

KATHOLIEKE UNIVERSITEIT LEUVEN
FACULTEIT DER GENEESKUNDE
DEPARTEMENT INWENDIGE ZIEKTEN
AFDELING HEPATOLOGIE

Role of hepatic stellate cells and vascular mediators in the pathophysiology of cirrhotic portal hypertension

Wim Laleman

Promotor: Prof. Dr. Frederik Nevens
Co-promotor: Prof. Dr. em. Johan Fevery

Thesis submitted in fulfillment of the requirements for the degree of
"Doctor in medical sciences"

2006

ACKNOWLEDGEMENT

Le véritable voyage de découverte ne consiste pas à chercher de nouveaux paysages, mais à avoir de nouveaux yeux. (Marcel Proust, 1871-1922)

Het schrijven van een doctoraatsthesis vormt voor elke doctorandus het ultieme orgelpunt van verschillende jaren vallen en opstaan, ontgoocheling en vreugde, verdwalen en uiteindelijk toch het juiste pad vinden tot aan de eindmeet van vandaag. Hoewel het pad van deze onderneming soms heel bochtig, onvoorspelbaar en mistig was, kon ik rekenen op vele medgezellen op deze lange tocht.

Prof. M. Vervenne, rector van de Katholieke Universiteit Leuven, Prof. M. Waer, vice-rector en voorzitter van de groep biomedische wetenschappen, alsook Prof. B. Himpens, decaan van de faculteit Geneeskunde, en alle professoren van deze zelfde faculteit wens ik te bedanken voor het immer "warme" en "voedende" milieu van onze Alma Mater, zowel te Leuven als aan de K.U.L.A.K. in Kortrijk. Het Nationaal Fonds voor Wetenschappelijk Onderzoek ben ik erkentelijk voor het verleende mandaat.

Mijn welgemeende en ongetwijfeld grootste dank gaat uit naar Prof. Dr. Frederik Nevens, promotor van dit proefschrift, om mij de mogelijkheid, maar tegelijk ook vrijheid, te geven om medische research te verrichten. Uw enthousiasme, hepatologisch-klinische en brede wetenschappelijke achtergrond en onuitputbare gedrevenheid vormden de fundamenten van dit proefschrift. Ook mijn co-promotor Prof. Dr. Em. Johan Fevery, wens ik te bedanken voor zijn blijvende interesse en steun.

De leden van jury, Prof. Dr. Jan Tack, Prof. Dr. Patrick Wouters, Prof. Dr. Ed Conway, Prof. Dr. Peter Verhamme en Prof. Dr. Peter Michielsen (Dept. Hepatogastroenterology, University Hospital Antwerpen), wil ik bedanken voor het kritisch nalezen en constructief becommentariëren van het voorliggende werk. I also wish to thank Prof. Dr. Didier Lebrec (Dept. of Hepatology, Hôpital Beaujon, Clichy, France) for taking the time to review this manuscript and to accept the invitation to participate in this jury.

Een thesis is zelden het werk van één persoon. Ik ben dan ook de volgende mensen erkentelijk in één of meerdere categorieën, gaande van praktisch-technische ondersteuning tot kritische terugkoppeling en bijstand of verstrooiing in de meest positieve zin van het

woord: Prof. Dr. David Cassiman, Prof. Dr. Chris Verslype, Lan Lin, Roger Servaes, Julien Stessel, Prof. Dr. Marc Van de Casteele, Tina Crabbé, Petra Windmolders, Ilse Bockx, Victor Petrov, Jos Van Pelt, Nelson Perez, Azam Katoonidazeh, Dr. Diethard Monbaliu, Katrien Vekemans, Kelly Bils, Rita Santy, Prof. Dr. Tania Roskams, Dr. Louis Libbrecht, Paula Aertsen, Prof. Dr. Raf Bisschops, Prof. Dr. Pieter Evenepoel en Prof. Dr. Alexander Wilmer. Heel in het bijzonder wil ik volgende 5 mensen uitdrukkelijk bedanken: Tamara Severi, met wie ik 4 jaar als "soul-mate" het labo hepatologie heb beleefd en die ondanks alles een onnavolgbaar voorbeeld van doorzettingsvermogen vormde. Ingrid Vander Elst, met wie ik menig uur in het "rattenkot" heb gesleten voor alle dierexperimenteel werk en oppuntstelling van ons dier- en perfusiemodel en zonder wiens nooit aflatende blijvende positieve motivering en technisch vernuft dit werk zeker niet zou zijn wat het vandaag geworden is. Marcel Zeegers, wiens onevenaarbare kennis en wetenschappelijke achtergrond de steunpilaar vormde in alle biochemische bepalingen van dit werk en bij wie ik altijd terecht kon met fundamentele vragen of … gewoon zomaar. Lien Van Landeghem, die mij in mijn laatste jaar ook ongelofelijk en belangeloos wist te helpen in een aantal cruciale experimenten en aan wie ik nu de fakkel doorgeef. Finaal, mijn oud-kotgenoot Wouter Mignon, die als computer-wizzard, niet alleen mijn thesis maar ook mezelf 2x wist te reanimeren uit de cyber-dood na weer eens een computer-crash (zonder back-ups).

De andere stafleden van de dienst Hepatologie, Prof. Dr. S. Yap en Prof. Dr. W. Van Steenbergen, alsook de stafleden van de dienst Gastroenterologie en Endoscopie, wens ik te bedanken voor hun blijvende interesse en positieve ondersteuning. Dr. John Verbrugghe, Dr. François D'Heygere, Dr. Marc Verhamme en Dr. Philippe Vergauwe ben ik eeuwig dank verschuldigd om mij obsessioneel-passioneel verslaafd te maken aan de Gastroentero-Hepatologie.

Mijn diepe dank gaat tot slot nog uit naar mijn ouders, die me onvoorwaardelijk en altijd alle kansen hebben geboden, alsook naar mijn zus en schoonbroer, schoonouders, schoonzussen en –broers, familie en vrienden voor de steun en vriendschap.

Omwille van alle steun, liefde, geduld en begrip, ben ik zonder enige twijfel het meest verschuldigd aan mijn vrouw Katrien en onze dochters Elise en Laura. Omdat dit proefschrift het enige is wat overschiet van de tijd dat ik niet bij hen was, wezenlijk of in gedachten, draag ik dit werk dan ook aan hen op.

TABLE OF CONTENTS:

ACKNOWLEDGEMENTS 3

TABLE OF CONTENTS 5

LIST OF ABBREVIATIONS 7

CHAPTER 1: INTRODUCTION: PORTAL HYPERTENSION: FROM PATHOPHYSIOLOGY TO CLINICAL PRACTICE. 9

1. INTRODUCTION 10
2. PATHOPHYSIOLOGICAL BASIS OF PORTAL HYPERTENSION 11
3. SUMMARY AND PERSPECTIVES 22
4. REFERENCES 23

CHAPTER 2: AIMS 27

CHAPER 3: A STABLE MODEL OF CIRRHOTIC PORTAL HYPERTENSION IN THE RAT: THIOACETAMIDE REVISITED 31

1. INTRODUCTION 32
2. MATERIALS AND METHODS 33
3. RESULTS 38
4. DISCUSSION 50
5. REFERENCES 53

CHAPTER 4: BOTH CA^{2+}-DEPENDENT AND –INDEPENDENT PATWAYS ARE INVOLVED IN RAT HEPATIC STELLATE CELL CONTRACTION AND INTRAHEPATIC HYPERRESPONSIVENESS TO METHOXAMINE 55

1. INTRODUCTION 56
2. MATERIALS AND METHODS 58
3. RESULTS 65
4. DISCUSSION 77
5. REFERENCES 81

CHAPTER 5: A ROLE FOR ASYMMETRIC DIMETHYLARGININE (ADMA) IN THE PATHOPHYSIOLOGY OF PORTAL HYPERTENSION IN BILIARY CIRRHOTIC RATS 83

1. INTRODUCTION 84
2. MATERIALS AND METHODS 86
3. RESULTS 90
4. DISCUSSION 103
5. REFERENCES 107

CHAPTER 6: BOTH THROMBOXANE A_2, A VASOCONSTRICTIVE CYCLO-OXYGENASE-METABOLITE, AND NITRIC OXIDE ARE INVOLVED IN THE INCREASED INTRAHEPATIC VASCULAR TONE ASSOCIATED WITH THIOACETAMIDE-INDUCED CIRRHOSIS IN THE RAT 109

1. INTRODUCTION 110
2. MATERIALS AND METHODS 113
3. RESULTS 116
4. DISCUSSION 128
5. REFERENCES 134

CHAPTER 7: NITROFLURBIPROFEN, A NITRIC OXIDE RELEASING DERIVATIVE OF FLURBIPROFEN, IMPROVES PORTAL HYPERTENSION THROUGH CORRECTION OF INTRAHEPATIC ENDOTHELIAL DYSFUNCTION AND HYPERRESPONSIVENESS IN THIOACETAMIDE CIRRHOTIC RATS 137

1. INTRODUCTION 138
2. MATERIALS AND METHODS 140
3. RESULTS 143
4. DISCUSSION 155
5. REFERENCES 158

CHAPTER 8: SUMMARY AND GENERAL CONCLUSIONS 159

HOOFDSTUK 8: SAMENVATTING 165

CURRICULUM VITAE 171

PUBLICATION LIST 173

LIST OF ABBREVIATIONS:

APB-t	aminopyrine breath test
ADMA	asymmetric dimethylarginine
Akt	serine-threonine kinase
α-SMA	α-smooth muscle actin
BDE	bile duct excised
cGMP	cyclic guanosine monophosphate
COX	cyclooxygenase
DAN	2,3-diaminonaphtalene
DDAH	dimethylarginine dimethylaminohydrolase
11-dehydro-TXB_2	11-dehydro-thromboxane B_2
eNOS	endothelial nitric oxide synthase
ET1	endothelin-1
HCT-1026	nitroflurbiprofen
HSC	hepatic stellate cell
HVPG	hepatic venous pressure gradient
IHVR	intrahepatic vascular resistance
L-NAME	N_ω-Nitro-L-arginine methyl ester hydrochloride
MAP	mean arterial pressure
MBF	mesenteric blood flow
MLCK	myosin light chain kinase
MLCP	myosin light chain phosphatase
NO	nitric oxide
NOx	nitrate/nitrite
PHT	portal hypertension
PKC	protein kinase C
PP	portal pressure
PPVL	partial portal vein ligation
RAA	renin-angiotensin-aldosteron
rMLC	regulatory light chain of myosin
SDMA	symmetric dimethylarginine
TAA	thioacetamide
TXA2	thromboxane A2
SRS	splenorenal shunt

Chapter 1

Introduction: Portal hypertension:

from pathophysiology to clinical practice.

adapted from

W. Laleman[1], L. Van Landeghem[1], A. Wilmer[2], J. Fevery[1] and F. Nevens[1].

Department of Hepatology[1] and Medical Intensive Care[2],
University Hospital Gasthuisberg, K.U. Leuven, Belgium.

Liver International 2005, 25: 1070-1090
Reprinted with permission of Blackwell publishing

1. INTRODUCTION

Portal hypertension (PHT) is characterized by an increase in portal vein pressure as a result of an impediment to portal flow. Most frequently, portal hypertension is caused by cirrhosis, either alcoholic in origin or due to chronic hepatitis B or C infection, and includes over 90% of patients with portal hypertension in Europe and the USA (1). Taking into account the high prevalence of hepatitis C worldwide and the emergence of non-alcoholic fatty liver disease, the incidence of PHT is not expected to decrease in the next decade (2). Many of the lethal complications of liver cirrhosis are directly related to the presence of portal hypertension, including haemorrhage from gastroesophageal varices, hepatic encephalopathy, ascites and functional renal failure. An innovating and challenging concept which has attained considerable attention over the last years is that PHT, in order to become clinically relevant, should increase above a critical threshold. The use of the invasive technique to measure the hepatic venous pressure gradient (HVPG), which reflects the gradient between the portal vein and vena cava pressure, has played a major role in the construct of this concept and has therefore become indispensable at least in clinical trials for PHT (1,3,4). It is now generally agreed that the HVPG should increase above a threshold of 12 mmHg for complications of PHT, such as ruptured oesophageal varices and ascites, to occur (5-7). Several clinical-haemodynamic correlations have supported the principle of critical threshold since longitudinal studies have demonstrated a decrease in variceal size and an increased short-term survival when the portal pressure gradient could be reduced below this threshold (8,9) or when a reduction in HVPG of at least 20% of the baseline values could be obtained (9-12). Moreover, over the last decade it has become clear that a decrease in portal pressure is not only protective against the short-term risk of variceal (re)bleeding but is also associated with a lower long-term risk of developing other complications (such as variceal rebleeding, ascites, hepatic encephalopathy, spontaneous

bacterial peritonitis and hepatorenal syndrome) and with an improved long-term survival in an 8 year follow-up period after the index variceal bleeding (13).

The available armamentarium to do so, however, is far from satisfactory. Since the introduction more than 20 years ago by Lebrec et al. (14) for the prevention of variceal rebleeding, and a few years later by Pascal et al. (15) for primary prophylaxis, non-selective beta-blockers, acting as splanchnic vasoconstrictors, have remained the cornerstone in the treatment of portal hypertension (16,17). However, only 30-40% of patients achieve a long-term decrease in portal pressure (9), whereas an additionally estimated 10 to 20% of patients discontinue beta-blockers due to intolerance (18,19). As a consequence, the search for potential new strategies is emergent and linked to the growing interest in the pathophysiology of portal hypertension.

2. PATHOPHYSIOLOGICAL BASIS OF PORTAL HYPERTENSION

According to Ohm's law ($\Delta P=QxR$), changes in portal venous pressure are proportional to alterations in blood flow and resistance. In the normal liver, intrahepatic resistance changes with variations in portal blood flow, thereby keeping portal pressure within normal limits. In cirrhosis however, both the intrahepatic resistance and splanchnic blood flow are increased (Fig. 1) (19,20). An increased resistance to portal blood flow is considered the primary factor in the pathophysiology of cirrhotic PHT and is located at the intrahepatic circulation. The increased portal venous inflow (splanchnic hyperemia) is typically observed in more advanced stages of PHT as the result of a marked arteriolar vasodilation in splanchnic organs draining into the portal vein. Such increased blood flow maintains and aggravates portal pressure despite the formation of an extensive network of collaterals and gives rise to the hyperdynamic systemic state, characterized by an increased heart rate, cardiac output, plasma volume and a low overall vascular resistance (19).

As a consequence it is possible to reduce portal pressure either by reducing portal resistance, portal blood inflow or both.

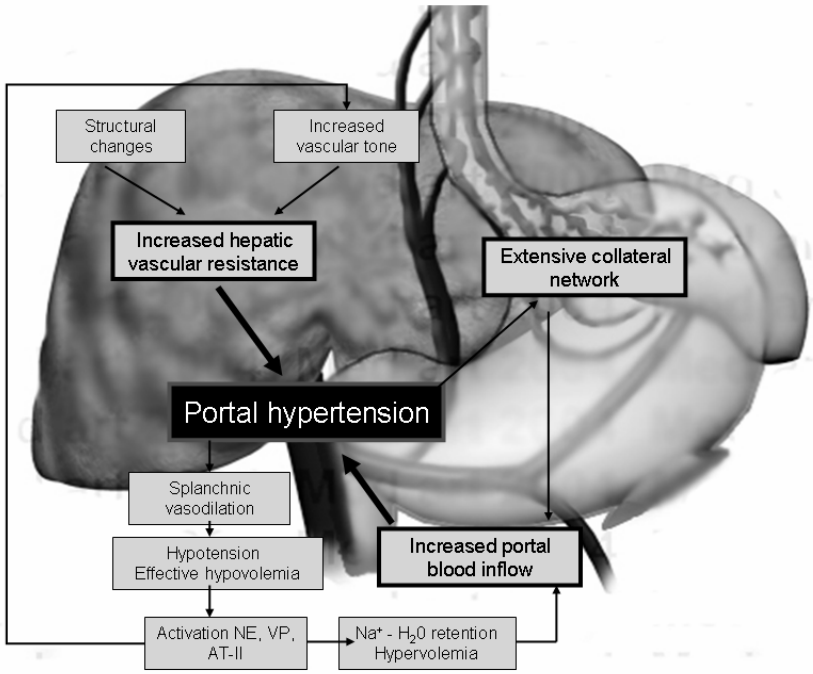


Fig. 1: Schematic overview of the pathophysiology of PHT.

(NE, norepinephrine; VP, vasopressin; AT-II, angiotensin-II)

2.1. Increased intrahepatic vascular resistance: cellular and humoral components

It has long been thought that the increase in intrahepatic vascular resistance (IHVR) was merely a mechanical consequence of the distortion of the liver vascular architecture by fibrosis, scarring and nodule formation, and therefore not amenable to pharmacological modification. Consequently, all attempts to decrease portal pressure pharmacologically were directed to reduce portal venous inflow by using vasoconstrictive agents, such as vasopressin derivatives, somatostatin or non-selective beta-blockers. The pioneering work by Bhatal and Grossmann (21) changed this dogma by demonstrating that a fraction of this increased IHVR liver could be reduced by vasodilators in an isolated perfused cirrhotic rat

liver. They estimated that this **active, dynamic modifiable component** of IHVR or **increased intrahepatic vascular tone**, accounted for 30% of the total IHVR, and suggested, as a basis for their findings, that an increased number of a special type of **contractile cells** in a strategic location within the cirrhotic nodule may modulate, through contraction, the resistance of the hepatic vascular bed to portal inflow. This hypothesis induced the search for contractile elements within the liver and for abnormalities in the mechanisms regulating cell contraction. Although other cellular elements such as the vascular smooth muscle cells of the intrahepatic vasculature (i.e. small portal venules in portal areas) may also be involved, many studies have pointed out a dominant role for activated hepatic stellate cells (HSC).

2.1.1. Perisinusoidal HSCs, as effectors of the increased vascular tone.

HSC (also known as lipocytes or Ito cells) are located in the perisinusoidal space of Disse beneath the endothelial barrier and represent 5 to 8% of all liver cells (22-26). In the normal liver, they have been suggested (but not proven) to have vasoregulating properties due to their long primary cytoplasmic processes, which are parallel to the sinusoidal endothelial wall, and second order branches sprouting out from these processes and which embrace the sinusoid and penetrate between hepatocytes toward neighbouring sinusoids (Fig. 2). Additionally, some HSC are in close contact with nerve endings, some of which contain neuropeptides, such as substance P, neuropeptide Y and somatostatin. What is certain is that in normal liver, HSC are mainly involved in the storage of vitamin A and synthesis of extracellular matrix components, matrix degrading metalloproteinases, cytokines and growth factors. During liver injury, perisinusoidal HSC undergo a striking morphologic and functional transition ("activation") from a "quiescent" storing cell to a "myofibroblast-like" phenotype with pro- fibrogenic (i.e. increased secretion of extracellular matrix constituents that collectively form the hepatic scar), contractile,

immuno-modulatory and migratory potential (26). Due to the expression of smooth muscle proteins, their strategical anatomical location around hepatic sinusoids and the acquisition of receptors for different vasoactive substances (see below), activated HSCs, by contraction, reduce the calibre of the sinusoid (Fig. 2) (23,27).

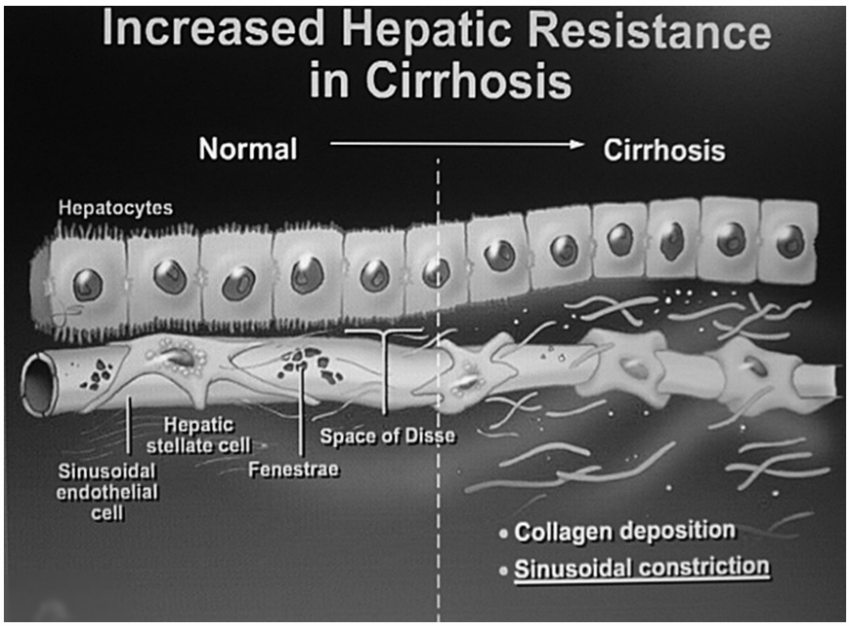


Fig. 2: Hepatic stellate cells in normal liver and cirrhosis

Based on these premises, it is assumed that contraction is similar to smooth muscle cells, leading to the subsequent connotation “smooth muscle-like”. However, in contrast to fibrogenesis, the basic biology of contraction by HSC remains enigmatic.

2.1.2 Vascular mediators, as regulators of vascular tone.

An additional feature in the development of the increased intrahepatic vascular tone is an imbalance in vasoactive substances. In cirrhosis, there is an overexpression locally and/or systemically of (neuro)humoral **vasoconstrictors**, such as norepinephrine, endothelins, angiotensin II and leukotrienes, leading to increased vascular tone of the cirrhotic liver as

well as to an exaggerated response ("hyperresponsiveness") of the hepatic vascular bed to some of these mediators (28,29). Of these vasoconstrictors endothelin-1 (ET-1) seems the most potent one. Both hepatic concentration and endothelin receptor expression are increased in human and experimental cirrhosis (30). The ET_A-receptor subtype, present on vascular contractile cells, causes vasoconstriction, while the ET_B-receptor subtype on endothelial cells is believed to cause vasorelaxation by stimulating endothelial nitric oxide synthase (eNOS) (28) (Fig. 3). Furthermore, ET-1 has also been reported to induce a strong pro-fibrogenic response, emphasizing its role not only in the active dynamic (i.e. increased intrahepatic vascular tone) but also in the "passive" (i.e. fibrosis and scarrification of the liver) component of intrahepatic resistance (31,32).

A second major player is angiotensin II (AT-II). Already in 1981, Arroyo et al. (33) showed that the renin-angiotensin-aldosterone system was implicated in the regulation of portal blood flow. Recently, Bataller et al. (34) described that stellate cells express the AT_1 receptor, which promotes contraction and proliferation of the HSCs. Additionally, as is the case with endothelin-1, an autocrine source of AT-II became apparent, indicating that stellate cells harbour all the components for local signalling in response to AT-II (35) (Fig. 3). Bataller et al. (36) also documented that angiotensin-II is a fibrogenic cytokine through the generation of radical oxygen species by NADPH oxidase stimulation, since inhibition of NADPH oxidase of the AT1-receptor attenuated liver injury and fibrosis.

A third factor is the influence of the adrenergic neurohumoral system. Oben et al. (37) tested the hypothesis that HSC respond to and produce sympathetic nervous system neurotransmitters. In cultured HSC and intact mice with liver injury, it was shown that HSCs expressed adrenoceptors and catecholamine biosynthetic enzymes and that they released norepinephrine (NE). In Dbh(-/-) mice, which lack dopamine beta-hydroxylase,

the liver- injury related fibrogenic responses were inhibited, suggesting an important role for neurohumoral factors (Fig. 3).

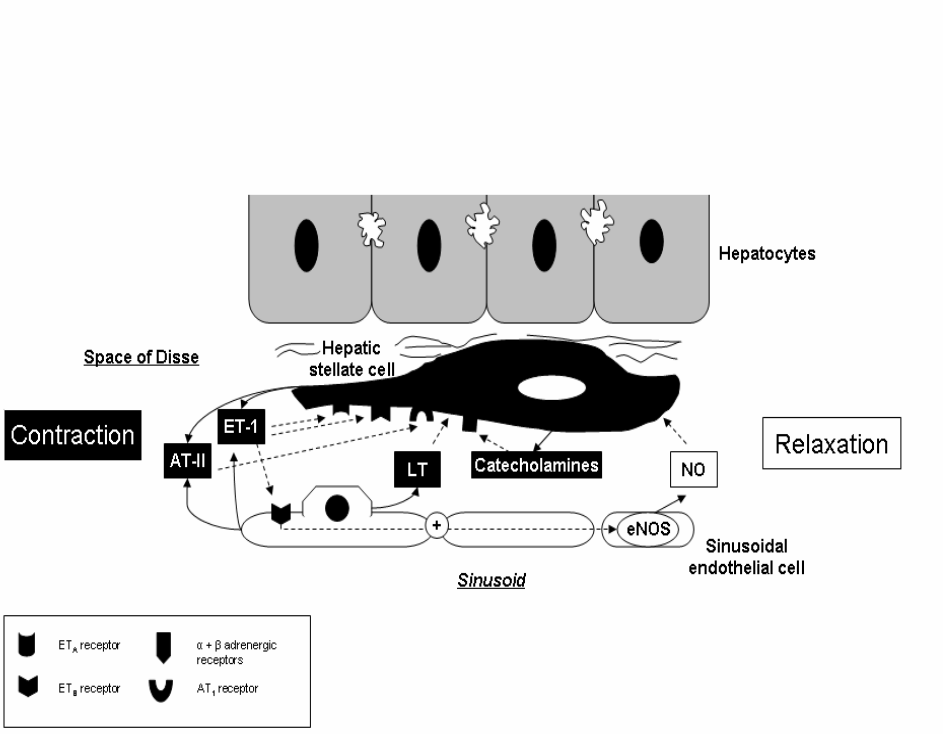


Fig. 3: Modulation of contraction/relaxation of activated HSC. (ET-1, endothelin-1; AT-II, angiotensin II; NO, nitric oxide; eNOS, endothelial nitric oxide synthase; LT, leukotrienes).

In contrast to the intrahepatic excess in vasoconstrictive potential, the intrahepatic production and/or availability of **vasodilators** remains insufficient. Nitric oxide (NO), the most renowned vasodilator substance, is a reactive, gaseous molecule with a half-life of 3-5 seconds, produced from L-arginine by one of the 3 nitric oxide synthase (NOS)-isoforms. These isoforms are categorized in 2 families of enzymes: endothelial cells (eNOS) and neurons (nNOS) contain a distinct "constitutive" NOS, whereas a wide variety of cells, mainly cells involved in inflammatory reactions, are capable of expressing the inducible form (iNOS). In the liver, both eNOS and iNOS can be active. In chronic liver injury, the

molecular basis of the intrahepatic NO-deficiency has uniformly been attributed to a decreased activity of the eNOS (38-40) (Fig. 3-4).

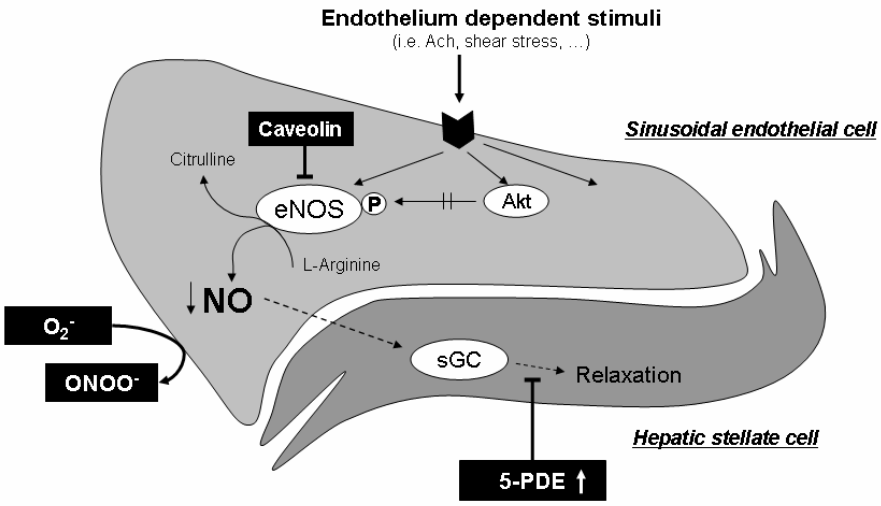


Fig. 4: Possible mechanisms involved in the decreased intrahepatic NO bioavailability: dysfunction of endothelial NO-synthase (eNOS) in the sinusoidal endothelial cell due to excessive inhibitory activity of caveolin, defective phosphorylation of eNOS by the serine-threonine kinase Akt or decreased translation of the eNOS protein or increased degradation of NO to peroxynitrite or of its second messenger cyclic guanosine 3',5'-monophosphate due to upregulated phosphodiesterases. (Ach, acetylcholine; sGC, soluble guanylate cyclase; O_2^-, superoxide; ONOO$^-$, peroxynitrite; 5-PDE, 5-phosphodiesterase)

Whether this dysfunction is due to diminished translation or to complex posttranslational modifications (such as the impaired serine-threonine kinase Akt activation of eNOS and/or increased interaction of eNOS with the inhibitory protein caveolin-1) remains currently under discussion (Fig. 4) (38-40).

Besides decreased production, there might also be an increased degradation of NO (by formation of peroxynitrite) due to enhanced superoxide activity as a result of superoxide dismutase deficiency, leading to diminished bioavailability of NO (41), and increased degradation of its second messenger cyclic guanosine 3',5'-monophosphate (cGMP) due to upregulated phosphodiesterases (42) (Fig. 4).

2.2 Splanchnic hyperemia and arterial vasodilation

The second contributing factor to portal hypertension is increased blood flow in the portal venous system. This is due to splanchnic arteriolar vasodilatation (43,44). The increase in blood flow is responsible for the maintenance and further aggravation of the portal hypertensive syndrome in conditions of increased IHVR, for high portal venous inflow per se is not sufficient to induce portal hypertension in the face of a healthy compliant liver (45). High portal inflow also explains why portal hypertension persists despite the presence of an extensive collateral network that may divert up to 80% of the portal blood flow (43). The splanchnic arteriolar vasodilation is due to increased levels of circulating vasodilator substances and reduced sensitivity ("hyporesponsiveness") to vasoconstrictors (44). Early studies mainly focused on the role of circulating vasodilator substances of splanchnic origin such as glucagon, vasoactive intestinal peptide, bile salts, platelet activating factor, substance P, calcitonin gene-related peptide and atrial natriuretic peptide (46), because these agents accumulate in chronic liver disease as a result of reduced hepatic metabolism and/or increased portosystemic shunting (47). The strongest evidence concerns **glucagon**, whereas for other substances controversy still exists (47-51). Elevated plasma glucagon levels are present in cirrhotic patients and in portal hypertensive rat models, and a partial decrease in splanchnic hyperemia has been obtained by infusion of glucagon antibodies or of somatostatin in portal hypertensive rats (52-55). Splanchnic hyperemia was also

obtained when glucagon levels were increased in healthy rats to values found in cirrhotic rats (53). Hyperglucagonemia would account for 30-40% of the splanchnic vasodilation in the chronic portal hypertensive state (53). These data clearly support a pathogenetic role for glucagon, and favour the use of somatostatin in the treatment of variceal hemorrhage. Paracrine vasoactive substances produced by the splanchnic vascular endothelium, such as respectively **NO** and **prostacyclin**, are also implicated in the pathogenesis of the portal hypertensive syndrome, since inhibition of respectively NO and prostanoid synthesis as well as removal of the endothelium, corrects, in large part, splanchnic and systemic hemodynamics in portal hypertensive rats (44,56). Moreover, crosstalk exists between both pathways (56). For the excess of NO in the splanchnic and systemic circulation, it has been previously assumed that the inducible isoform of NOS (iNOS) was responsible. This was based on the hypothesis of Vallance and Moncada (57), who proposed that endotoxemia, sometimes present in cirrhosis, induces expression of iNOS in vessel walls. However, this hypothesis could not be validated because iNOS was not significantly upregulated in the splanchnic and systemic vasculature of cirrhotic animals and because dexamethasone, known to inhibit iNOS expression, did not prevent the hyperdynamic circulation from developing (58,59). The major enzymatic source of the vascular NO overproduction was shown to be eNOS (58-61). An important role in the upregulation of eNOS in this context has been attributed to chronic increases in shear stress stimulation in endothelial cells as a result of the increased portal tributary blood flow and the hyperdynamic circulation (62-64). The pathogenetic relationship between shear stress and arterial vasodilation was further reinforced by the observation that long-term β-blockade in partial portal vein ligated rats corrected arterial hyporeactivity to vasoconstrictors and systemic eNOS overexpression, suggesting possible mechanisms of action of beta-blockade either indirectly by decreasing cardiac output by β_1 receptors or either through a direct vascular β_2

effect (62). In addition to shear stress, several other factors, such as vascular endothelial growth factor (VEGF) (65,66) and proinflammatory cytokines (67) have also been associated with enhanced systemic eNOS activity. Of particular interest is work by Groszmann et al (67), who have shown that tumor necrosis factor alpha (TNF-α), a proinflammatory cytokine, was induced in mesenteric lymph nodes by bacterial translocation and accumulated in the serum. This TNF-α production was associated with elevated levels of tetrahydrobiopterin (BH_4), a TNF-α-stimulated co-factor and enhancer of eNOS-derived NO biosynthesis in mesenteric vasculature, and establishes a link between pro-inflammatory cytokines and eNOS-derived NO production in the absence of inducible NOS.

In addition to NO, carbon monoxide has also been implicated in contributing to the mesenteric vascular hypo-responsiveness of portal hypertensive rats (68).

These pathophysiological insights form the basis to use vasoconstrictors such as vasopressin, somatostatin and non-selective adrenergic beta-blockers in the treatment of PHT.

2.3. The hyperdynamic circulation

In a more advanced phase, patients with cirrhosis and portal hypertension exhibit a typical "hyperdynamic" circulation with increased cardiac output, heart rate and plasma volume and decreased arterial blood pressure and systemic vascular resistance (69). These hemodynamic changes are initially induced by splanchnic, and later on by peripheral vasodilatation, leading to reduced systemic vascular resistance and an abnormal distribution of the blood volume with a reduced central or "effective" blood volume as key elements. The basis for this phenomenon is thought to originate either from the presence of excess circulating vasodilators that escape hepatic degradation or bypass the liver through

portosystemic shunting or from increased shear stress in the systemic circulation, as discussed above (62-64,70). The low arterial pressure and central hypovolemia lead to the activation of several counter-regulatory systems, such as the renin-angiotensin-aldosteron system (RAAS), the sympathetic nervous system and the non-osmotic release of arginine vasopressin, in an attempt to maintain a stable perfusion pressure by means of vasoconstriction and sodium and water retention. The above mentioned "hyporesponsiveness" of the splanchnic vascular wall to vasoconstrictor agents explains why the hyperdynamic circulation increases with progression of the disease despite increasing activation of these homeostatic vasoconstrictor systems (69). Furthermore, persistent activation of these systems appears to worsen the active component of intrahepatic resistance and promotes vasoconstriction with ischemia and subsequent formation of oxidative stress in essential end-organs. This complex interplay between enhanced vasodilatation in one vascular territory and vasoconstriction in another, plays a central role in the development of the multi-organ disturbance in cirrhosis (71). This diversity in vascular reactions within one cirrhotic patient may be either due to locally increasing levels of endogenous vasoconstrictors compared to the vasodilators, due to relative "underfilling" of the vasodilated systemic circulation or to a change in vascular reactivity (69,70). The presence and severity of the hyperdynamic circulation in patients with cirrhosis may significantly affect the patient's prognosis on a short term basis. Several studies have already emphasised the relation between the degree of arterial hypotension in cirrhosis and the severity of hepatic dysfunction, hepatic decompensation and survival (72,73).

3. SUMMARY AND PERSPECTIVES

Complications of portal hypertension are responsible for morbidity and mortality in patients with cirrhosis. Decreasing portal pressure has therefore become a major target in treating these patients. Due to the unavailability of reliable, safe and effective alternatives, currently, therapy is limited to the use of beta-blockers, which reduce portal pressure through a reduction in portal and collateral blood flow. However, only half of the treated patients achieve the preset hemodynamic goals and there remains the potential for further impairment of liver function due to a decrease in total hepatic flow. The recent demonstration of a functional component in the increased IHVR in cirrhosis has prompted further studies to investigate mechanisms involved in this abnormality, both cellular as humoral, in order to set the framework for a rational approach to the treatment of PHT. The present thesis hopes to support this quest.

4. REFERENCES

1. Wongcharatwaree S, Groszmann RJ. Diagnosing portal hypertension. Baillieres Best Pract Res Clin Gastroenterol 2000; 14: 881-894.
2. Ramesh S, Sanyal AJ. Hepatitis C and nonalcoholic fatty liver disease. Semin Liv Dis 2004; 24: 399-413.
3. Myers JD, Taylor WJ. An estimation of portal venous pressure by occlusive catherization of a hepatic venule. J Clin Invest 1951; 30: 662-663.
4. Groszmann RJ, Wongcharatrawee S. The hepatic venous pressure gradient: anything worth doing should be done right. Hepatology 2003; 39: 280-282.
5. Garcia-Tsao G, Groszmann RJ, Fischer RL, et al. Portal pressure, presence of gastroesophageal varices and variceal bleeding. Hepatology 1985; 5: 419-424.
6. Casado M, Bosch J, Garcia-Pagan JC, et al. Clinical events after transjugular intrahepatic portosystemic shunt : correlation with hemodynamic findings. Gastroenterology 1998; 114: 1296-1303.
7. Vorobioff J, Groszmann RJ, Picabea E, et al. Prognostic value of hepatic venous pressure gradient measurements in alcoholic cirrhosis: a 10-year prospective study. Gastroenterology 1996; 11: 701-709.
8. Groszmann RJ, Bosch J, Grace ND, et al. Hemodynamic events in a prospective randomized trial of propranolol versus placebo in the prevention of a first variceal hemorrhage. Gastroenterology 1990; 90: 1401–1407.
9. Feu F, Garcia-Pagan JC, Bosch J, et al. Relation between portal pressure response to pharmacotherapy and risk of recurrent variceal haemorrhage in patients with cirrhosis. Lancet 1995; 346: 1056–1059.
10. Escorsell A, Bordas JM, Castaneda B, et al. Predictive value of the variceal pressure response to continued pharmacological therapy in patients with cirrhosis and portal hypertension. Hepatology 2000; 31: 1061-1067.
11. Merkel C, Bolognesi M, Sacerdoti D, et al. The hemodynamic response to medical treatment of portal hypertension as a predictor of clinical effectiveness in the primary prophylaxis of variceal rebleeding. Hepatology 2000; 32: 930-934.
12. Villuanueva C, Balanzo J, Novella MT, et al. Nadolol plus isosorbide mononitrate compared with sclerotherapy for the therapy for prevention of variceal rebleeding. N Engl J Med 1996; 334: 1624-1629.
13. Abraldes JG, Tarantino I, Turnes J, et al. Hemodynamic response to pharmacological treatment of portal hypertension and long-term prognosis of cirrhosis. Hepatology 2003; 37: 902-908.
14. Lebrec D, Poynard T, Hillon P, Benhamou JP. Propanolol for the prevention of recurrent gastrointestinal bleeding in patients with cirrhosis: a controlled study. N Engl J Med 1981; 305: 1371-1374.
15. Pascal JP, Calès P. Propanolol in the prevention of first upper gastrointestinal tract hemorrhage in patients with cirrhosis of the liver and esophageal varices. N Engl J Med 1987; 317: 856-861.
16. D'Amico G, Pagliaro L, Bosch J. The treatment of portal hypertension: a meta-analytic review. Hepatology 1995; 22: 332-354.
17. D'Amico G, Pagliaro L, Bosch J, et al. Pharmacological treatment of portal hypertension: an evidence-based approach. Semin Liv Dis 1999; 19: 475-505.
18. Villeneuve JP, Pomier-Layrargues G, Infante-Rivard C, et al. Propanolol for the prevention of recurrent variceal rebleeding in cirrhosis : a controlled trial. Hepatology 1986; 6: 1239-1243.
19. Bosch J, Garcia-Pagan JC. Complications of cirrhosis. I. Portal hypertension. J Hepatol 2000; 32 (Suppl. 1): 141-156.
20. Bosch J, Groszmann RJ, editors: Portal hypertension: pathophysiology and treatment. Oxford: Blackwell; 1994.
21. Bhatal PS, Grossman HJ. Reduction of the increased intrahepatic vascular resistance of the isolated perfused cirrhotic rat liver by vasodilators. J Hepatol 1985; 1: 325-337.
22. Pinzani M, Failli P, Ruocco C, et al. Fat-storing cells as liver-specific pericytes. Spatial dynamics of agonist-stimulated intracellular calcium transients. J Clin Invest 1992; 90: 642-646.
23. Kawada N, Tran-Thi TA, Klein H, et al. The contraction of hepatic stellate (Ito) cells stimulated with vasoactive substances. Possible involvement of endothelin-1 and nitric oxide in the regulation of the sinusoidal tonus. Eur J Biochem 1993; 213: 815-823.
24. Rockey DC, Housset CN, Friedman SL. Activation-dependent contractility of rat hepatic lipocytes in culture and in vivo. J Clin Invest 1993; 92: 1795-1804.

25. Cassiman D, Roskams T. Beauty is in the eye of the beholder: emerging concepts and pitfalls in hepatic stellate cell research. J Hepatol 2002; 37: 527-535.
26. Friedman SL. Seminars in medicine of the Beth Israel Hospital, Boston. The cellular basis of hepatic fibrosis. Mechanisms and treatment strategies.
N Engl J Med 1993; 328: 1828-35.
27. Zhang JX, Pegoli WJ, Clemens MG, et al. Endothelin-1 induces direct constriction of the hepatic sinusoids. Am J Physiol 1994; 266: G624-G632.
28. Rockey DC. Vascular mediators in the injured liver. Hepatology 2003; 37: 4-12.
29. Graupera M, Garcia-Pagan JC, Titos E, et al. 5-lipoxygenase inhibition reduces intrahepatic vascular resistance of cirrhotic rat livers: A possible role of cysteinyl-leukotrienes. Gastroenterology 2002; 122: 387-393.
30. Ghandi CR, Sproat LA, Subbotin VM. Increased hepatic endothelin-1 levels and endothelin receptor density in cirrhotic rats. Life Sci 1996; 58: 55-62.
31. Rockey DC, Chung JJ. Endothelin antagonism in experimental hepatic fibrosis. Implications for endothelin in the pathogenesis of wound healing. J Clin Invest 1996; 98: 1381-1388.
32. Cho JJ, Hocher B, Herbst H, et al. An oral endothelin-A receptor antagonist blocks collagen synthesis and deposition in advanced rat liver fibrosis. Gastroenterology 2000; 118:1169-1178.
33. Arroyo V, Bosch J, Mauri M, et al. Effect of angiotensin-II blockade on systemic and hepatic hemodynamics and on the renin-angiotensin-aldosterone system in cirrhosis with ascites. Eur J Clin Invest 1981; 11: 221-229.
34. Bataller R, Ginès P, Nicolas JM, et al. Angiotensin induces contraction and proliferation of human hepatic stellate cells. Gastroenterology 2000; 118: 1149-1156.
35. Bataller R, Ginès P, Lora J, et al. Evidence for a local renin-angiotensin system in human liver: expression in activated hepatic stellate cells. Hepatology 2001; 34: 399A.
36. Bataller R, Schwabe RF, Choi YH, et al. NADPH oxidase signal transduces angiotensin II in hepatic stellate cells and is critical in hepatic fibrosis. J Clin Invest 2003; 112: 1383-1394.
37. Oben JA, Roskams T, Yang S, et al. Hepatic fibrogenesis requires sympathetic neurotransmitters. Gut 2004; 53: 438-445.
38. Van de Casteele M, Omasta A, Janssens S, et al. In vivo gene transfer of endothelial nitric oxide synthase decreases portal pressure in anaesthetised carbon tetrachloride cirrhotic rats. Gut 2002; 51: 440-445.
39. Shah VJ, Toruner M, Haddad F, et al. Impaired endothelial nitric oxide synthase activity associated with enhanced caveolin binding in experimental cirrhosis in the rat. Gastroenterology 1999; 117: 1222–1228.
40. Moralez-Ruiz M, Cejudo-Martin P, Fernandez-Varo G, et al. Transduction of the liver with activated Akt normalizes portal pressure in cirrhotic rats. Gastroenterology 2003; 125: 522-531.
41. Van de Casteele M, Van Pelt JF, Nevens F, et al. Low NO bioavailability in CCl_4 cirrhotic rat livers might result from low NO synthesis combined with decreased superoxide dismutase activity allowing superoxide-mediated NO breakdown: a comparison of two portal hypertensive rat models with healthy controls. Comp Hepatol 2003 ; 2: 2.
42. Loureiro-Silva MR, Iwakiri Y, Abraldes JG, Haq O, Groszmann RJ. Increased phosphodiesterase-5 expression is involved in the decreased vasodilator response to nitric oxide in cirrhotic rat livers. J Hepatol 2006; 44: 886-893.
43. Vorobioff J, Bredfeldt J, Groszmann RJ. Hyperdynamic circulation in a portal hypertensive rat model: a primary factor for the maintenance of chronic portal hypertension. Am J Physiol 1983; 244: G52-G56.
44. Wiest R, Groszmann RJ. The paradox of nitric oxide in cirrhosis and portal hypertension: Too much, not enough. Hepatology 2002; 35: 478-491.
45. Sikuler E, Groszmann RJ. Interaction of flow and resistance in maintenace of portal hypertension in a rat model. Am J Physiol 1986; 250: G205-G212.
46. Möller S, Bendtsen F, Henriksen JH. Vasoactive substances in the circulatory dysfunction of cirrhosis. Scand J Clin Lab Invest 2001; 61: 421-430.
47. Benoit JN, Barrowman JA, Harper SA, et al. Role of humoral factors in the intestinal hyperemia associated with chronic portal hypertension. Am J Physiol 1984; 247: E486-E493.
48. Genecin P, Polio J, Colombato LA, et al. Role of bile acids do not mediate the hyperdynamic circulation in portal hypertensive rats. Am J Physiol 1990; 259: G21-G25.
49. Thomas SH, Joh T, Benoit JN. Role of bile acids in splanchnic hemodynamic response to chronic portal hypertensive rats. Dig Dis Sci 1991; 36: 1243-1248.
50. Fernandez M, Casadevall M, Schuligoi R, et al. Neonatal capsaicin treatment does not prevent splanchnic vasodilation in portal hypertensive rats. Hepatology 1994; 20: 1609-1614.

51. Lee SS, Sharkey KA. Capsaicin treatment blocks development of hyperkinetic circulation in portal hypertensive rats. Am J Physiol 1993; 264: G868-G873.
52. Gomis R, Fernandez-Alvarez J, Pizcueta M, et al. Impaired function of pancreatic islets from rats with portal hypertension resulting from cirrhosis and partial vein ligation. Hepatology 1994; 19: 1257-1261.
53. Silva G, Navasa M, Bosch J, et al. Hemodynamic effects of glucagon in portal hypertension. Hepatology 1990; 11: 668-673.
54. Kravetz D, Bosch J, Arderiu MT, et al. Effects of somatostatin on splanchnic hemodynamics and plasma glucagons in portal hypertensive rats. Am J Physiol 1988; 254: G322-G325.
55. Benoit JN, Zimmerman B, Premen AJ, et al. Role of glucagons in splanchnic hyperemia of chronic portal hypertension. Am J Physiol 1986; 251: G674-G678.
56. Fernandez M, Garcia-Pagan JC, Casadevall M, et al. Acute and chronic cyclooxygenase blockade in portal hypertensive rats: influence on nitric oxide biosynthesis. Gastroenterology 1996; 110: 1529-1535.
57. Vallance P, Moncada S. Hyperdynamic circulation in cirrhosis: a role for nitric oxide ? Lancet 1991; 1: 776.
58. Martin P, Xu D, Niederberger M, et al. Upregulation of endothelial constitutive NOS: a major role in the increased NO production in cirrhotic rats. Am J Physiol 1996; 270: F494-F499.
59. Fernandez M, Garcia-Pagan JC, Casadevall M, et al. Evidence against a role for inducible nitric oxide synthase in the hyperdynamic circulation of portal hypertensive rats. Gastroenterology 1995; 108: 1487-1495.
60. Wiest R, Shah VJ, Sessa W, et al. Nitric oxide overproduction by eNOS precedes the hyperdynamic circulation in portal hypertensive rats. Am J Physiol 1999; 276: G1043-51.
61. Cahill PA, Redmond EM, Hodges R, et al. Increased endothelial nitric oxide synthase activity in the hyperaemic vessels of portal hypertensive rats. J Hepatol 1996; 25: 370-378.
62. Pateron D, Tazi KA, Sogni P, et al. Role of aortic nitric oxide synthase 3 (eNOS) in the systemic vasodilation of portal hypertension. Gastroenterology 2000; 119: 196-2000.
63. Braillon A, Lee S, Girod C, et al. Role of portosystemic shunts in the hyperkinetic circulation of the portal hypertensive rat. J Lab Clin Med 1986; 108: 543-548.
64. Tazi KA, Barrière E, Moreau R, et al. Role of shear stress in aortic eNOS up-regulation in rats with bilairy cirrhosis. Gastroenterology 2002; 122: 1869-1877
65. Akiyoshi F, Sata M, Suzuki H, et al. Serum vascular endothelial growth factor levels in various liver diseases. Dig Dis Sci 1998; 43: 41-45.
66. Bouloumie A, Schini-Kerth VB, Busse R. Vascular endothelial growth factour up-regulates nitric oxide synthase expression in endothelial cells. Cardiovasc Res 1999; 41: 509-510
67. Wiest R, Das S, Cadelina G, et al. Bacterial translocation in cirrhotic rats stimulates eNOS-derived NO production and impairs mesenteric vascular contractility. J Clin Invest 1999; 104: 1223-1233.
68. Fernandez M, Lambrecht RW, Bonkovsky H. Increased heme oxygenase activity in splanchnic organs from portal hypertensive rats: role in modulating mesenteric vascular reactivity. J Hepatol 2001; 34: 812-817.
69. Blendis L, Wong F. The hyperdynamic circulation in cirrhosis: an overview. Pharm Therap 2001; 89: 221-231.
70. Henriksen JH, Kizska-Kanowitz M, Bendtsen F, et al. Review article: volume expansion in patients with cirrhosis. Aliment Pharmacol Ther 2002; 16: 12-23.
71. Arroyo V, Jimenez W. Complications of cirrhosis. II. Renal and circulatory dysfunction. Light and shadows in an important clinical problem. J Hepatol 2000; 32: 157-170.
72. Llach J, Ginès P, Arroyo V, et al. Prognostic value of arterial pressure, endogenous vasoactive systems, and renal function in cirrhotic patients admitted to the hospital for the treatment of ascites. Gastroenterology 1988 ; 94: 482-487.
73. Fernandez-Esparrach G, Sanchez-Fueyo A, Ginès P, et al. A prognostic model for predicting survival in cirrhosis with ascites. J Hepatol 2001; 34: 46-52.

Chapter 2

Aims of the thesis

GENERAL AIM:

To study the role of hepatic stellate cells (HSCs) and vascular mediators in the increased intrahepatic vascular tone, that is commonly associated with cirrhotic PHT.

SPECIFIC AIMS:

Since representative cirrhotic animal models and tools to selectively evaluate IHVR are vital to the study of cirrhotic PHT, we first aimed to characterize and optimize a new animal model of cirrhosis and to study intrahepatic vascular tone in an "in-situ liver perfusion model" (Aim 1).

In a next step, we aimed to further unravel the mechanisms, both cellular and humoral, involved in the pathogenesis of the increased intrahepatic vascular tone (Aim 2) associated with cirrhosis and portal hypertension. Finally, we aimed to assess potential therapeutic utility of these cellular and humoral targets by pharmacological intervention (Aim 3).

Specific aims:

1. To develop a stable, reproducible and homogenous animal model of cirrhosis by the use of the hepatotoxin thioacetamide in order to study hemodynamic characteristics of portal hypertension.
2. To further unravel mechanisms involved in the pathogenesis of the increased hepatic vascular tone associated with cirrhosis

    1.1. The cellular compartment: hepatic stellate cells

    In vitro characterisation of contractile properties of HSCs and pathways involved in their contraction with subsequent assessment of the relevance of these pathways in the perfused cirrhotic rat liver

1.2. The humoral compartment:

1. The impaired intrahepatic vasodilator capacity: a role for an endogenous, circulating nitric oxide synthase inhibitor: asymmetric L-dimethylarginine (ADMA)
2. The excessive intrahepatic vasoconstrictor capacity: a role for thromboxane A_2 (TXA_2), a cyclooxygenase-metabolite

3. To evaluate the effect of NO-donating non-steroidal anti-inflammatory drugs (nitro-NSAIDs) on cirrhotic portal hypertension, a potential new pharmacostrategy: selective hepatic NO donation and TXA_2-inhibition, combining the best of 2 worlds.

Chapter 3

A stable model of cirrhotic portal hypertension in the rat: thioacetamide revisited

adapted from

W. Laleman[1], I. Vander Elst[1], M. Zeegers[1], R. Servaes[1], L. Libbrecht[2], T. Roskams[2], J. Fevery[1] and F. Nevens[1]

Department of Hepatology[1] and Pathology[2],
University Hospital Gasthuisberg, K.U. Leuven, Belgium.

Eur J Clin Invest 2006; 36: 242-249.
Reprinted with permission of Blackwell publishing

1. INTRODUCTION

Cirrhosis is currently ranked as one of the ten most common causes of death in the Western world and remains therefore a major health issue (1). Since ethical considerations limit experimental procedures in humans, there is a need for animal models, mimicking the human situation as closely as possible. Essential for an animal model of cirrhosis is a high degree of resemblance to human cirrhosis, high reproducibility and homogeneity and a low mortality, taking into consideration currently defined Animal Care guidelines. Currently, the carbon-tetrachloride (CCl_4) hepatotoxin-induced model of micronodular cirrhosis, mimicking human non-biliary cirrhosis, is considered the "golden standard" rat model of cirrhosis (2). However, it is associated with major drawbacks such as low reproducibility resulting from a mortality rate that averages 30% during induction, poor homogeneity (meaning that the extent of cirrhosis varied between different intoxicated animals) and a rather low resemblance to human cirrhosis since typical features of human cirrhosis, such as nuclear atypia, mitoses and nodular parenchymal regeneration, resulting in a more typical distorted architecture, are not so prominent. Additionally, inhalation with CCl_4 seems to be the sole way of achieving a high yield of cirrhosis which might pose potential health hazards for the investigator using it (2-5).

A potential alternative to these above-mentioned problems is the induction of cirrhosis in the rat with the hepatotoxin thioacetamide (TAA), which is suggested to have more in common with human cirrhosis (4). The problem with TAA until now was inconsistent production of cirrhosis (varying from 3 to 7 months (6)) when administered orally. To overcome these inconveniences, Li et al. (7) recently suggested an intoxication protocol during 12 weeks which adapts the dose of TAA in drinking water according to the weekly body weight, as originally described for intragastric administration of CCl_4 by Proctor and Chatamra (8). We aimed to reevaluate the TAA model using this protocol and to

investigate the optimal duration of exposure in order to obtain all typical features of portal hypertension, including intrahepatic endothelial dysfunction, and cirrhosis.

2. MATERIALS AND METHODS

2.1. Animal model

Male Wistar rats, weighing 200-250 g, were divided into three groups. For each group, 4 animals served as healthy, age-matched controls. Groups 1 and 2 consisted of 8 animals each, which were intoxicated with TAA (Sigma, Bornem, Belgium) for 6 and 12 weeks respectively, while group 3 (n=10) was given TAA for 18 weeks. From the start and in all groups, the concentration of TAA in the drinking water was 0.03%. Thereafter, concentrations were adapted weekly according to the body weight, aiming to keep individual body weights between the 200 and 250g, as described (7). Practically, TAA concentrations were augmented (decreased) with 50% if the weight increased (decreased) more than 20g weekly or if the overall weight increased (decreased) more than 60g.

2.2. Characteristics

2.2.1. Biochemical analysis

At the end of hemodynamic measurements, blood samples were taken by puncture of the aortic bifurcation and collected in dry or lithium-heparin containing Vacutainer tubes (Becton-Dickinson), depending the need for serum or plasma. Liver (AST, ALT, gamma-glutamyltransferase, alkaline phosphatase, total bilirubin and albumin) and renal function tests (serum Na^+, creatinine, blood urea nitrogen) were assayed by automated procedures.

2.2.2. Histological assessment

Liver biopsies were taken randomly and fixed in Bouin. Afterwards, samples were embedded in paraffin, sectioned and mounted on slides and stained with haematoxylin and eosin or Sirius-red.

2.2.3. Intrahepatic nitric oxide synthase (NOS) activity assay

In the group of 18 weeks intoxication, the conversion of L-^{3}H-arginine to L-^{3}H-citrulline was used to determine NOS activity, as described with slight modifications (9). Briefly, fresh liver was homogenized in buffer (250 mM sucrose; 5 mM $MgCl_2x6H_2O$; TrisHCl 50 mM pH 7.4) to a final concentration of 0.2g wet weight of liver/mL. Samples, containing100 µL of homogenate, were incubated with 100 µL of buffer (40 mM Hepes pH 7.4; 1 mM reduced β-NADPH; 2 mM $CaCl_2$; 12 µM arginine in final amount, containing 0.45 µCi L-2,3-^{3}H-arginine (Dupont Products, Boston, USA)) for 10 min at 37°C. To determine NOS activity, duplicate samples were incubated for 10 min in the presence or absence of N^{G}-nitro-L-arginine-methyl ester (L-NAME, 20mM). The reaction was stopped by 1 mL stop buffer (10 mM EGTA; 1 mM citrulline; 100 mM PIPES pH 5.5). One mL of this mix was then applied to a cation-binding Dowex W50 column (Fluca, Buchs, USA) equilibrated with NaOH till pH 10. The column was eluted with 3 mL distilled water and 12 mL of scintillation fluid was added. Each sample was counted in a Liquid Scintillation Analyser (Tri-Carb-1900, Packard, USA). L-NAME inhibitable activity was determined as specific NOS activity.

2.2.4. In vivo hemodynamic measurements

Measurement of portal pressure and mean arterial pressure (Dataq Instruments, Akron, Ohio, USA) were carried out under pentobarbital anaesthesia (Nembutal, 60mg/mL, Sanofi, Brussels, Belgium) to allow cannulation of the carotid artery (PE-10 tubing, Portex, Kent, UK) and portal vein (Insyte-W 24 Gauge, Becton Dickinson, Erembodegem, Belgium) (10). Additionally in some experiments, mesenteric blood flow (MBF, i.e. flow in the superior mesenteric artery mesenteric blood flow) and the flow through the splenorenal shunt (SRS), were determined by use of a 1-mm non-constrictive perivascular flow probe (1RB, Transonic, Ithaca, USA) connected to a T-206-flow meter (Transonic) (11,12).

2.2.5. In situ liver perfusion

For the investigation of normal hepatic microcirculation and the derangements caused herein by cirrhosis, a **flow-controlled liver perfusion system** was introduced in our lab (with the helpful assistance of Prof. Dr. Garcia-Pagan, Liver Unit, Barcelona) (Fig. 1) (13-15). Briefly, after laparotomy, a ligature was passed around the suprarenal portion of the inferior vena cava. The portal vein was cannulated with a 14G catheter and the liver was perfused with Krebs'solution (NaCl 118mM, KCl 4.7 mM, $MgCl_2$ 1.2mM, NaH_2PO_4 1.2mM, $NaHCO_3$ 25mM, $CaCl_2$ 2.5mM, HEPES 20mM, pH 7.4) pumped (Masterflex, Vernon Hills, IL) from a reservoir into an overflow chamber via a PALL Ultipor filter (Pall, East Hills, USA) and oxygenated via a silastic tubing oxygenator (Sophysa, Nijvel, Belgium) at 37 ± 0.5°C.

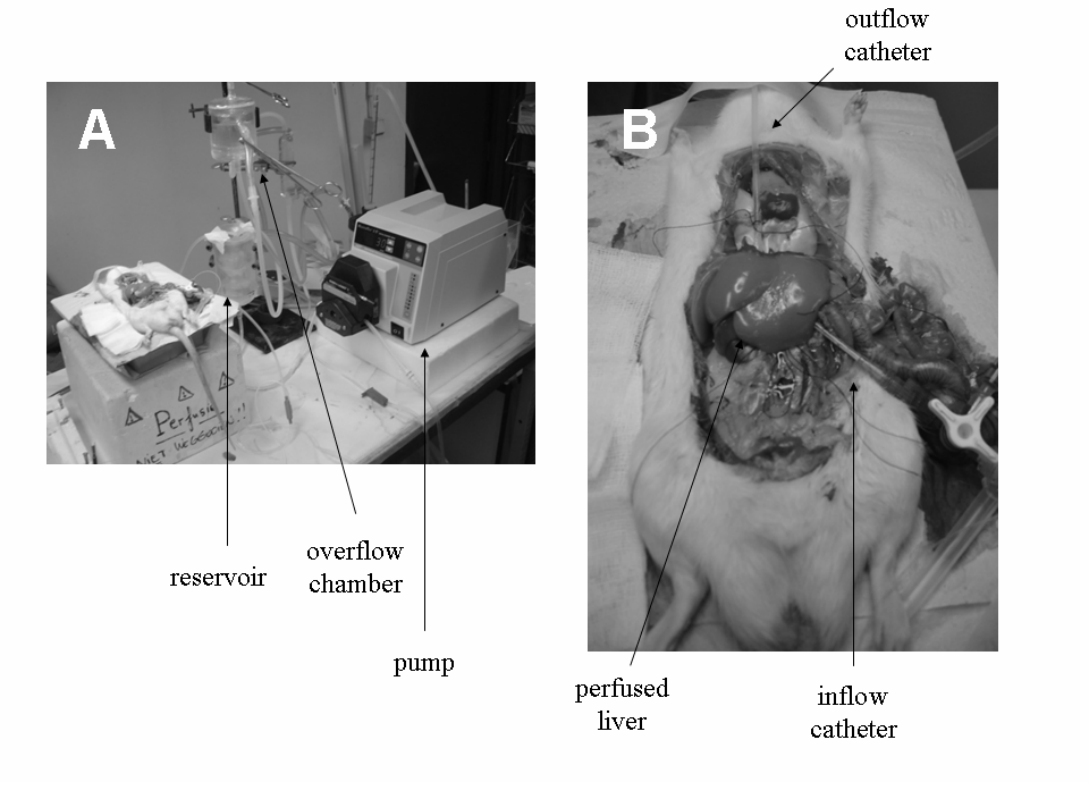


Fig. 1. A & B. In-situ liver perfusion of the rat.

The abdominal aorta and inferior vena cava were cut below the ligature, allowing the exsanguination of the animal and the escape of the perfusate. Following thoracotomy, the right atrium was cannulated (PE-240; Portex, Kent, UK) and the catheter was advanced up to the outlet of the hepatic vein. When the perfused effluent was clear, the system was closed and recirculation was set up with a volume of 150 mL at a constant flow of 35 mL/min. An ultrasonic flow probe (T201, Transonic System) and a pressure gauge were placed in line, immediately upstream of the inlet cannula, to continuously monitor portal flow and perfusion pressure. Another pressure transducer was placed immediately downstream of the outlet cannula for measurement of the ouflow pressure.

Criteria of liver viability included gross appearance of the liver, stable perfusion pressure (starting value ± 1 mmHg) and a stable buffer pH (7.4 ± 0.1) during an initial 30 min stabilization period. If any of the viability criteria were not met, the experiment was terminated.

Total intrahepatic resistance was evaluated by performance of flow-pressure curves.

Endothelial function was assessed by performing concentration-effect curves to cumulative doses of acetylcholine (10^{-7} to 10^{-5} M, one log increase every 1.5 minutes) after a 5 minute precontraction of the liver with the α_1-adrenergic agonist methoxamine 10^{-4} M (13,14).

Responsiveness to vasoconstrictors was documented by performing dose-response curves to cumulative doses of methoxamine (10^{-6} to 10^{-4}M, one log increase every 5 minutes) (15).

2.2.6. Measurement of vasoactive substances

Serum samples were assayed for nitrate/nitrite (NOx), a parameter of NO production, and for 11-dehydro-thromboxane B_2 (11-dehydro-TXB_2), a stabile non-renal- nor thrombocyte-derived metabolite of thromboxane A_2 (TXA_2) (16-19). NOx levels were measured by means of a fluorometric method, using 2,3-diaminonaphtalene (20), whereas levels of 11-

dehydro-TXB_2 were determined by using a commercially available enzyme immunoassay (Caymann Chem, Michigan, USA).

2.3. Statistics

Statistical analysis was performed using SigmaSTAT 2.0 (Jandel, San Rafael, California, USA). Data are given as mean ± SEM. For comparison of multiple groups, analysis of variance (ANOVA) was used, or analysis of variance on ranks (ANOVA-on-ranks) when appropriate. When significant, subsequent multiple comparisons were performed. If only two conditions were compared, the unpaired Student's t-test was used or Mann-Whitney in case of failed normality. The slopes of the different flow-perfusion curves were calculated by regression analysis. *P*-values below 0.05 were considered significant.

3. RESULTS

In the first part of the study we analyzed chronological differences between the different groups with regard to general characteristics, biochemistry, histopathology and hemodynamic alterations with associated changes in vasoactive substances. In the second part, we studied intra- and extrahepatic hemodynamic anomalies typical of cirrhosis in animals intoxicated for 18 weeks.

3.1. The animal model : general characteristics (Table 1)

All control animals survived the study and in the TAA group, there were no deaths after 6 and 12 weeks of intoxication. At 6 weeks of intoxication, except for body weight, no differences were observed compared to control. In 5 repeated series of rats intoxicated for 18 weeks (n=56), 9 rats died (mortality 16%). In the present series of 18 weeks, 1 rat died during anaesthesia. Ascites to a mild degree was present at 18 weeks in 40% of rats.

Table 1: Baseline characteristics of intoxicated versus control rats at 6, 12 and 18 weeks.

	6 weeks		**12 weeks**		**18 weeks**	
	TAA (n=8)	**Control (n=4)**	**TAA (n=8)**	**Control (n=4)**	**TAA (n=9)**	**Control (n=4)**
Body weight (g)	238 ± 9*	412 ± 7*†	237 ± 4*	468 ± 19*†	231 ± 5*	524 ± 7*†
Liver (g/100g b.w.)	4.72 ± 0.32‡	3.83 ± 0.18	5.71 ± 0.45*‡	3.40 ± 0.09*	7.63 ± 0.34*‡	3.35 ± 0.15*
Spleen (g/100g b.w.)	0.28 ± 0.01‡	0.24 ± 0.01	0.39 ± 0.03‡	0.22 ± 0.03	0.59 ± 0.03*‡	0.17 ± 0.01*
APB-t constant	-5.8 ± 1.6*	-17.4 ± 0.2*	-4.4 ± 0.6*	-16.4 ± 2.3*	-4.8 ± 0.79*	-16 ± 5*

Data expressed as mean ± SEM. $^{*}P < 0.05$ vs age-matched control, $^{\dagger}P < 0.05$ vs different control groups, $^{\ddagger}P < 0.05$ 18 vs 6 and 12 weeks.

Abbreviations: TAA, thioacetamide; APB-t constant, aminopyrine breath test constant

3.2. Biochemical analysis

In addition to already raised bilirubin and alkaline phosphatase levels at 6 weeks of TAA, serum biochemical analysis showed decreased albumin levels and raised concentrations of gamma-glutamyltranspeptidase from 12 weeks onwards with an additional marked ALT increase at 18 weeks (Table 2).

Table 2 : Renal and liver function tests in function of duration of intoxication and for each time point compared to healthy controls.

	6 weeks		12 weeks		18 weeks	
	TAA	**Control**	**TAA**	**Control**	**TAA**	**Control**
	(n=8)	**(n=4)**	**(n=8)**	**(n=4)**	**(n=9)**	**(n=4)**
Sodium (mEq/L)	142.7 ± 1.0	142.5 ± 1.5	141.4 ± 1.1	141.7 ± 1.0	143.4 ± 1.5*	137.2 ± 0.06*
Potassium (mEq/L)	4.9 ± 0.3	4.3 ± 0.1	5.2 ± 0.2	4..9 ± 0.2	5.1 ± 0.2	4.9 ± 0.4
Creatinine (mg/dL)	0.54 ± 0.02‡	0.54 ± 0.01	0.58 ± 0.02‡	0.57 ± 0.02	0.64 ± 0.01*‡	0.72 ± 0.02*
Albumin (g/L)	33.5 ± 0.7†	35.2 ± 0.5	29.5 ± 1.1*†	34.1 ± 1.2*	29.5 ± 0.2*†	35.0 ± 0.8*
ALT (IU/L)	62 ± 4‡	68 ± 2	79 ± 6‡	74 ± 4	141 ± 7*‡	79 ± 10*
Alk Phosph (IU/L)	583 ± 43^{*+}	327 ± 35*	702 ± 57*	242 ± 26*	806 ± 40^{*+}	131 ± 73*
γ-GT (IU/L)	3 ± 0.2†	3 ± 0	20 ± 4*†	3 ± 0*	18 ± 2*†	3 ± 0*
Bilirubin (mg/dL)	0.76 ± 0.21*‡	0.1 ± 0*	0.44 ± 0.06*‡	0.1 ± 0*	0.24 ± 0.04*‡	0.1 ± 0*

Data expressed as mean ± SEM. $^{*}P < 0.05$ vs age-matched control, $^{\ddagger}P < 0.05$ 18 vs 6 and 12 weeks, $^{\dagger}P < 0.05$ 18 and 12 weeks vs 6 weeks TAA, $^{+}P < 0.05$ 18 vs 6 weeks TAA.

Abbreviations: TAA, thioacetamide; ALT, alanine aminotransferase; Alk Phosph, alkaline phosphatase; γ-GT, gamma-glutamyltranspeptidase.

3.3. Histopathology

With increasing time of intoxication, the gross appearance of the liver changed from normal over a dull, irregular "salt & pepper" like appearance at 6 weeks, to a nodular and eventually clearly macronodular liver at 12 and 18 weeks, respectively (Fig. 2.A-D).

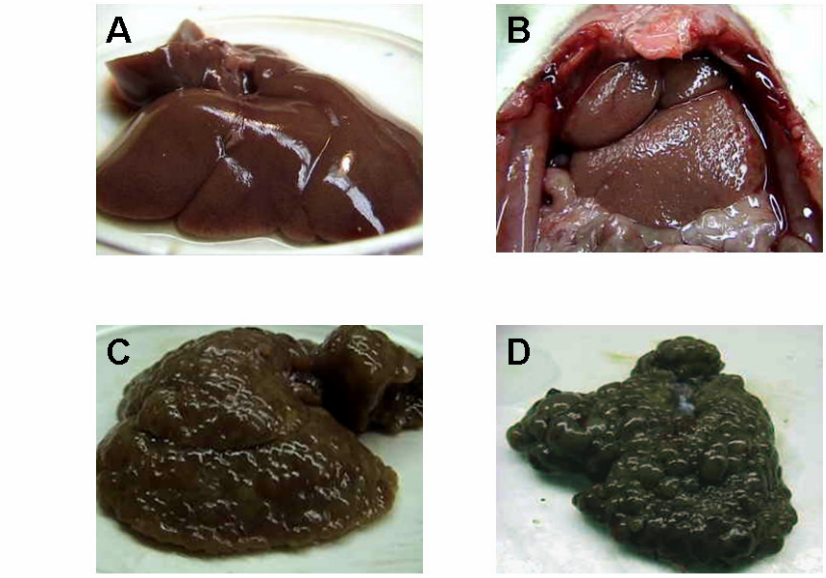


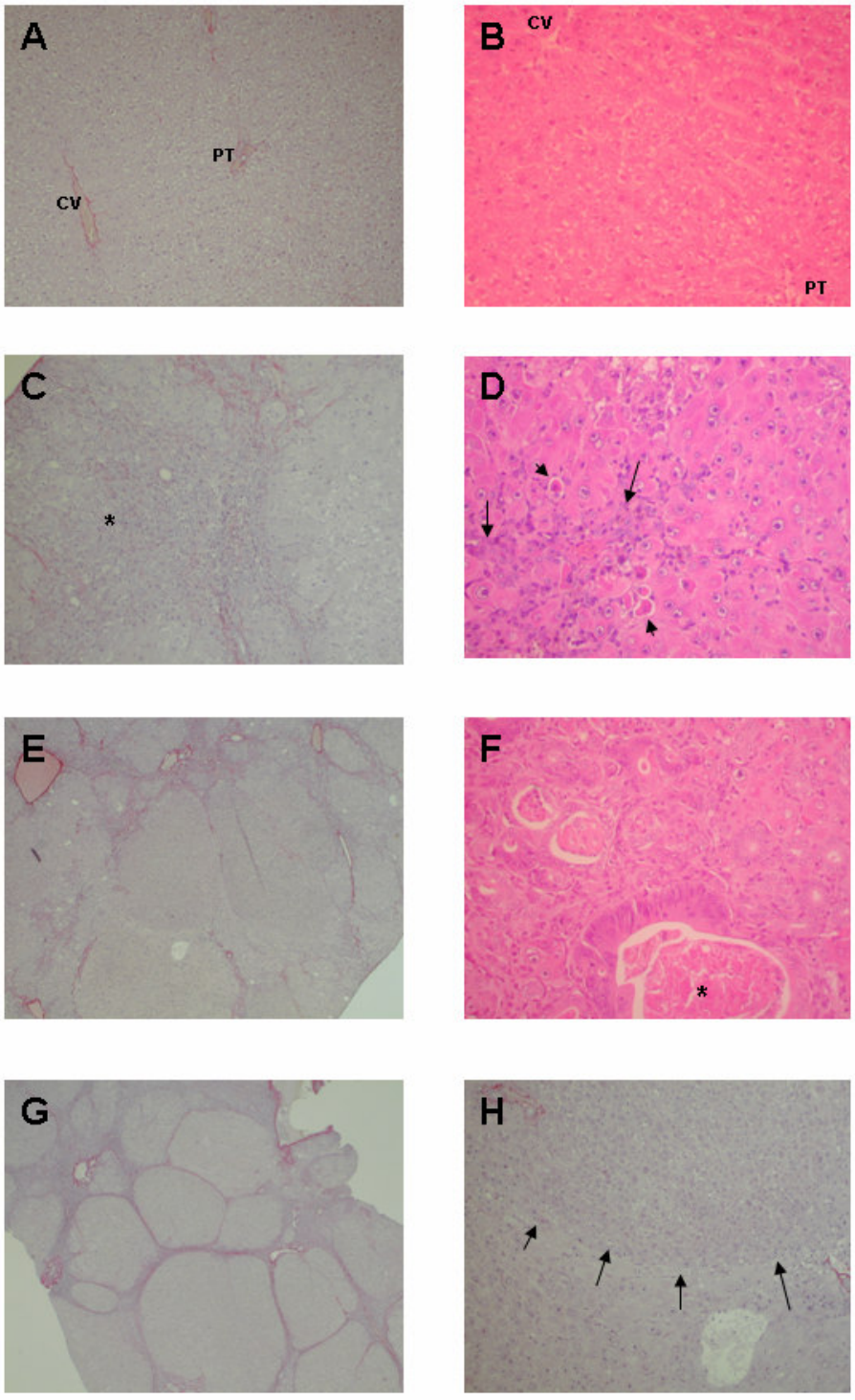
Fig. 2: Macroscopic appearance of livers at different time points of intoxication : Normal liver (A), liver after 6 (B), 12 (C) and 18 weeks of TAA (D).

Microscopical examination (Fig. 3. A-H) showed comparable histopathological changes in the different animals within a group. After 6 weeks of TAA intoxication, Sirius-red stain showed periportal fibrosis (Fig. 3.C). The portal tracts showed a mixed inflammatory infiltrate, consisting of mononuclear and polymorphonuclear leucocytes. At the periphery of the portal tracts, ductular reaction associated with polymorphonuclear leucocytes, resulted in cholangiolitis. The portal vein was patent. The parenchyma showed large cell change (nuclear and cellular enlargement with normal nucleocytoplasmic ratio, sign of replicative senescence), oncocytic change and mitotic figures as a sign of regeneration.

Apopototic bodies of hepatocytes were prominent. Some steatosis was present (Fig. 3.D). At 12 weeks, Sirius-red stain illustrated fine threadery fibrosis with formation of portal-portal and portal-central septa (Fig. 3.E). Small nodules of parenchyma were focally sequestrated. However, most areas were still in an advanced septal stage. The portal tracts showed presence of polymorphonuclear leucocytes in the lumen of interlobular bile ducts, as a sign of cholangitis. In the portal tracts, an excess of tubular ductular structures were present. These ductules showed vacuolisation of their cytoplasm, nuclear anisokaryosis and sometimes basophilia of their cytoplasm. These changes were consistent with dysplastic (premalignant) changes in ductules. At the periphery of the portal tracts strands of small oval cells were seen, not forming tubular structures and clearly different from the larger bile ductular structures in the center of the portal tractcs. Inflammation in the portal tracts was comparable to 6 weeks. The parenchyma showed large cell and small cell change, oncocytic and focal fatty change. These are considered 'dysplastic' changes (Fig. 3.F). In addition, nodule-in-nodule aspect was observed as a sign of high grade dysplasia. In these nodules, rosette formation (reorganisation of hepatocytes into duct-like structures with a lumen) was prevalent. At 18 weeks, fully established cirrhosis was present in all animals (10/10) with formation of portal-central shunts (Fig. 3.G). Expanded portal tracts consisted of ductular structures, showing signs of atypia: nuclear crowding, anisokaryosis, basophilia of cytoplasm. True invasive cholangiocarcinoma was not yet present. Occasional mitotic figures were seen. In the parenchyma, nodule-in-nodule aspect was often present (Fig. 3.H). The parenchyma showed the same dysplastic changes as at 12 weeks, but nodule-in-nodule appearance with signs of high grade dysplasia/early cancer rosette formation, nuclear crowding, large and small cell change, mitotic figures) was much more prevalent.

Fig. 3 : Microscopical examination of livers at different times of intoxication.

A. Sirius-red stain of normal control showing normal liver architecture: PT, portal tract; CV, central vein (original magnification x 25).
B. H&E stain of normal control: PT, portal tract; CV, central vein (original magnification x 100)
C. Sirius-red stain at 6 weeks of TAA intoxication: expansion of portal tracts (asterix) is seen (original magnification x 25).
D. H&E stain after 6 weeks TAA intoxication: expansion of portal tracts by oval cells (ductular) reaction (long arrows). The parenchyma shows many apoptotic bodies (short arrows), anisokaryosis, inflammation and clear cell change (upper middle of figure) (original magnification x 160).
E. Sirius-red stain at 12 weeks of TAA intoxication showing advanced septal fibrosis with early nodule transformation (original magnification x 25).
F. H&E stain at 12 weeks showing a portal tract with tubular ducts and ductules. Some (asterix) show high-grade dysplastic changes, high nucleocytoplasmic ratio, crowding of nuclei and mitotic figures) (original magnification x 160).
G. Sirius-red stain at 18 weeks of TAA intoxication showing fully established cirrhosis (original magnification x 25).
H. Sirius-red stain at 18 weeks of TAA intoxication illustrating “nodule in nodule” formation (arrows). Upper part is high-grade dysplastic nodule with compact growth pattern, while the lower part shows surrounding parenchyma with lower nucleocytoplasm index and “large cell change” (original magnification x 100).


A
PT
CV
B
CV
PT
C
*
D
E
F
*
G
H

3.4. Hemodynamic characterization

Cirrhogenesis was paralleled by development of the portal hypertensive syndrome. At 6 weeks of intoxication, there were no signs of portal hypertension nor of systemic hypotension, as compared to age-matched controls. In contrast, portal hypertension was clearly present after 12 weeks (11 ± 0.4 vs 5.9 ± 0.4 mmHg, $P<0.001$, n=8) and 18 weeks (12.1 ± 0.8 vs 5.6 ± 0.5 mmHg, $P<0.001$, n=9) (Fig. 4), which was associated with splenomegaly at these same time points (Table 1).

Mean arterial pressure at 12 weeks was still comparable to controls (P =0.350), while at 18 weeks systemic hypotension was present compared to age-matched controls (88 ± 8 vs 137 ± 4 mmHg, P=0.008, n=9) (Fig. 5) as well as compared to 6 and 12 weeks TAA (n=8 each, $P<0.05$ vs 18 weeks).

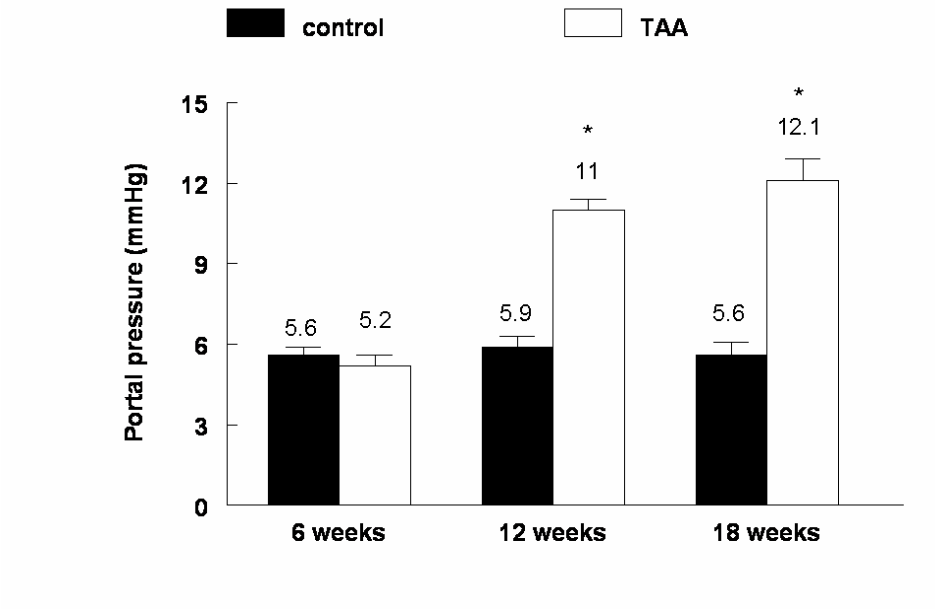


Fig. 4. Evolution of portal pressure in the different groups

*P < 0.001 vs control and TAA 6 weeks

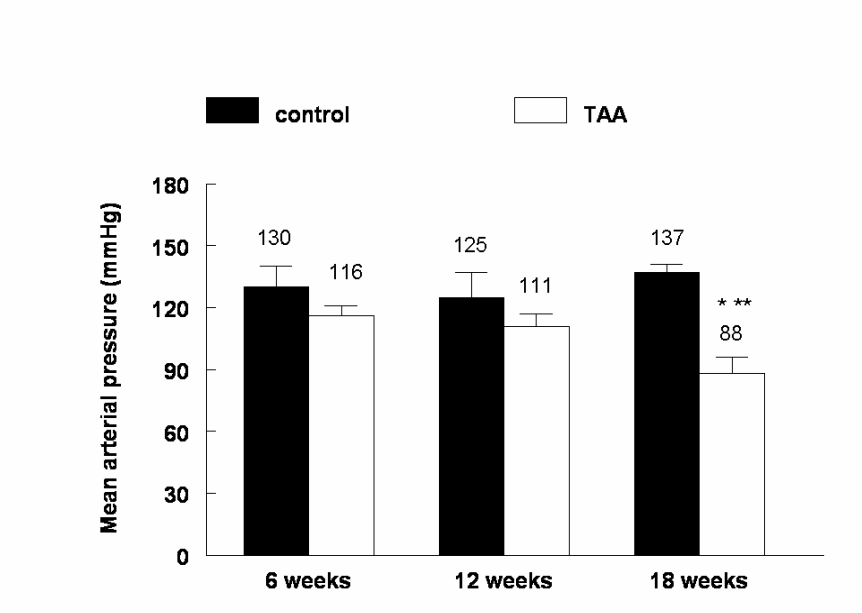
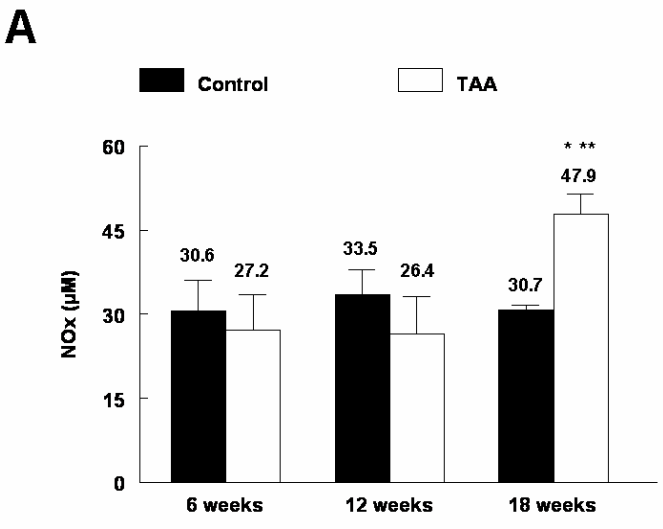


Fig. 5. Evolution of mean arterial pressure in the different groups

*$P < 0.001$ vs control, **$P < 0.05$ vs 6 and 12 weeks TAA

Increased levels of nitrate/nitrite (NOx) (Fig. 6.A), a parameter of NO production, and of 11-dehydro-TXB_2 (Fig. 6.B), a stable non-platelet-derived metabolite of TXA_2, paralleled the hemodynamic measurements.



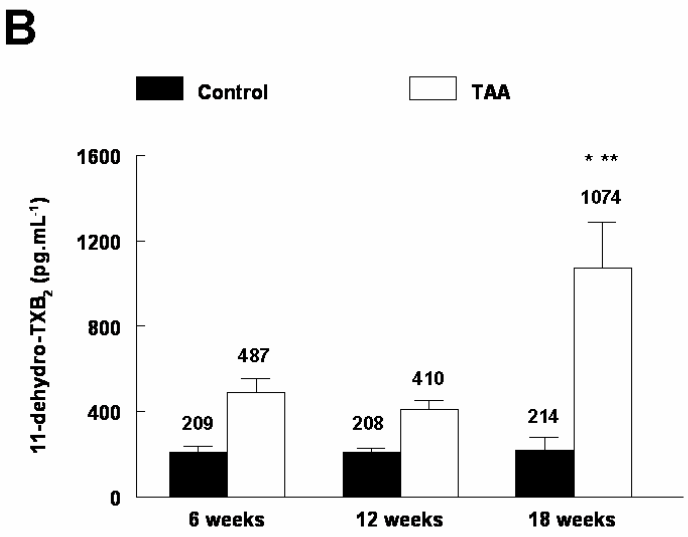
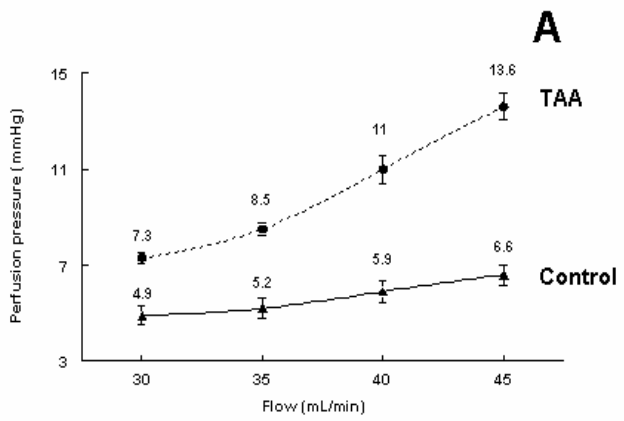
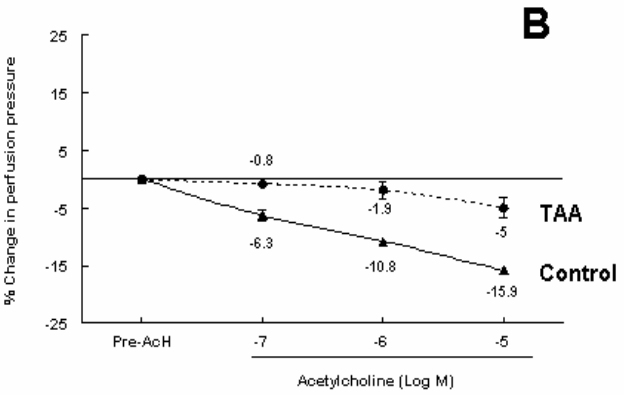


Fig. 6: Levels of vasoactive substances: NO products (NOx; NO^{2-} and NO^{3-}) (A) and 11-dehydro-TXB_2 (stable end metabolite of TXA_2) (B) with increasing duration of TAA administration vs controls. *$P < 0.05$ vs age-matched controls, **$P < 0.05$ 18 vs 6 and 12 weeks of TAA.

3.5. Evaluation of intra- and extrahepatic hemodynamic parameters at 18 weeks TAA.

In cirrhotic animals, an increased total intrahepatic vascular resistance was found since the increase in perfusion pressure at each flow rate and the pressure-flow slope (0.48 ± 0.03 vs 0.09 ± 0.02 [cirrhosis vs co], $P<0.001$) were significantly greater than in control rats (Fig. 7.A). Additionally, cirrhotic livers exhibited a significantly lower relaxation to cumulative doses of acetylcholine (Fig. 7.B) and a hyperresponsiveness to methoxamine (Fig. 7.C).


A
Perfusion pressure (mmHg)
15
11
7
3
13.6
11
8.5
7.3
6.6
5.9
5.2
4.9
TAA
Control
30
35
40
45
Flow (mL/min)


B
% Change in perfusion pressure
25
15
5
-5
-15
-25
-0.8
-1.9
-5
-6.3
-10.8
-15.9
TAA
Control
Pre-AcH
-7
-6
-5
Acetylcholine (Log M)

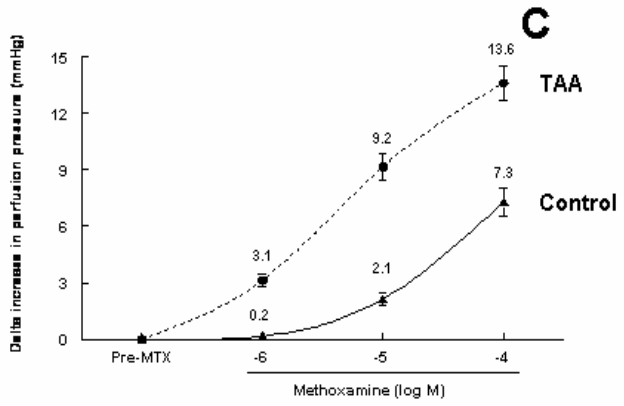

C
Delta increase in perfusion pressure (mmHg)
15
12
9
6
3
0
13.6
9.2
7.3
3.1
2.1
0.2
TAA
Control
Pre-MTX
-6
-5
-4
Methoxamine (log M)

Fig. 7: Evaluation of intrahepatic hemodynamic parameters through in-situ liver perfusion at 18 weeks TAA versus control. A. Flow-perfusion curve. The increase in perfusion pressure was greater in cirrhotic animals as demonstrated by a significantly greater perfusion pressure at each flow rate ($P < 0.001$ cirrhotic vs normal liver, n=5 each). B. Endothelial function assessment showing significantly less vasorelaxation in cirrhotic livers as compared to control livers following cumulative doses of acetylcholine 10^{-7} to 10^{-5}M ($P < 0.001$, n=5 each). C. Responsiveness to vasoconstrictors, illustrating a hyperresponse in cirrhotic livers compared to normal liver following cumulative doses of methoxamine 10^{-6} to 10^{-4}M ($P < 0.001$, n=5 each).

The impaired vasorelaxation capacity in cirrhotic rats was further supported by the in vitro documentation of decreased specific NOS activity in these same rats (1.1 ± 0.2 pmol/mg protein/minute vs 3.6 ± 0.4 pmol/mg protein/minute , $P<0.001$).

Extrahepatically, we detected the presence of splanchnic hyperemia and increased splenorenal shunting (Fig. 8).

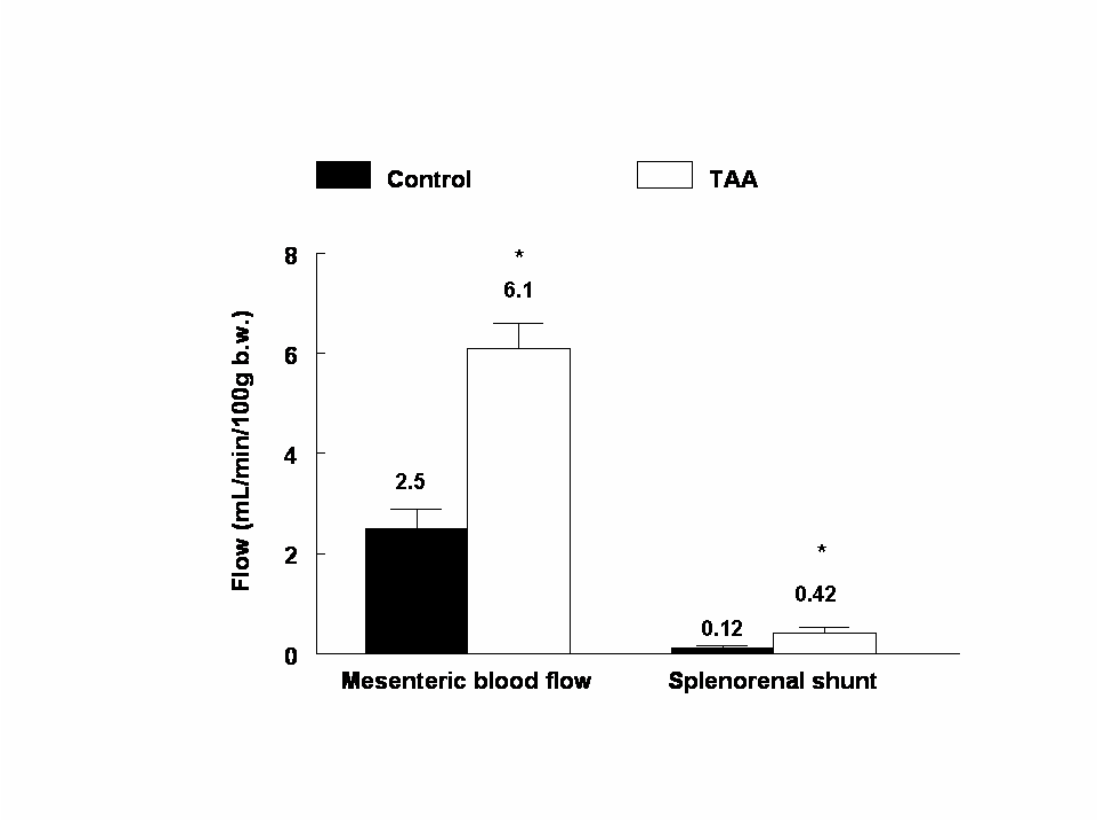


Fig. 8: Difference in flow in the superior mesenteric artery (MBF, mesenteric blood flow) and in the splenorenal shunt (SRS) after 18 weeks TAA vs controls (n=6 each) (*$P < 0.05$ vs control).

4. DISCUSSION

TAA is a long-known hepatotoxin, which through bioactivation by the mixed function oxidase system to acetamide and thioacetamide-S-oxide, and eventually the hyperreactive thioacetamide-S-dioxide, causes centrilobular necrosis and ultimately cirrhosis (21-23). Administrating TAA via drinking water is an easy, atraumatic and inexpensive method and largely attains the intended target, namely the liver, thereby limiting extrahepatic toxicity in contrast to intraperitoneal or subcutaneous injection and inhalation. Although effective, the main drawback until now has been the heterogeneous production of cirrhosis, which was recently overcome by Li (7) by individualizing the dose of TAA to weekly weighed body weight during 12 weeks, resulting in a homogenous and reproducible model. However, since we could neither find the presence of cirrhosis in all animals nor the typically associated hyperdynamic state during this 12 week protocol, we aimed to chronologically reevaluate the model by focusing on cirrhogenesis and additionally associated features of portal hypertension.

In the present model the development of cirrhosis presents as a multi-step process starting off histopathologically with hepatitis at 6 weeks, proceeding to a stadium of advanced septal fibrosis at 12 weeks and finally to cirrhosis at 18 weeks. Only at 18 but not 12 weeks, as reported by Li (7), the full spectrum of histological alterations typical of cirrhosis was observed: parenchymal cell damage and death, nodular parenchymal regeneration, resulting in distorted architecture, and complete fibrous vascularized septa, the hallmark of the 'true cirrhotic state' (24,25). In addition, administration of TAA also led to the emergence of dysplasia, a premalignant change frequently seen in human chronic liver disease (estimated to be present in 82% of cirrhotic livers (26)) and considered causative of hepatocellular carcinoma and cholangiocarcinoma (27-29). In our model, severe dysplasia of both cholangiocytes and hepatocytes was observed after 18 weeks of intoxication. With

regard to hepatocyte dysplasia, both large-cell and small-cell dysplastic foci were noted and low and high grade dysplastic nodules. We also documented an evolution from dysplastic foci at 6 weeks over dysplastic nodules at 12 weeks to highly prevalent high-grade dysplastic nodules at 18 weeks (29). Therefore, the TAA model might be useful in studies unravelling molecular and morphological features of preneoplastic lesions and hepato- and cholangio-carcinogenesis during an exposure of at least 18 weeks.

Biochemically, in contrast to previously reported (7), we observed a gradual decrease in liver synthetic capacity over time, associated with progressive cholestasis and hepatocellular injury, features typical of decompensated cirrhosis in humans (30).

The proposed model also resulted in a stable model of intrahepatic portal hypertension with the typical hyperdynamic circulation. At 6 weeks no differences were noticeable with regard to portal and systemic pressure, whereas at 12 weeks portal pressure was elevated but without affecting systemic pressure, contrasting earlier documented findings (7). At 18 weeks portal hypertension was associated with arterial hypotension, suggesting reduced peripheral vascular resistance (2,31-33). The increasing splenomegaly further supported the progressive development of the portal hypertensive syndrome over time (34). We have to mention that these measurements were done under pentobarbital-anesthesia, which occasionally can cause altered systemic hemodynamics, suppression of the sympathic nervous system and reduction of renal blood flow (10). On the other hand, more and more ethical committees on animal research consider the performance of invasive hemodynamic measurements in freely moving awake animals as unethical.

Additionally at 18 weeks, we demonstrated the presence of increased total intrahepatic vascular resistance since perfusion pressure rose in parallel with increasing flow while in normal liver the perfusion pressure remained stable over the range of flow rates used.

Although, anatomical abnormalities, as described above, are the main cause of the

increased vascular resistance to portal blood flow through the cirrhotic liver, enhanced intrahepatic vascular tone has also been demonstrated in cirrhotic patients (35) and other cirrhotic rat models (36). Hyperresponsiveness of the hepatic vascular bed to increased locally or systemically produced vasoconstrictors, amongst others TXA_2, exaggerated by impaired production and/or availability of vasodilators, mainly nitric oxide, constitute the major intrinsic mechanisms for the increased vascular tone in cirrhosis (31-33,37-41). In our model, at 18 weeks of TAA, we could confirm the presence of both this exaggerated response to vasoconstrictors and endothelial dysfunction. These findings were further reinforced by decreased hepatic NOS activity and elevated serum levels of TXA_2, in agreement with current literature (31-33,37-41). With regard to the splanchnic and systemic hemodynamic dysfunction, we confirmed that at week 18 the arterial hypotension in this cirrhotic rat model was associated with splanchnic hyperemia and increased portosystemic shunting. Moreover, these hemodynamic anomalies were associated with increased systemic levels of NO, a key pathogenetic molecule in this context (41).

In conclusion, we demonstrated that TAA, adapted to weekly changes of body weight, should be given for 18 weeks in rats in order to obtain a homogeneous and reproducible model of macronodular cirrhosis associated with the typical histological, biochemical and hemodynamic changes seen in man. Therefore, TAA might represent a good alternative for the CCl_4-model, to study a variety of aspects of chronic liver disease.

5. REFERENCES

1. Stewart SF, Day CP. The management of alcoholic liver disease. J Hepatol 2003;38(Suppl): 2-13.
2. Lee FY, Groszmann RJ. Experimental models in the investigation of portal hypertension. Ascites Ren Dysfunct Liv Dis Pathog Diagn Treat 1999;1: 365-378.
3. Dashti H, Jeppsson B, Hägerstrand I, et al. Thioacetamide- and carbon tetrachloride-induced liver cirrhosis. Eur Surg Res 1989;21: 83-91.
4. Ariosto F, Riggio O, Cantafora A, et al. Carbon tetrachloride-induced experimental cirrhosis in the rat: a reappraisal of the model. Eur Surg Res 1989;21: 280-286.
5. Colombato LA, Robin M, Pomier-Layrargues G, Huet PM. Animal models of portal hypertension. In: Holstege A, Hahn EG, Scholmerich J, eds. Portal hypertension – Proceedings of the 79th Falk Symposium. Kluwer Academic Publishers, 1995: 3-14.
6. Petermann H, Vogl S, Schulze E, Dargel R. Chronic liver injury alters basal and stimulated nitric oxide production and 3H-thymidine incorporation in cultured sinusoidal endothelial cells from rats. J Hepatol 1999;31: 284-292.
7. Li X, Benjamin IS, Alexander B. Reproducible production of thioacetamide-induced macronodular cirrhosis in the rat with no mortality. J Hepatol 2002;36: 488-493.
8. Proctor E, Chatamra K. High yield micronodular cirrhosis in the rat. Gastroenterology 1982;83: 1183-1190.
9. Shah V, Cao S, Hendrickson H, Yao J, Katusic ZS. Regulation of hepatic eNOS by caveolin and calmodulin after bile duct ligation in rats. Am J Physiol Gastrointest Liver Physiol 2001; 280: G1209-1216.
10. Van Roey G, Lijnen P, Verbesselt R, Verbruggen A, Fevery J. Effect of narcotic agents and bleeding on systemic and renal hemodynamics in healthy and CCl4-treated cirrhotic rats. Clin Sci 1997; 93: 549-556.
11. Calès P, Oberti F, Veal N, et al. Splenorenal shunt blood flow by transit time ultrasound as an index of collateral circulation in portal hypertensive rats. Hepatology 1998; 28: 1269-1274.
12. Fernandez M, Garcia-Pagan JC, Casadevall M, et al. Acute and chronic cyclooxygenase blockade in portal-hypertensive rats: influence on nitric oxide biosynthesis. Gastroenterology 1996; 110: 1529-1535.
13. Gupta TK, Toruner M, Chung MK, Groszmann RJ. Endothelial dysfunction and decreased production of nitric oxide in the intrahepatic microcirculation of cirrhotic rats. Hepatology 1998; 28: 926-931.
14. Graupera M, Garcia-Pagan JC, Pares M, Abraldes JG, Rosello J, Bosch J, Rodes J. Cyclooxygenase-1 inhibition corrects endothelial dysfunction in cirrhotic rat livers. J Hepatol 2003; 39: 515-521.
15. Graupera M, Garcia-Pagan JC, Abraldes JG, et al. Cyclooxygenase-derived products modulate the increased intrahepatic resistance of cirrhotic rat livers. Hepatology 2003; 37: 172-181.
16. Lawson, J.A., Patrono, C., Ciabattoni, G.*, et al.* Long-lived enzymatic metabolites of thromboxane B_2 in the human circulation. Anal Biochem 1986;155:198-205.
17. Metabolism of thromboxane B2 in man. Identification of twenty urinary metabolites. Roberts LJ, Sweetman BJ, Oates JA. J Biol Chem 1981;25;256:8384-8393.
18. Roberts, L.J., II, Sweetman, B.J., Payne, N.A., et al. Metabolism of thromboxane B_2 in Man. Identification of the major urinary metabolite. J Biol Chem 1977;252:7415-7417.
19. Westlund, P., Granström, E., Kumlin, M., et al. Identification of 11-dehydro-TXB_2 as a suitable parameter for monitoring thromboxane production in the human. Prostaglandins 1986;31:929-960.
20. Wink DA, Grisham MB, Miles MA, Nims RW, Kusha MC, Pacelli R, Teague D. Determination of selectivity of reactive nitrogen oxygen species for various substrates. Meth Enz 1996; 268: 120-130.
21. Chieli E, Malvaldi G. Role of the microsomal FAD-containing monooxygenase in the liver toxicity of thioacetamide-S-oxide. Toxicology 1984;31: 41-52.
22. Brodehl J. Thioacetamid in der experimentellen Leberforschung. Klin Wschr 1961;39: 956-62.
23. Porter WR, Neal RA. Metabolism of thioacetamide and thioacetamide-S-oxide by rat liver microsomes. Drug Metab Dispos 1978;6: 379-388.
24. Desmet VJ, Roskams T. Cirrhosis reversal: a duel between dogma and myth. J Hepatol 2004;40: 860-867.
25. Roskams T, Baptista A, Bianchi L, et al. Histopathology of portal hypertension: a practical guideline. Histopathology 2003;42: 2-13.
26. Le Bail B, Bernard PH, Carles J, Balabaud C, Bioulac Sage P. Prevalence of liver cell dysplasia and association with HCC in a series of 100 cirrhotic liver explants. J Hepatol 1997;27: 835-842.
27. Libbrecht L, Desmet V, Roskams T. Preneoplastic lesions in human hepato-carcinogenesis. Liver International 2005;25: 1-12.

28. Kojiro M, Roskams T. Early hepatocellular carcinoma and dysplastic nodules. Semin Liver Dis 2005;25: 133-142.
29. Libbrecht L, Desmet V, Vandamme B, Roskams T. The immunohistochemical phenotype of dysplastic foci in human liver: correlation with putative progenitor cells. J Hepatol 2000;33: 76-84.
30. Sherlock S, Dooley J. Hepatic cirrhosis. In: Sherlock S, Dooley J, editors. Diseases of the liver and biliary system. Oxford, Blackwell publishing; 2002. p. 365-380.
31. Bosch J, Garcia-Pagan JC. Complications of cirrhosis. I. Portal hypertension. J Hepatol 2000; 32(S1): 141-156.
32. Arroyo V, Jimenez W. Complications of cirrhosis. II. Renal and circulatory dysfunction. Lights and shadows in an important clinical problem. J Hepatol. 2000;32 (Suppl 1): 157-170.
33. Laleman W, Van Landeghem L, Wilmer A, Fevery J, Nevens F. Portal hypertension: from pathophysiology to clinical practice. Liver Int 2005;25: 1079-1090.
34. Bolognesi M, Merkel C, Sacerdoti D, Nava V, Gatta A. Role of spleen enlargement in cirrhosis with portal hypertension. Dig Liver Dis 2002;34: 144-150.
35. Navasa M, Chesta J, Bosch J, Rodes J. Reduction of portal pressure by isosorbide-5-mononitrate in patients with cirrhosis. Effects on splanchnic and systemic hemodynamics and liver function. Gastroenterology 1989;96: 1110-1118.
36. Bhathal PS, Grossman HJ. Reduction of the increased portal vascular resistance of the isolated perfused cirrhotic rat liver by vasodilators. J Hepatol 1985;1: 325-337.
37. Graupera M, Garcia-Pagan JC, Pares M, et al. Cyclooxygenase-1 inhibition corrects endothelial dysfunction in cirrhotic rat livers. J Hepatol. 2003;39: 515-521.
38. Pinzani M, Milani S, De Franco R, et al. Endothelin 1 is overexpressed in human cirrhotic liver and exerts multiple effects on activated hepatic stellate cells. Gastroenterology 1996;110: 534-548.
39. Rockey DC, Chung JJ. Reduced nitric oxide production by endothelial cells in cirrhotic rat liver: endothelial dysfunction in portal hypertension. Gastroenterology 1998;114: 344-351.
40. Van De Casteele M, Van Pelt JF, Nevens F, Fevery J, Reichen J. Low NO bioavailability in CCl4 cirrhotic rat livers might result from low NO synthesis combined with decreased superoxide dismutase activity allowing superoxide-mediated NO breakdown: A comparison of two portal hypertensive rat models with healthy controls. Comp Hepatol 2003;2: 2.
41. Wiest R, Groszmann RJ. The paradox of nitric oxide in cirrhosis and portal hypertension: too much, not enough. Hepatology 2002;35: 478-491.

Chapter 4

Both Ca^{2+}-dependent and -independent pathways are involved in rat hepatic stellate cell contraction and intrahepatic hyperresponsiveness to methoxamine.

adapted from

W. Laleman[1], L. Van Landeghem[1], T. Severi[1], I. Vander Elst[1], M. Zeegers[1], R. Bisschops[2], J. Van Pelt[1], T. Roskams[3], D. Cassiman[1], J. Fevery[1] and F. Nevens[1].

Department of Hepatology[1], Gastroenterology[2], Histopathology[3],

University Hospital Gasthuisberg, K.U. Leuven, Belgium.

Am J Physiol Gastrointest Liver Physiol. 2006, in press

1. INTRODUCTION

During chronic liver injury, hepatic stellate cells (HSCs) undergo a process of activation from a quiescent "storing" to a highly proliferative "myofibroblast-like" phenotype. Besides a fibrogenic response, this activation process also leads to the acquisition of enhanced contractile properties. Both the scarrification process as the increased contractility of HSCs have been implicated in the increased intrahepatic vascular resistance to portal flow, but especially the recognition that hypercontractile HSCs participate in the increased intrahepatic vascular tone, provide the rationale for targeting these cells for the treatment of portal hypertension in advanced chronic liver disease (1-3). Due to the expression of smooth muscle proteins and the strategic anatomical location around hepatic sinusoids, a resemblance to pericytes or vascular smooth muscle cells has been proposed, leading to the assumption of a "smooth muscle-like" contraction pattern (1,3-5). Yet this supposed "smooth muscle-like" contraction pattern of activated HSCs conflicts with the presumed transition to a "myofibroblast-like" activated HSC phenotype. In smooth muscle cells, contraction is mainly powered by Ca^{2+} -dependent myosin activation. Increased intracellular Ca^{2+}-levels, either via inositol triphosphate (IP_3) or Ca^{2+} influx through L-type channels, give rise to the activation of the Ca^{2+}/calmodulin-dependent myosin light chain kinase (MLCK), which in turn results in increased phosphorylation of the regulatory light chain of myosin (rMLC). Phosphorylation of rMLC allows the myosin ATPase to be activated by actin, leading to actomyosin cross-bridging and cell contraction (6,7). In non-muscle cells, including activated HSCs, increased phosphorylation of rMLC has also been correlated with increased contractility (8,9). However, in contrast to smooth muscle cells, several studies favour non-Ca^{2+}-dependent contraction pathways as the key event in force generation by myofibroblasts, of which the rho-A signalling and protein kinase C dependent pathways are the most relevant (10-12). Both of these pathways inhibit myosin

light chain phosphatase (MLCP) activity, leading to delayed degradation of phosphorylated rMLC and thus promoting contraction (7,10).

Since the contribution of these different pathways are not yet fully elucidated for HSC contraction, we therefore aimed 1) to define the relative role of Ca^{2+}-dependent and -independent pathways in the actomyosin interaction of HSCs (Fig. 1), using a three-dimensional stress-relaxed-collagen-lattice contraction model, 2) to compare the degree of Ca^{2+}-dependency of vascular smooth muscle cells, cardiac myofibroblasts and activated hepatic stellate cells and 3) to determine the relevance of these in vitro findings in the increased intrahepatic vascular resistance (IHVR) associated with thioacetamide-induced cirrhosis in the rat.

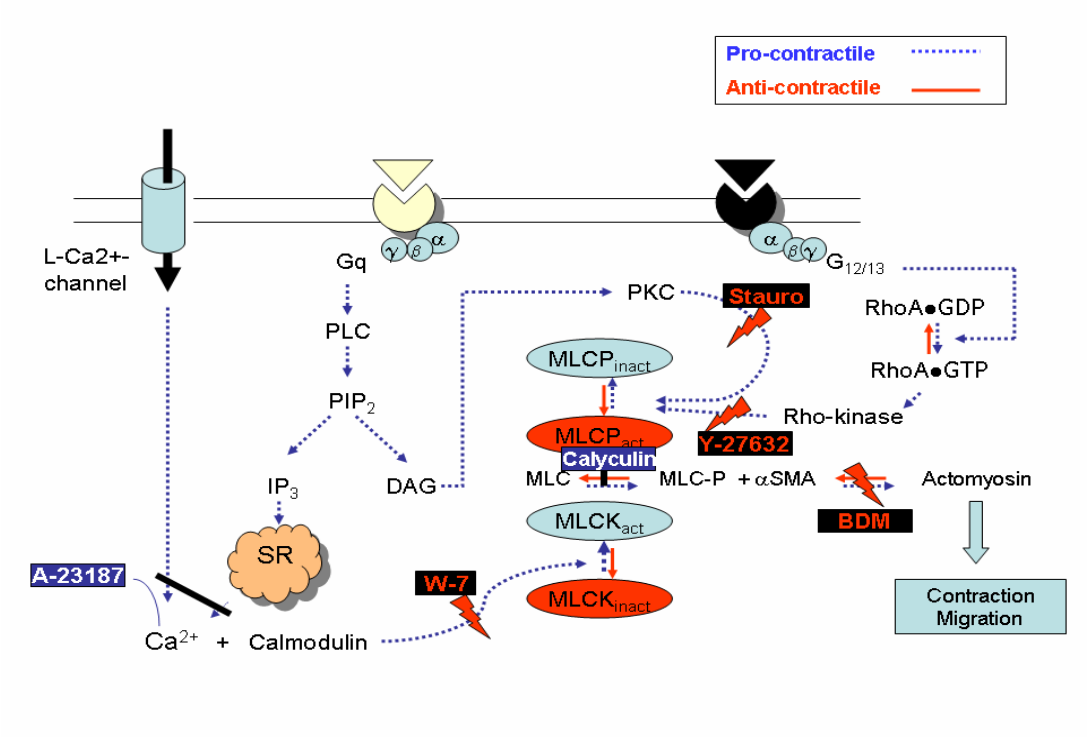


Fig. 1: Proposed model for the regulation of agonist-promoted hepatic stellate cell contraction. Actomyosin interaction is determined by the interaction between α-smooth muscle actin (α-SMA) and the phosphorylated myosin light chain (MLC-P). Phosphorylation of MLC is regulated by myosin light chain kinase (MLCK), which is

activated by Ca^{2+}-dependent pathways, involving increased intracellular Ca^{2+} and calmodulin. On the other hand, inactivation of myosin light chain phosphatase (MLCP), regulated by the Ca^{2+}-independent protein kinase C (PKC) and Rho-kinase, also leads to sustained phosphorylated MLC and therefore increased contraction. The site-specific inhibitors and agonist used in the study are also mentioned in this model: A-23187, a Ca^{2+} -ionophore; W-7, a calmodulin-mediated MLCK-inhibitor; stauro (staurosporin), a PKC-inhibitor; Y-27632, a Rho-kinase-inhibitor; calyculin, a MLCP-inhibitor; BDM (2,3-butanedione 2-monoxim), a nonmuscle myosin ATPase-inhibitor.

2. MATERIAL AND METHODS

2.1. Cell isolation and culture

Rat hepatic stellate cells were ***isolated*** using a sequential collagenase type IV (Sigma , St. Louis, MO) and pronase E (Merck,Darmstadt, Germany) perfusion technique (13-15). Purification was obtained by density gradient centrifugation using Optiprep 9% (harvesting density <1.053) (Nycomed, Sweden) (13,14). Viability was routinely over 95%, as determined by trypan blue exclusion. Purity was assessed by phase-contrast microscopy after 24-48 h of culture on plastic and showed large proportions of typical HSC (homogeneous cultures of stellate-shaped cells, > 30% containing cytoplasmic lipid droplets) (Fig. 2.A). The cells were seeded on uncoated plastic culture dishes and cultured in William's E medium (Gibco, Belgium) supplemented with 10% FCS, 0.6 IU/mL insulin, 2mM glutamine and 1% antibiotic –antimycotic solution. The medium was renewed every 48 hours. Characterization of in vitro activated rat hepatic stellate cell (or myofibroblast-like) cultures, established by culturing enriched HSC fractions on plastic, was performed by staining with anti-α-smooth muscle actin (α-SMA) (Fig. 2.B-C), anti-desmin and

synaptophysin, which have been shown to be characteristic and highly specific expression markers of HSCs in both the fibrotic rat and human liver (helpful assistance Prof. T. Roskams) (13,15). Experiments were performed between the first and third passage (1:3 split ratio) using three independent cell lines.

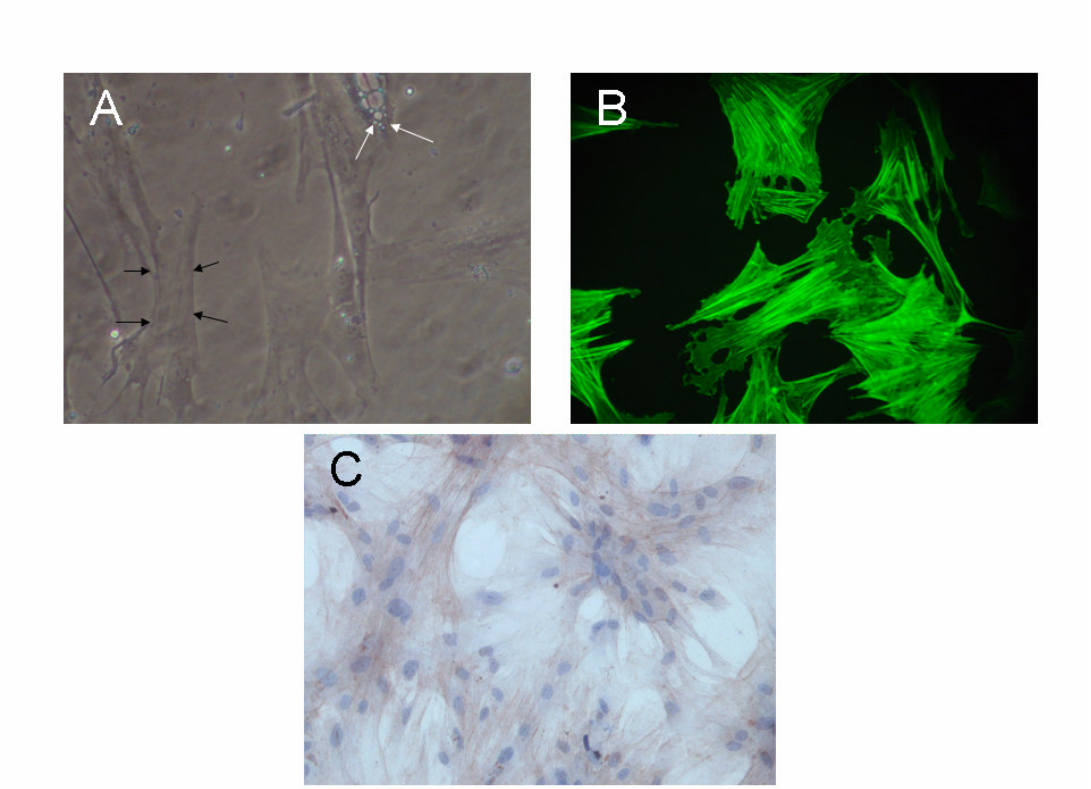


Fig. 2: Characterization of "culture-activated" hepatic stellate cells.

A. Phase-contrast microscopy after 24-48 h of culture on plastic showing elongated stellate shaped cells (black arrows) with the presence of minimal cytoplasmic lipid droplets (white arrows) (original magnification x 200), B. and C. Illustration of the presence of α-smooth muscle actin, a highly-specific marker of HSCs, by a phalloidin-probe, (B) and immunohistochemistry (C), respectively (both original magnification x 200).

Rat cardiac ventricular myofibroblasts and rat aortic vascular smooth muscle cells were a gift of Dr. V. Petrov (Department of Molecular and Cardiovascular research, K.U.L.) and Prof. Dr. S. Janssen (Center for Transgene Technology and Gene Therapy, K.U.L), respectively (16,17).

2.2. Three-dimensional stress-relaxed collagen lattice contraction model

For the study of HSC contraction capacity in vitro, we used a *three-dimensional hydrated collagen lattice model*. At present, this provides the most potent model *in vitro* to examine the reciprocal mechanical interactions that occur between cells and the extracellular matrix, and how these can influence the formation and function of the myofibroblast (18-22). Endogenous tension (also called pre-stress) can be generated in the collagen matrix by tethering the lattice (Fig. 3). Once this pre-stress is established, it is maintained at a relatively constant level over long periods of time. If the collagen lattice is released from its points of attachment - such that stress in the matrix is lost - the cells rapidly contract and subsequently lose their stress fibres and fibronexus adhesion complexes.

Practically, hydrated collagen gels were prepared using rat tail tendon collagen I (Becton-Dickinson, Bedford, MA), adjusted to physiological strength and pH with 1 N NaOH and 10xPBS at 4°C. Afterward, the collagen solution was mixed with a HSC suspension so that the final solution resulted in a collagen concentration of 1.5 mg/mL and 250000 cells/mL. A 500µl aliquot of the collagen solution was then cast into a 24-well tissue culture plate (Falcon, Meylan, France) and covered after 1 hour with culture medium (1mL/well) in order to ascertain adequate gelation. Afterward, the polymerized collagen matrix containing HSCs remained attached to the culture dish for 24 hours leading to mechanical loading ("stressed"), as such mimicking the in vivo geometric and mechanical conditions of HSCs (19,20,22).

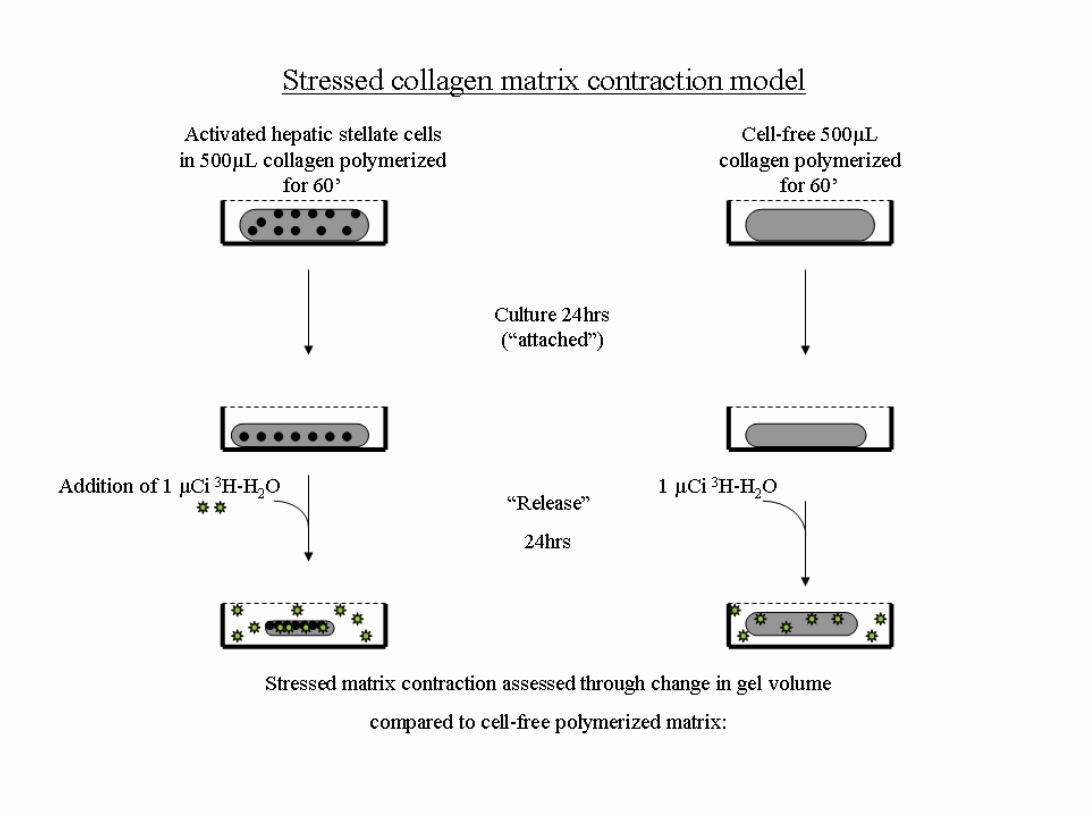


Fig. 3: Principle of the stressed collagen matrix contraction model based on the partioning of tritiated H_2O between gel phase and surrounding medium:

$$CPM_{gel}/V_{gel} = CPM_{medium}/V_{medium}$$

$$V_{med} = 1000\mu L$$

$$\mathbf{V_{gel}\ (\mu L) = [CPM_{gel}/CPM_{med}]*1000}$$

(CPM = counts per minute, measure of amount of ^3H_2O)

Control gels provide estimates for the precontraction volume and allow to express relative changes in volume (% contraction):

$$\mathbf{Contraction\ (\%) = V_{control} - V_{HSCgel}/V_{control} * 100}$$

After 24 hours, stabilized lattices were washed with 1xPBS, followed by addition of 1 mL serum-free culture medium per well containing 1µCi ^3H_2O (Amersham Biosciences, Roosendaal, The Netherlands). To initiate matrix contraction, the mechanically stressed matrices were released by gentle circumferential dislodgement of the lattice ("relaxation"). Cell-mediated contraction was measured by determining the relative partitioning of ^3H_2O

between the gel phase and the surrounding medium following 24 hours of contraction, thereby allowing estimation of gel phase volumes. More specifically, the separate tritium activities of medium and gel phase were measured in 10mL of oscillation fluid (Perkin Elmer) using a TRI-Carb 1900CA liquid scintillation analyser (Packard, Meriden, USA). Control cell-free gels provided estimates for the precontraction volume and allowed us to express relative changes in volume (% contraction). All data are derived from experiments using at least 3 sets of 3 collagen lattices using culture-activated HSCs from 3 different rat HSC isolations. For the experiments comparing contraction of VSMCs, HSCs and cardiac myofibroblasts, the same set-up was used as for HSCs. In these specific experiments, the extent of contraction was expressed relative to fetal calf serum (FCS)-induced contraction in order to allow comparison between cell types.

2.3. Inhibitors and agonists affecting contractility (Fig.1)

Depending on the experiment, FCS 10%, the α_1-adrenergic agonist methoxamine 10^{-4} M (Sigma) or the Ca^{2+}-ionophore A23187 (Sigma) were used as agonists. Mostly, FCS was used because its ease of use, high availability and its ability to elicit an even powerful contraction as endothelin-1 (23). Actomyosin interaction, the end-target of both Ca^{2+}-dependent and Ca^{2+}-independent pathways, was studied by the use of 2,3-butanedione 2-monoxim [BDM], a nonmuscle myosin ATPase-inhibitor (Sigma). The following kinase inhibitors were used: the calmodulin-mediated MLCK-inhibitor W7 (Sigma), the Rho-kinase-inhibitor Y-27632 (Calbiochem, La Jolla, USA) and the PKC-inhibitor staurosporin (Sigma). The kinase inhibitors and BDM were added to agonist-free collagen lattices 5 minutes prior to addition of an agonist and release. To evaluate the effect of increased intracellular Ca^{2+} on contraction in the different cell types, the Ca^{2+}-ionophore A23187 was used in agonist-free conditions. To investigate the effect of inhibition of MLCP, calyculin (Calbiochem) was added to Ca^{2+}-depleted and normal (Ca^{2+}-containing) lattices.

The former lattices were obtained by washing lattices with Ca^{2+}-free PBS1x (3x2 min, each), followed by Ca^{2+}-free PBS1x + 3mM EGTA (2x5 min each, then 14 min) and a final set of washes with Ca^{2+}-free PBS1x + 3mM EGTA + 0.01µM A23187 (3x2 min, each). The final washing step allowed depletion of intracellular Ca^{2+}.

2.4. Western blotting for rMLC and P-rMLC

HSCs, cultured for 24 hours in the presence of W-7, Y-27632, staurosporin or FCS alone, were harvested and homogenized in lysis buffer (Tris-HCL 0.125 M, 4% SDS, 20% glycerol, 0.02% bromophenol blue, DTT 0.2M). After heat denaturation (100°C for 5') and centrifugation (13.000xg for 10'), equal amounts of protein (6.5µg) were separated by a 7% SDS-PAGE gel and then transferred onto a nitrocellulose Protran membrane (Schleicher& Schuell, Dassel, Germany). The membranes were blocked with 5% blocking solution (milkpowder) in PBS1x for 1 ½ hour at room temperature to avoid nonspecific binding. Thereafter, blots were incubated overnight with primary antibodies against regulatory myosin light chain (rMLC) and phosphorylated rMLC (P-rMLC) (1:200, Santa Cruz, CA, USA). The next day, the membranes were incubated with horseradish peroxidase-conjugated secondary antibody (SwaR-HRP 1:500 Prosan, Merelbeke, Belgium) and immunoreactivity was visualized using chemiluminescence detection (ECL-plus, Amersham Biosciences). Membranes were stained with a Ponceau staining to confirm equal protein loading and transfer between lanes. Densitometric quantification of Western blot signal intensity was performed with Un-Scan-IT Gel Software (Silk Scientific, Utah, USA) and calculated as a percentage relative to the mean value of HSCs treated only with FCS.

2.5. Fluo-4-visualization of intracellular calcium

HSCs, grown on glass coverslips, were incubated with 5µM Fluo-4 + 0.025% pleurionic acid (Molecular Probes) in FCS-free conditions. Coverslips were subsequently transferred

to the coverglass chamber of the confocal scanning microscope (Nikon TE 300, Noran Oz). Cells were observed and photographed prior to, during and after addition of FCS-free medium containing 0.01μM A23187.

2.6. Rat model of TAA-induced cirrhosis*:* see Chapter 3

2.7. In-situ liver perfusion

The detailed description of the perfusion model and its modalities were described in Chapter 3. In TAA cirrhotic and control rats (n=25, each), we studied the effect of the α_1-agonist methoxamine on intrahepatic vascular resistance (IHVR) with and without preincubation with W-7, Y-27632 and staurosporin by in-situ liver perfusion.

3. RESULTS

In the first part of this section, HSC contraction was investigated in vitro by use of the stress-relaxed-collagen-lattice contraction model. In the second part, the in vitro findings were corroborated with in vivo experiments in the in-situ perfused rat liver.

3.1. In vitro results

3.1.1. Relevance of intracellular Ca^{2+} and Ca^{2+}-dependent pathways in HSC-mediated gel-contraction

Increasing Ca^{2+} intracellularly in serum-free conditions with A23187, a Ca^{2+}-ionophore, was demonstrated by means of confocal Ca^{2+}-imaging, which showed a rapid and transient rise in intracellular Ca^{2+} within seconds (Fig. 4).

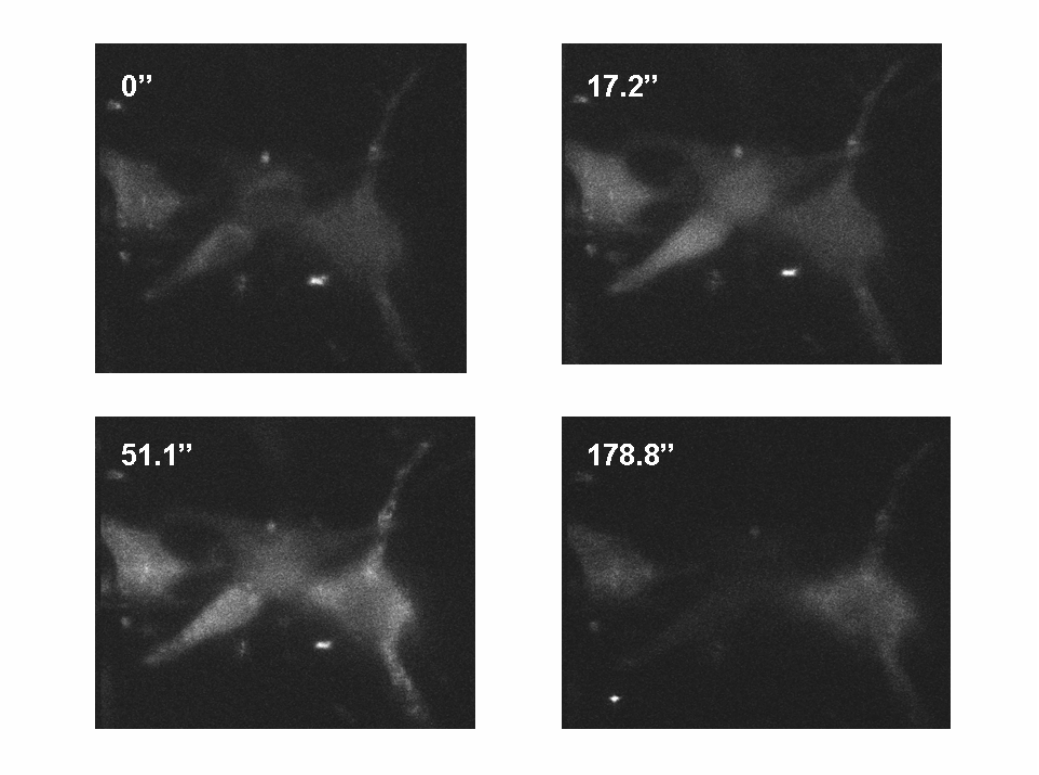


Fig. 4: Increasing Ca^{2+} intracellularly in serum-free conditions with A23187, a Ca^{2+}-ionophore, was demonstrated by means of confocal Ca^{2+}-imaging at different time points (time 0”, 17.2”, 51.1”, 178.8”).

A dose-response curve with A23187 showed maximal contraction of 54.7 ± 1.8% at 0.01µM after 24 hours (Fig. 5).

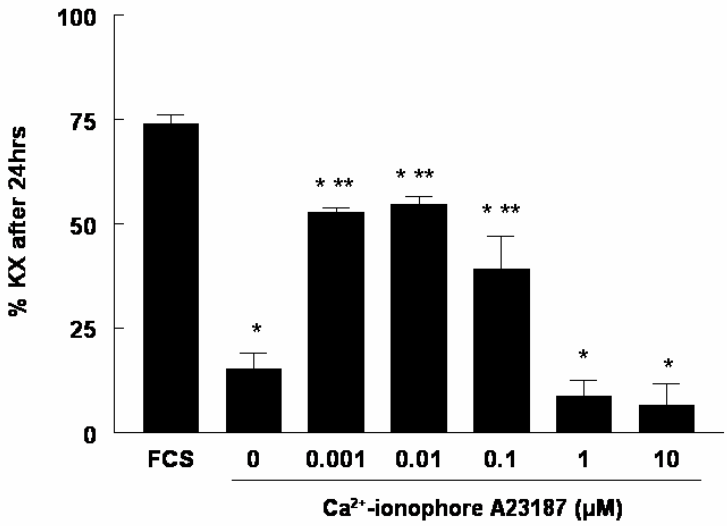


Fig. 5: Dose-response curve in HSCs to A23187, a Ca^{2+}-ionophore, in serumt-free conditions, showing that elevation in intracellular Ca^{2+} is insufficient to cause a maximal contraction (*$P < 0.001$ vs FCS, ** $P < 0.001$ vs 0, 1 & 10µM A23187).

Since this amounts only to 75.6 ± 1.8% of FCS-promoted-contraction, increasing intracellular Ca^{2+} appears insufficient to exclusively cause contraction (Fig. 6).
The equivalent maximal contraction relative to FCS-induced contraction generated in VSMCs and cardiac myofibroblasts amounted to 85.1 ± 2.3% and 34.6 ± 2.1%, respectively ($P < 0.001$ vs the equivalent effect in HSCs) (Fig. 6).

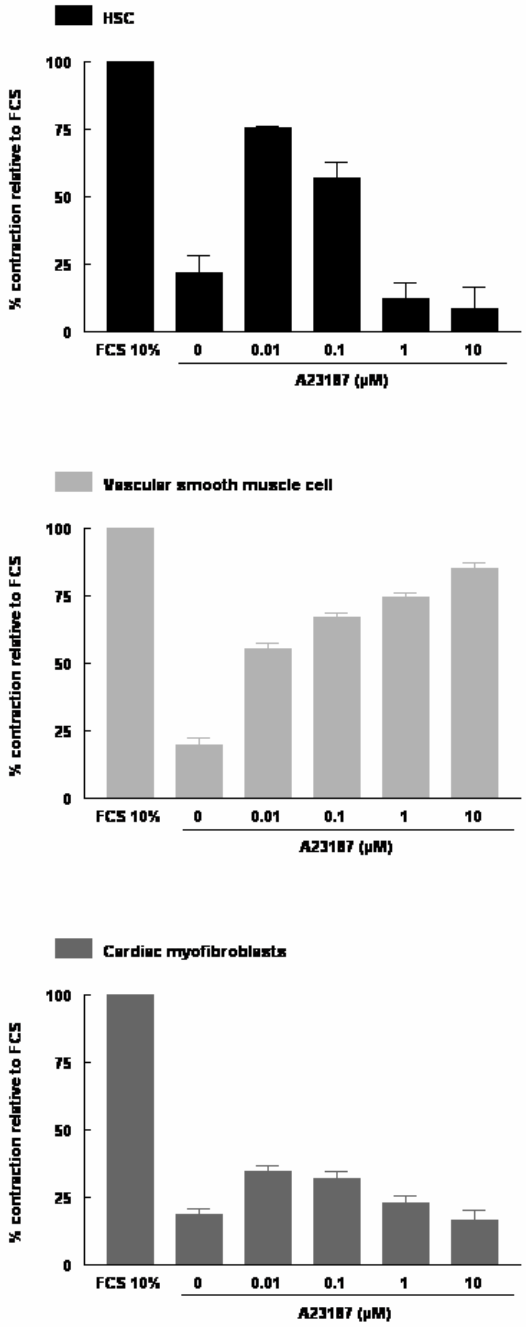


Fig. 6: Comparison of the degree of Ca^{2+}-depedency of contraction, expressed as extent of contraction relative to FCS-promoted contraction, between hepatic stellate cells (HSC), vascular smooth muscle cells and cardiac myofibroblasts.

The downstream effector of the Ca^{2+}-dependent pathway, MLCK, was inhibited using W-7, an inhibitor of calmodulin-mediated activation of MLCK. This resulted in an attenuation of FCS-mediated collagen-lattice contraction to 17.6 ± 2% at 10^{-4}M (vs 77.4 ± 1.2% for control, $P < 0.001$) (Fig. 7).

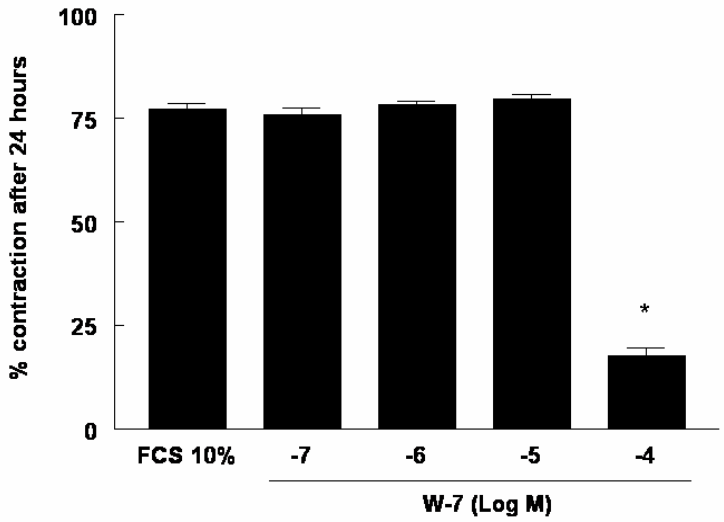


Fig. 7: Dose-response curve to W-7, an inhibitor of calmodulin-mediated myosin light chain kinase activation, on hepatic stellate cell contraction (* $P < 0.001$ vs FCS).

When the effect of W-7 (10^{-4}M) was evaluated on maximal Ca^{2+}-induced contraction (induced by 0.01 µM A23187 in FCS-free conditions), Ca^{2+}-induced contraction was inhibited (16.8 ± 2.7% vs 54.7 ± 1.8%, $P < 0.001$), further strengthening the suggestion that calmodulin is indeed the downstream target of Ca^{2+}-dependent pathways.

3.1.2. Relevance of Ca^{2+}-independent pathways in HSC-mediated gel-contraction

First, MLCP, the supposed converging end-point of the Ca^{2+}-independent pathways, was inhibited using calyculin, a type-1 phosphatase-inhibitor. Calyculin (10^{-9}M) was able to induce contraction of HSC-embedded collagen lattices in the absence of FCS (53.7% vs 15.3% FCS-free, $P < 0.05$) (Fig. 8).

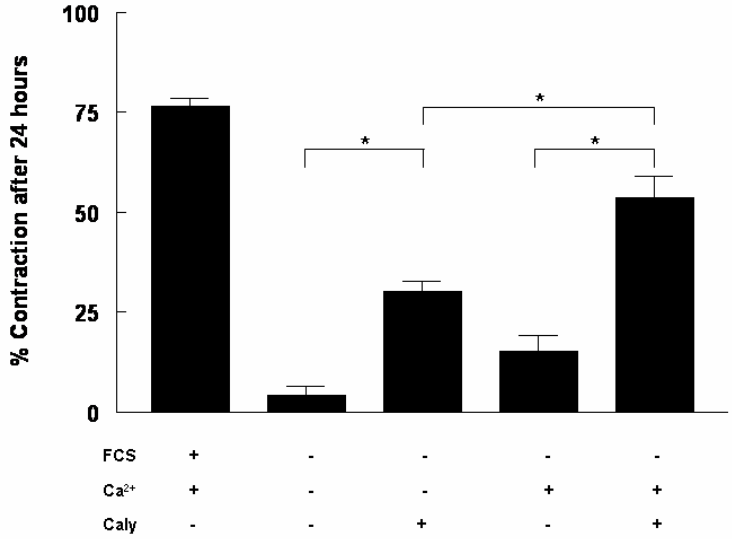


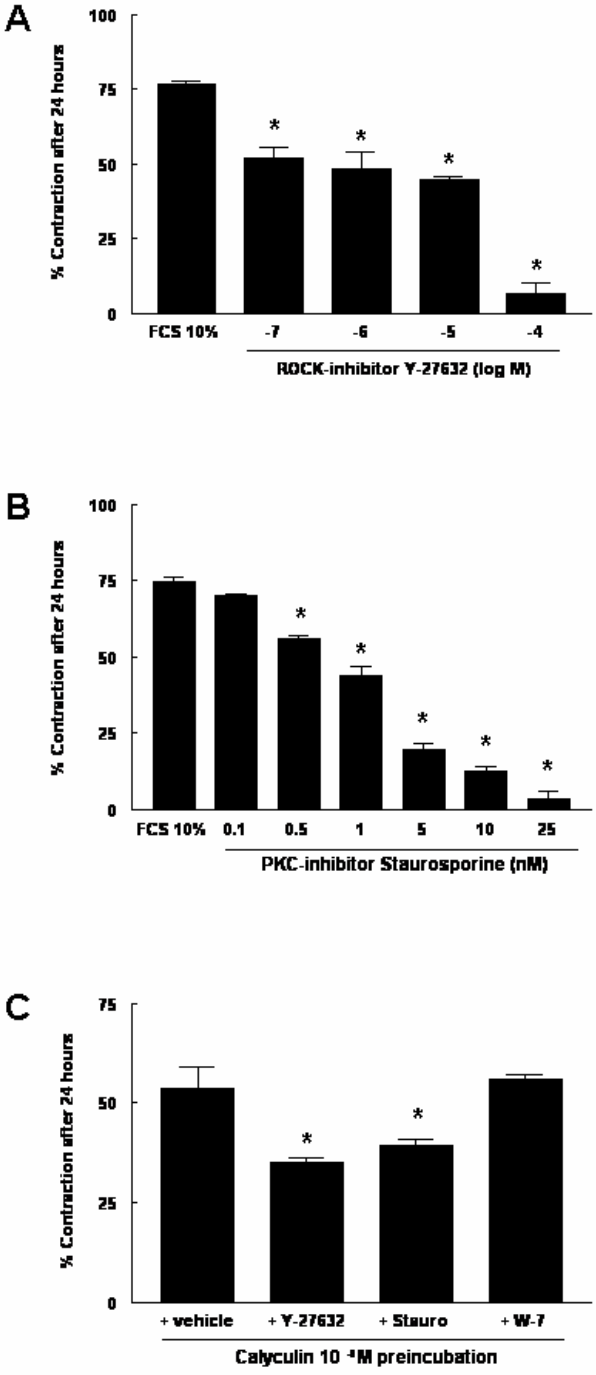
Fig. 8: Phenomenon of Ca^{2+}-sensitization. Inhibition of myosin light chain phosphatase by calyculin 10^{-9}M increases % contraction in response to a specific level of Ca^{2+} (*$P < 0.05$).

To further specify the relative contribution of MLCP-activity in HSC-mediated contraction, HSC contraction was examined under Ca^{2+}-depleted and Ca^{2+}-containing conditions in the presence or absence of calyculin 10^{-9}M. In Ca^{2+}-depleted conditions, contractility was enhanced when MLCP was inhibited (4 ± 2.3 vs 30 ± 2.7, P=0.002) (Fig. 8).

In Ca^{2+}-containing lattices, a similar effect as in Ca^{2+}-depleted conditions was observed when MLCP was inhibited (15.3 ± 3.8 vs 53.7 ± 5.2, P=0.004), but the degree of contraction was increased compared to the Ca^{2+}-depleted conditions. These data not only illustrate a role for MLCP in the regulation of HSC contraction in addition to increasing levels of intracellular Ca^{2+}, but also document its involvement in "Ca^{2+}-sensitization". This phenomenon aims at improving contraction by use of Ca^{2+} that is available, rather than by inundating the cell with excessive Ca^{2+}. More specifically, the amount of force generated to a specific level of Ca^{2+} is increased by inhibiting MLCP.

Known inactivating upstream signalling pathways of MLCP, more specifically Rho-associated kinase and PKC mediated pathways, were evaluated next. Y-27632 and staurosporin, their respective inhibitors, dose-dependently attenuated FCS-promoted HSC contraction (Fig. 9.A&B). In contrast, Y-27632 (10^{-4}M) and staurosporin (25nM), which both inhibited FCS-promoted contraction by greater than 85%, inhibited calyculin-promoted contraction respectively by maximally 35% and 27%, strengthening the hypothesis that MLCP is their downstream target. Furthermore, W-7 (10^{-4}M), an inhibitor of calmodulin-mediated activation of MLCK, did not change calyculin-promoted contraction at all, suggesting its unimportance in the regulation of MLCP (Fig. 9.C).

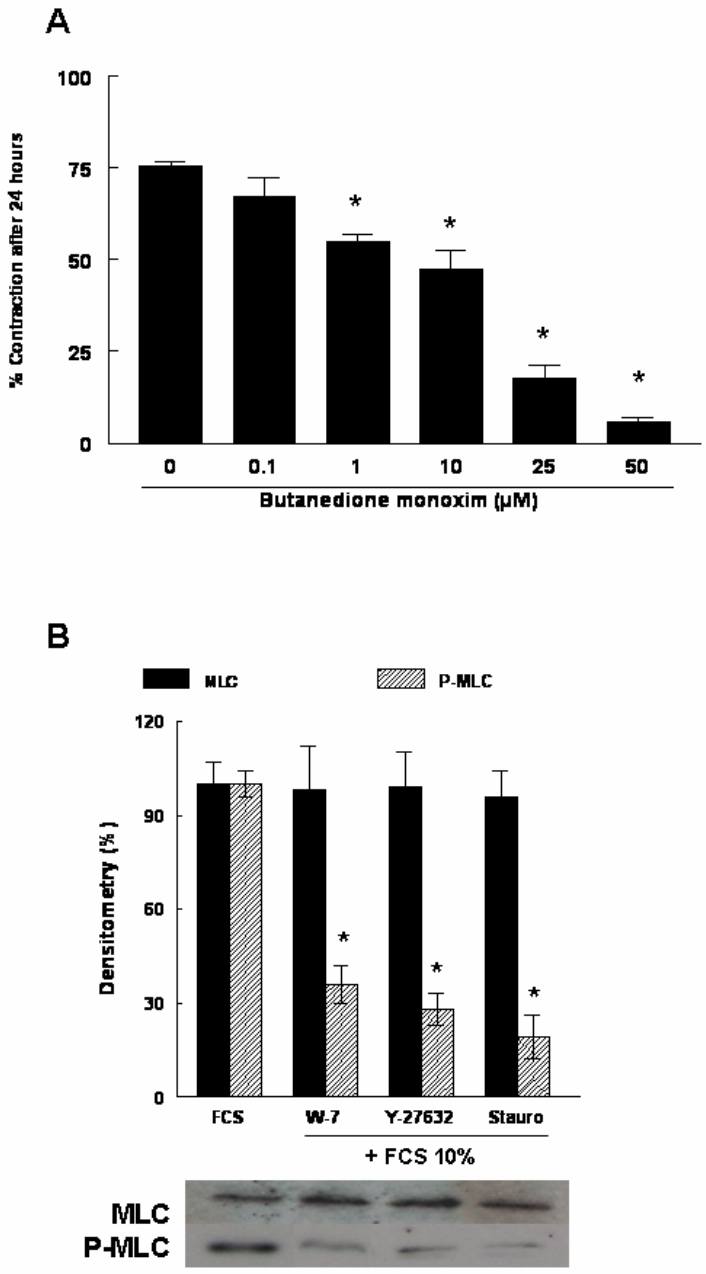
Fig. 9: Relevance of Ca^{2+}-independent pathways and their end-target myosin light chain phosphatase: A. dose-response curve to the Rho-kinase inhibitor Y-27632 (*P < 0.001 vs FCS alone), B. dose-response curve to the protein kinase C-inhibitor staurosporin (*P < 0.001 vs FCS alone) and C. relevance of the rho-kinase and protein kinase C pathway in the regulation of myosin light chain phosphatase since pre-incubation with calyculin 10^{-9}M largely counteracted inhibition of contraction by Y-27632 10^{-4}M and staurosporin 25nM (*P < 0.05 vs calyculin + vehicle and calyculin + W-7).


A
% Contraction after 24 hours
100
75
50
25
0
*
*
*
*
FCS 10%
-7
-6
-5
-4
ROCK-inhibitor Y-27632 (log M)
B
% Contraction after 24 hours
100
75
50
25
0
*
*
*
*
*
FCS 10%
0.1
0.5
1
5
10
25
PKC-inhibitor Staurosporine (nM)
C
% Contraction after 24 hours
75
50
25
0
*
*
+ vehicle
+ Y-27632
+ Stauro
+ W-7
Calyculin 10 -8M preincubation

3.1.3. Relevance of actomyosin interaction in HSC-mediated contraction

To assess whether the end-point of Ca^{2+}-dependent and -independent pathways was indeed dependent on actomyosin involvement, butanedione monoxim (BDM), a nonmuscle myosin II-Ca^{2+}-ATPase-inhibitor, was added to the culture-medium prior to release. This led to a dose-dependent decrease in FCS-promoted contraction, indicating the requirement of actomyosin interaction in the contraction of stress-relaxed HSC-embedded collagen matrices (Fig. 10.A). To further substantiate the involvement of the calmodulin/MLCK-, Rho-kinase- and PKC-mediated pathways in this actomyosin interaction, we additionally examined the phosphorylation of MLC by Western blot analysis. Densitometric analysis of MLC and P-MLC (Fig. 10.B) shows constitutive expression of MLC in all conditions. Addition of W-7 (10^{-4}M), Y-27632 (10^{-4}M) and staurosporin (25nM) decreased the amount of phosphorylation of MLC compared to control conditions (FCS) ($P< 0.001$ vs the degree of phosphorylation in control conditions).

Fig. 10: Relevance of actomyosin interaction in HSC-mediated contraction and its regulation by Ca^{2+}-dependent and –independent pathways: A. dose-response curve to butanedione monoxim, a nonmuscle myosin II-Ca^{2+}-ATPase-inhibitor (*$P < 0.05$ vs FCS alone), B. Densitometric analysis of western blot of phosphorylated myosin light chain (P-MLC) and MLC in the presence of FCS alone or combined with W-7 10^{-4}M, Y-27632 10^{-4}M and staurosporin 25nM (* $P < 0.001$, n=3 per condition). A representative blot is shown.


A
100
75
50
25
0
% Contraction after 24 hours
*
*
*
*
0
0.1
1
10
25
50
Butanedione monoxim (µM)
B
MLC
P-MLC
120
90
60
30
0
Densitometry (%)
*
*
*
FCS
W-7
Y-27632
Stauro
+ FCS 10%
MLC
P-MLC

3.1.4. Relevance of Ca^{2+}-dependent and -independent pathways in the presence of the α_1-adrenergic agonist methoxamine

To finally exclude the possibility that these pathways were relevant exclusively during FCS-stimulation, we repeated the experiments with W-7, Y-27632 and staurosporin in the presence of the α_1-adrenergic agonist methoxamine, for which activated HSCs express the receptors and the biosynthetic enzymes (24). Except for basal conditions comparing only both agonists, we observed no differences to FCS-induced contraction in the presence of W-7, Y-27632 and staurosporin (Fig. 11).

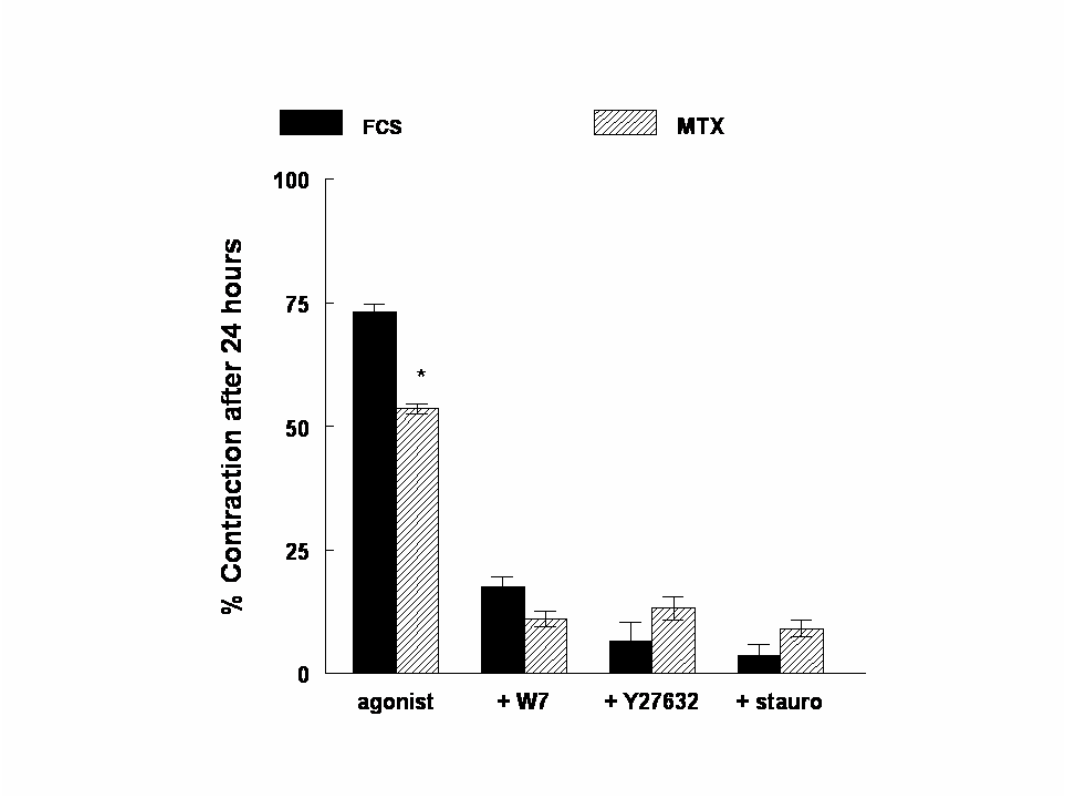


Fig. 11: Relevance of Ca^{2+}-dependent (W-7 10^{-4}M) and -independent pathways (Y-27632 10^{-4}M and staurosporin 25nM) in the presence of the α_1-adrenergic agonist methoxamine 10^{-4}M (MTX) (*$P < 0.05$ methoxamine vs FCS).

3.2. Results in the in-situ perfused normal and cirrhotic rat livers

In agonist-free conditions, the basal IHVR of cirrhotic rat livers was already increased compared to normal rat livers (0.22 ± 0.01 vs 0.13 ± 0.01 mmHg.min.ml^{-1} for control, P<0.001) (Fig. 12).

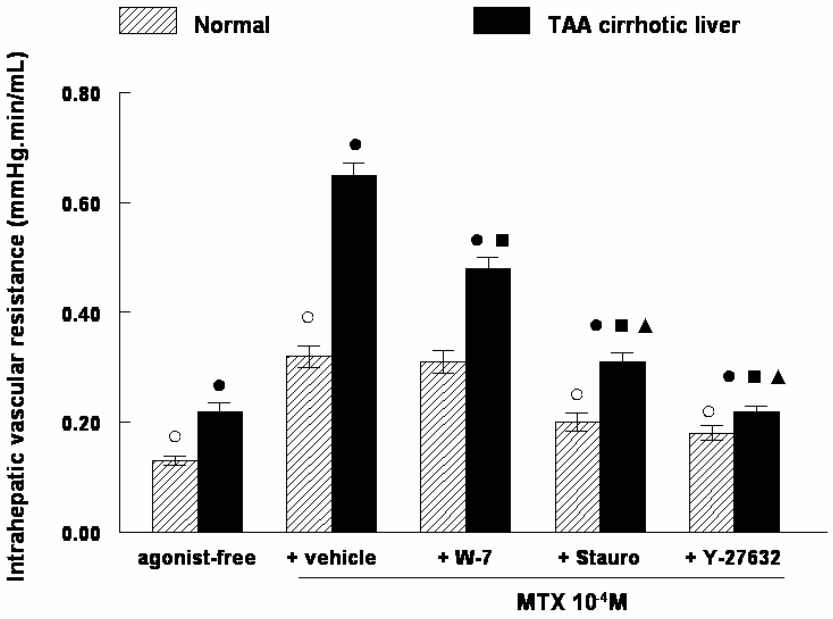


Fig. 12. Relevance of Ca^{2+}-dependent (W-7 10^{-4}M) and -independent pathways (Y-27632 10^{-4}M and staurosporin 25nM) in the in-situ perfused normal and thioacetamide-induced cirrhotic rat liver (n=5 per condition). Both Ca^{2+}-dependent and –independent pathways were shown to be involved in the hyperresponsiveness of the cirrhotic liver to methoxamine since inhibition of these pathways attenuated the increased intrahepatic vascular resistance with a predominance of the Ca^{2+}-independent pathways, mediated through protein kinase C- and RhoA-mediated signalling cascades. ● $P < 0.05$ vs TAA + MTX, ■ $P < 0.05$ vs TAA + W-7, ▲ $P < 0.05$ vs TAA + Y-27632, ○ $P < 0.05$ vs normal rat liver + MTX

Abbreviations: TAA, thioacetamide; MTX, methoxamine

Addition of methoxamine (10^{-4}M) led to an increase in IHVR in both the cirrhotic and the normal perfused rat liver (0.65 ± 0.02 vs 0.32 ± 0.02mmHg.min.ml^{-1} respectively, *P*<0.001) (Fig. 12).

In the cirrhotic perfused rat liver, the response to methoxamine was aggravated compared to the normal perfused rat liver (Δ increase in IHVR TAA 0.39 ± 0.03 mmHg.min.ml^{-1} vs 0.21 ± 0.02 mmHg.min.ml^{-1} for control, *P*=0.001), which is consistent with the phenomenon of "hyperresponsiveness" to vasoconstrictors in cirrhosis. Preincubation with Y-27632 10^{-4}M , staurosporin 25nM and W-7 10^{-4}M in the cirrhotic rat liver, significantly reduced this hyperresponsiveness to methoxamine by 66.8 ± 1.3%, 52.4 ± 2.7% and 28.7 ± 2.8% respectively, suggesting a predominant involvement of Ca^{2+}-independent pathways in the increased active IHVR associated with cirrhosis (Fig. 12). In the normal liver, we noted a reduction in IHVR only after inhibition of Ca^{2+}-independent pathways and to a lesser extent than found in cirrhosis: 43.1 ± 4.2% (*P*=0.008 vs TAA+Y27632) and 40.2 ± 4.2% (*P*=0.038 vs TAA+stauro) (Fig 12).

4. DISCUSSION

Accumulating evidence indicates that the contractile force generated by activated HSCs not only drives scar contraction in cirrhosis but also modulates hepatic microcirculation (1,3-5,9,11). Both aspects affect the increased intrahepatic resistance to portal flow, and therefore make HSCs interesting targets for the treatment of portal hypertension. Because of their apparent key role, considerable effort has been made to elucidate the regulation that governs contractile force generation in these cells. At present, it is generally assumed that activated HSCs have a "smooth-muscle cell-like" Ca^{2+}-dependent contraction pattern (2-5,25). This contention is founded on different observations, such as a functional and ultrastructural resemblance to pericytes (4), the expression of smooth muscle proteins (like α-smooth muscle actin and myosin II) (2,9), the expression of L-type voltage operated Ca^{2+}-channels (25) and the fact that agonists that are known to cause contraction in HSCs are associated with increases in intracellular Ca^{2+} (3-5). Although persuasive, these observations are challenged heretofore by a lack of direct evidence proving that an increase in intracellular Ca^{2+} indeed mediates force generation, and by an apparent contradiction in terminology, as witnessed in the " smooth-muscle cell-like contraction pattern of a myofibroblast-like activated HSC".

In contrast to previous studies, we applied a three-dimensional stress-relaxed collagen lattice contraction model to study the contractility of HSCs (11,22). The reasons herefore are two-fold. First, cell adhesion, analogous to the in vivo-situation, occurs three-dimensionally to attachment sites made upon protein fibrils rather than two-dimensionally along a protein-coated interface (like for contraction studies using confocal calcium-imaging or when growing HSCs on top of polymerized collagen lattices). This model therefore mimics the reciprocal geometric and mechanical relationships with the surrounding matrix which HSCs entertain in vivo (22). Second, the relevance of stressed

gels follows from the observation that in the cirrhotic liver the injured liver tissue is tethered in a way that cell contraction will inevitably increase stress in the surrounding matrix, resulting in a mechanical feedback which is missing in classically used unrestrained gels ("floating gels") as well as in classical two-dimensional assays, as mentioned earlier. Using this in vitro model, we first tested the premise that force generation in HSCs is Ca^{2+}-dependent. We demonstrated that although the Ca^{2+}/calmodulin mediated MLCK activity is necessary for HSC contraction, elevation of intracellular Ca^{2+} was insufficient to cause maximal contraction. These results contrasted with the demonstrated properties of vascular smooth muscle cell in which gradual elevation of intracellular Ca^{2+} ultimately led to a similar efficient contraction as obtained after agonist-stimulation, proving the dominance of Ca^{2+}-dependent pathways in these cells (6,7,10,11). In cardiac myofibroblasts, quite the reverse phenomenon was observed, since these cells, like other types of myofibroblasts (11), appeared almost Ca^{2+}-insensitive. These observations clearly refute any comparison for HSCs with smooth muscle cells and myofibroblasts, making terms like "smooth-muscle-cell-like" and "myofibroblast-like" inappropriate in this context.

The inability of increased intracellular Ca^{2+} to promote maximal contraction suggests that activated HSCs have an additional mechanism to the Ca^{2+}/calmodulin-dependent MLCK that is critical in regulating contractility. We therefore tested Ca^{2+}-independent pathways. Since these pathways are thought to converge in the inactivation of MLCP, resulting in delayed degradation of phosphorylated rMLC and thefore decreased contraction, we first focused on this enzyme (8-11,26). We demonstrated that the phosphatase-inhibitor calyculin, in the absence of any agonist, could promote HSC contraction, proving its involvement in the regulation of force generation. To further specify its role in this regulation, we examined HSC contraction under Ca^{2+}-depleted or Ca^{2+}-containing conditions in the presence or absence of calyculin. These experiments showed that

inhibition of MLCP increased the amount of contraction independently of the level of intracellular Ca^{2+}, a phenomenon known as Ca^{2+}-sensitization (7,10). In smooth muscle cells, this phenomenon has been extensively described and is mainly attributed to the inhibition of MLCP (7). Several mechanisms have been identified in these cells to inactivate MLCP, amongst which most importantly the phosphorylation of the regulatory subunit of MLCP by the Rho/Rho-kinase pathway and the inhibition of the catalytic subunit of MLCP mediated by the PKC-dependent pathway (7,10,26,27). For HSCs, to our knowledge the concept of Ca^{2+}-sensitization is novel. Reviewing the two mentioned mechanisms which are considered to be the main regulating factors in smooth muscle cells in this process, we observed surprising parallels in HSCs. First, we and others, in different conditions, could document a role for the rhoA-signalling pathway, since preincubation with the Rho-kinase inhibitor Y-27632 attenuated contraction and decreased phosphorylation of regulatory myosin light chain, the rate-limiting step in actomyosin interaction (12,28-30). Furthermore, we also proved that the rhoA signalling pathway acts through MLCP, since pre-incubation with calyculin, a phosphatase-inhibitor, largely counteracted inhibition of contraction by Y-27632. This suggests that Rho-kinase, a serine/threonine kinase, phosphorylates MLCP and inhibits phosphatase activity, resulting in delayed degradation of phosphorylated regulatory myosin light chain and thus protracted contraction. Second, we also revealed a role for the PKC-dependent pathway. Staurosporine, a PKC-inhibitor, prevented FCS- and methoxamine-promoted contraction and decreased phosphorylation of regulatory myosin light chain. Similarly as for RhoA-inhibition, calyculin also almost completely opposed inhibition of contraction by staurosporin, identifying MLCP as the end-target of this pathway as well. These results indicate an auxiliary role for PKC to the RhoA-pathway as a G-protein coupled effector of Ca^{2+}-sensitization.

It should be taken into account that the inhibitors used to block the different pathways are highly specific but not exclusive to their intended target. In addition, a role for MLC phosphorylation-independent regulatory mechanisms is postulated in smooth muscle cells (7). Our data show that Ca^{2+}-dependent (MLCK-related) and Ca^{2+}-independent (MLCP-related) pathways are important in HSC contraction, but these findings do not exclude the presence or absence of alternative, more discrete pathways. The study of these will require more selective experimental tools and models, which are lacking at the moment.

To correlate our in vitro findings to the in vivo situation, we reevaluated these pathways in the in-situ perfused liver. We first confirmed the presence of an exaggerated response to methoxamine in the cirrhotic rat liver compared to the normal liver, illustrating the known phenomenon of intrahepatic hyperresponsiveness to vasoconstrictors in the cirrhotic liver (chapter 3). Both Ca^{2+}-dependent and –independent pathways were shown to be involved in this hyperresponsiveness of the cirrhotic liver since inhibition of these pathways attenuated the increased intrahepatic vascular resistance. A predominance of the Ca^{2+}-independent pathways, mediated through the PKC- and RhoA-mediated signalling cascades was demonstrated.

In conclusion, we have shown that both Ca^{2+}-dependent and Ca^{2+}-independent pathways are necessary for a HSC-specific contraction pattern, which distinguishes them from both myofibroblasts and smooth muscle cells. These in vitro findings are consistent with the data obtained in the cirrhotic liver where both pathways were involved, with Ca^{+}-independent pathways predominating. A better understanding of the intracellular signal transduction mechanisms leading to HSC contraction and the demonstration of their relevance in the establishment of increased intrahepatic vascular resistance in the cirrhotic liver might lead to the identification of novel targets for the treatment of portal hypertension.

5. REFERENCES

1. Laleman W, Van Landeghem L, Wilmer A, et al. Portal hypertension: from pathophysiology to clinical practice. Liver Int 2006; 25: 1079-1090.
2. Friedmann SL. Seminars in medicine of the Beth Israel Hospital, Boston. The cellular basis of hepatic fibrosis. Mechanisms and treatment strategies. N Engl J Med 1993; 328: 1828-1835.
3. Reynaert H, Thompson MG, Thomas T, et al. Hepatic stellate cells: role in microcirculation and pathophysiology of portal hypertension. Gut 2000; 50: 571-581.
4. Pinzani M, Failli P, Ruocco C, et al. Fat-storing cells as liver-specific pericytes: spatial dynamics of agonist-stimulated intracellular calcium transients. J Clin Invest 1992; 90: 642-646.
5. Rockey DC. Vascular mediators in the injured liver. Hepatology 2003; 37: 4-12.
6. Taylor DA, Stull JT. Calcium dependence of myosin light chain phosphorylation in smooth muscle cells. J Biol Chem 1998; 263: 14456-14462.
7. Pfitzer G. Invited review: regulation of myosin phosphorylation in smooth muscle. J Appl Physiol 2001; 91: 497-503.
8. Kolodney MS, Elson EL. Correlation of myosin light chain phosphorylation with isometric contraction of fibroblasts. J Biol Chem 1993; 268: 23850-23855.
9. Saab S, Tam SP, Tran BN, et al. Myosin mediates contractile force generation by hepatic stellate cells in response to endothelin-1. J Biomed Sci 2002; 9: 607-612.
10. Somlyo AP, Somlyo AV. Signal transduction by G-proteins, Rho-kinase and protein phosphatase to smooth muscle and non-muscle myosin II. J Physiol 2000; 522: 177-185.
11. Parizi M, Howard EW, Tomasek JJ. Regulation of LPA-promoted myofibroblast contraction: role of Rho, myosin light chain kinase, and myosin light chain phosphatase. Exp Cell Res 2000; 254: 210-220.
12. Kawada N, Seki S, Kuroki T, et al. ROCK inhibitor Y-27632 attenuates stellate cell contraction and portal pressure increase induced by endothelin-1. Bioch Biophys Res Comm 1999; 266: 296-300.
13. Cassiman D, Denef C, Desmet VJ, et al. Human and rat hepatic stellate cells express neurotrophins and neurotrophin receptors. Hepatology 2001; 33: 148-58.
14. Alpini G, Phillips JO, Vroman B, et al. Recent advances in the isolation of liver cells. Hepatology 1994; 20: 494-514.
15. Cassiman D, Roskams T. Beauty is in the eye of the beholder: emerging concepts and pitfalls in hepatic stellate cell research. J Hepatol 2002; 37: 527-535.
16. Petrov VV, Fagard RH, Lijnen PH. Arginine-aminopeptidase in rat cardiac fibroblastic cells participates in angiotensin peptide turnover. Cardiovascular Research 2004; 61: 724-735.
17. Janssens S, Flaherty D, Nong Z, et al. Human endothelial nitric oxide synthase gene transfer inhibits vascular smooth muscle cell proliferation and neointima formation after balloon injury in rats. Circulation 1998; 97: 1274-1281.
18. Elsdale T, Bard J. Collagen substrata for studies on cell behaviour. J Cell Biol 1972; 54: 626-637.
19. Tomasek JJ, Gabbiani G, Hinz B, Chaponnier C, Brown RA. Myofibroblasts and mechanoregulation of connective tissue remodelling. Nat Rev Mol Cell Biol 2002; 3: 349-63.
20. Nakagawa S, Pawelek P, Grinnell F. Extracellular matrix organization modulates fibroblast growth and growth factor responsiveness. Exp Cell Res 1989; 182: 572-582.
21. van Bockxmeer FM, Martin CE, Constable IJ. Effect of cyclic AMP on cellular contractility and DNA synthesis in chorioretinal fibroblasts maintained in collagen matrices. Exp Cell Res 1984; 155: 413-421.
22. Grinnell F. Fibroblast biology in three-dimensional collagen matrices. TrendsCell Biol 2003; 13: 264-269.
23. Rockey DC, Housset CN, Friedman SL. Activation-dependent contractility of rat hepatic lipocytes in culture and in vivo. J Clin Invest 1993; 92: 1795-1804.
24. Oben JA, Roskams T, Yang S, et al. Hepatic fibrogenesis requires sympathetic neurotransmitters. Gut 2004; 53: 438-445.
25. Bataller R, Gasull X, Gines P, et al. In vitro and in vivo activation of rat hepatic stellate cells results in de novo expression of L-type voltage-operated calcium channels. Hepatology 2001; 33: 956-962.
26. Harnett KM, Cao W, Biancani P. Signal-transduction pathways that regulate smooth muscle function I. Signal transduction in phasic (esophageal) and tonic (gastroesophageal sphincter) smooth muscles. Am J Physiol Gastrointest Liver Physiol 2005; 288: G407-G416.
27. Nobe H, Nobe K, Paul RJ. Fibroblast fiber contraction: role of protein kinase C and Rho kinase in activation by thromboxane A_2. Am J Physiol Cell Physiol 2003; 285: C1411-C1419.
28. Yanase M, Ikeda H, Matsui A, et al. Lysophosphatidic acid enhances collagen gel contraction by hepatic stellate cells: association with rho-kinase. Biochem Biophys Res Commun 2000; 277: 72-78.

29. Yanase M, Ikeda H, Ogata I, et al. Functional diversity between Rho-kinase- and MLCK-mediated cytoskeletal actions in a myofibroblast-like hepatic stellate cell line. Biochem Biophys Res Commun 2003; 305: 223-228.
30. Melton AC, Datta A, Yee HF Jr. $[Ca2+]_i$-independent contractile force generation by rat hepatic stellate cells in response to endothelin-1. Am J Physiol Gastrointest Liver Physiol 2006; 290: G7-G13.

Chapter 5

A role for asymmetric dimethylarginine (ADMA) in the pathophysiology of portal hypertension in biliary cirrhotic rats.

adapted from

W. Laleman[1], A. Omasta[1], M. Van de Casteele[1] , M. Zeegers[1],
I. Vander Elst[1], L. Van Landeghem[1], T. Severi[1], J. Van Pelt[1], T. Roskams[2],
J. Fevery[1] and F. Nevens[1]

Department of Hepatology[1] and Histopathology[2],
University Hospital Gasthuisberg, KU Leuven, Belgium

Hepatology 2005, 42:1382-1390.
Editorial Hepatology 2005; 42: 1255-1257
Reprinted with permission of John Wiley & Sons, Inc.

1. INTRODUCTION

Portal hypertension (PHT) is a major complication of cirrhosis, irrespective of its etiology. The initial event in the pathogenesis of cirrhotic PHT is an increase in intrahepatic vascular resistance (IHVR) to portal flow, whereas the increase in splanchnic blood flow maintains and aggravates the syndrome (1,2). Although the increased IHVR is primarily caused by structural changes, such as fibrosis, thrombosis and nodule formation, a non-structural, dynamic vascular component has also been demonstrated (3). This increased hepatic vascular tone is mainly driven by activated hepatic stellate cells and results from an imbalance between vasodilator and vasoconstrictor forces. More specifically, there is increased production of vasoconstrictors, such as endothelin-1, thromboxane A_2 and angiotensin II, which is unopposed due to reduced bioavailability of nitric oxide (NO), a potent intrahepatic vasodilator (4-7). The molecular basis of the intrahepatic NO-deficiency has uniformly been attributed to decreased activity of the endothelial NOS-isoform, eNOS (4-6,8) (Fig. 1). However, the mechanisms of this endothelial dysfunction remain ill-defined and might even differ depending on the cause of the underlying liver disease (8-10).

In the early 1990's, Vallance et al. (11) reported that NO synthesis could be inhibited by an endogenous circulating amino acid: the asymmetric dimethylarginine (ADMA). ADMA as well as its vasoinactive stereoisomer, the symmetric dimethylarginine (SDMA), are synthesized by enzymatic methylation of L-arginine residues in proteins and released during proteolysis. In contrast to SDMA, which is entirely eliminated by renal excretion, ADMA is mainly metabolized to citrulline and dimethylamine by the liver enzyme dimethylarginine dimethylaminohydrolase (DDAH) (12,13). Consequently, it was suggested that impaired liver function led to increased plasma levels of ADMA (13,14). Several recent studies have linked ADMA to endothelial dysfunction and to cardiovascular

diseases, such as arterial hypertension and multi-organ failure (12,14). The specific intrahepatic hemodynamic effects of ADMA remain, however, unclear.

The aim of the present study was to evaluate in three different portal hypertensive rat models whether the pathophysiology of PHT might differ depending on the etiology of cirrhosis and to determine whether ADMA, an endogenous NOS inhibitor, could play a role herein (Fig. 1).

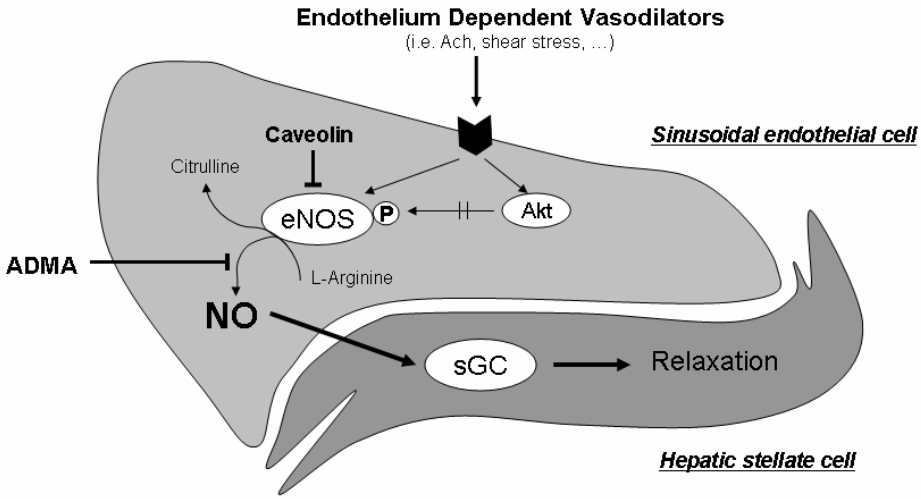


Fig. 1. Possible mechanisms involved in eNOS dysfunction in the sinusoidal endothelial cell: excessive inhibitory activity of caveolin, defective phosphorylation of eNOS by the serine-threonine kinase Akt and ADMA, an "imposter" for arginine (the substrate of eNOS) (Ach, acetylcholine; sGC, soluble guanylate cyclase) (adapted from [15]).

2. MATERIALS AND METHODS

2.1. Models of portal hypertension

In this study, different models of portal hypertension were used:

- *Biliary cirrhosis* resulted from bile duct excision (BDE) (16). At laparotomy, the bile duct was cut between a ligature close to the liver hilum and one close to the duodenum. Experiments on this model were performed 4 weeks later.
- *Thioacetamide cirrhosis (TAA)*, as a model of non-biliary cirrhosis, was described in chapter 3.
- *Partial portal vein ligation (PPVL)*, as a model of extra-hepatic PHT, was obtained by placing a 21G needle on the portal vein, after which a non-resorbable surgical thread (Polypropylene 5.0) was ligated around vein and needle. Afterwards, the needle was withdrawn (17). Three weeks later, experiments were carried out in PPVL rats.
- *Sham operation*. During laparotomy, duodenum, portal vein and bile duct were exposed. After 15 minutes the abdomen was closed with 2.0 Dexon thread. These rats served as controls.

2.2. In vivo hemodynamic measurements (Chapter 3)

2.3. Biochemical analysis

Besides biochemical analysis of plasma (Chapter 3), urine analysis was performed to determine creatinine clearance. This latter was measured by collecting urine from the rats 24 hours before the hemodynamic study and was determined by the following formula: $([\text{creatinine}]_{\text{urinary}}/[\text{creatinine}]_{\text{plasma}})$ x volume of urine collected over 24 hours, expressed per hour and per 100 g body weight.

2.4. Aminopyrine breath test

Hepatocyte microsomal function was assessed by the aminopyrine breath test, performed as described (18). The ABT-k represents the aminopyrine breath test constant and is the

regression coefficient (multiplied by 1000) of the least square regression of the measured radioactivity in the samples followed over time.

2.5. NOS activity assay (see chapter 3)

2.6. Western blot and immunohistochemistry for eNOS

2.6.1. Immunohistochemical staining

Samples of fresh liver were snap frozen in liquid nitrogen-cooled isopentane and stored at -70°C. For eNOS immunohistochemistry, a three step indirect immunoperoxidase staining method was used, as described previously (19). Intensity of sinusoidal staining was blindly and semi-quantitavely scored as 0 (no reactivity), +1 (weak), +2 (moderate), +3 (strong). For each specimen, 10 different high power fields were scored and the mean value +/- SEM was used as the final score.

2.6.1. Western blot for eNOS

Fresh liver was homogenized in Chaps Buffer (40% glycerol; 0.2M $K_2PO_4x7H_2O$, pH 7.2; 20mM Chaps (Sigma, St.Louis, USA)) to a final concentration of 0.25g wet weight of liver/mL. The protein concentration was quantified according to Bradford (20). Equal amounts of protein (100 µg) from each sample were separated by 7.5% SDS/PAGE. In preliminary work, a linear correlation between densitometric values and increasing amounts of protein was certified for the range used. The separated proteins underwent electrophoretic transfer onto a nitrocellulose Protran membrane (Schleicher & Schuell, Dassel, Germany). These membranes were blocked in blotto-Tween at 4°C overnight and thereafter incubated at room temperature with mouse monoclonal IgG against eNOS (Transduction Labs, Lexington, USA) (1:500). This was followed by 90' incubation with a secondary antibody (peroxidase-conjugated rabbit anti-mouse immunoglobulin, Dako) and visualized using chemiluminescence (ECL, Amersham, Netherlands). Membranes were stained with a Ponceau staining to confirm equal protein loading and transfer between

lanes. Densitometric quantification of Western blot signal intensity was performed with Un-Scan-IT Gel Software (Silk Scientific, Utah, USA) and calculated as a percentage of the mean value from sham-operated livers.

2.7. In situ liver perfusion system

The hepatic vascular response to ADMA was evaluated using a flow-controlled liver perfusion system, as described in detail in chapter 3.

To evaluate the effect of ADMA and other substances on IHVR in healthy rats, the liver was preconstricted with the α_1-adrenergic agonist methoxamine at a concentration of 10^{-4}M. Five minutes later, ADMA 10^{-3} M, vehicle (saline), SDMA 10^{-3} M, L-NAME 10^{-3} M or the combination of ADMA 10^{-3} M and L-NAME 10^{-3} M , dissolved in equal volumes, were added during a 1 minute period. Afterwards, concentration-effect curves to cumulative doses of acetylcholine (10^{-7} to 10^{-5} M, one log increase every 1.5 min) (Sigma) were performed for each condition. Similar experiments were performed in BDE and TAA cirrhotic rats, in which the effect of ADMA 10^{-3} M (n=5) was compared to vehicle (n=5). The concentration of ADMA was chosen based on a previously performed dose-response curve between 10^{-6} and 10^{-3}M (not shown). L-NAME is an inactive prodrug that upon hydrolyzation is bioactivated to N^G-nitro-L-arginine (L-NNA), a direct inhibitor of NOS. The response to cumulative doses of acetylcholine was calculated as percent change in perfusion pressure.

2.8. Determination of dimethylarginines and NOx

ADMA was determined in rat plasma, bile and perfusates by subsequent solid phase extraction, derivatization with phenylisothiocyanate and separation with liquid chromatography and UV detection. For solid phase extraction, plasma was added to a polymeric cationic-exchanger (Oasis-MCX, Waters, Milford, USA). Following elution, subsequent derivatization with phenylisothiocyanate was performed according to the

manufacturers instructions (Waters). For calibration and identification, arginine, ADMA and SDMA (Merck, Darmstadt, Germany) were used. In general, derivatization of an amino acid with phenylisothiocyanate leads to the formation of phenylthiocarbamyl -amino acids. Separation of these latter amino acids was obtained by reversed phase high-performance liquid chromatography. Separation was carried out according to Teerlinck et al. (21). Samples were spiked with known amounts of these amino acids for peak identification, recovery and quantification. A calibration curve (1-20 nmol ADMA) was constructed with a detection limit of 200 pmol per liter.

Levels of NOx in perfusates were determined by the method described in chapter 3.

In the perfusion experiments with normal rats, 2 mL perfusate samples were taken just before the administration of methoxamine and immediately after the dose-response to acetylcholine. The difference in NOx production between these two moments of sampling was calculated for each condition. At these same time points, ADMA levels were determined in perfusates of normal, BDE and TAA cirrhotic rats, incubated with either vehicle or ADMA 10^{-3}M. Subsequently, removal rates (RR) were calculated by the equation $RR = 100 \times (1- C_{after}/C_{before})$ with C_{after} being the perfusate level at the end of the experiment and C_{before} being the injected ADMA dose of 10^{-3}M.

3. RESULTS

In the first part of the experiments, differences in intrahepatic eNOS protein level and activity as well as ADMA plasma levels were evaluated in different portal hypertensive rat models. In the second part, the hemodynamic effect and metabolic fate of ADMA was further studied in the perfused normal and biliary and non-biliary cirrhotic rat liver.

3.1. Baseline characteristics of the different experimental groups (Table 1)

Portal pressure was significantly increased in the portal hypertensive rat models. Mean arterial pressures were lower in portal hypertensive rats than in sham operated controls, indicating the presence of the hyperdynamic state.

Table 1 : Characteristics of the different portal hypertensive models and sham-operated control group.

	Sham (n=10)	**TAA** (n=9)	**BDE** (n=10)	**PPVL** (n=10)
Portal pressure (mmHg)	5.7 ± 0.1	12.1 ± 0.8*	13.5 ± 0.9*	12.5 ± 0.9*
Mean arterial pressure (mmHg)	127 ± 4.7	88 ± 8*,**	110 ± 4.7*	109 ± 3.8*
Serum creatinine (mg%)	0.6 ± 0.03	0.6 ± 0.01	0.4 ± 0.03***	0.7 ± 0.03
Serum Na^{+} (mEq/L)	143.2 ± 0.7	143.4 ± 1.5	141.1 ± 1.0	143.7 ± 1.2
Creatinine clearance (mL/h/100g)	9.0 ± 0.4	9.9 ± 0.5	10.2 ± 0.5	9.0 ± 0.3
AST (U/L)	56.7 ± 5.3	192.3 ± 14.4$^{\Delta}$	99.7 ± 22.6	60.0 ± 25.1
γGT (U/L)	2.0 ± 0.0	18 ± 2*	19.5 ± 4.2*	3.2 ± 1.2
Bilirubin (mg%)	0.1 ± 0.0	0.24 ± 0.04†	9.8 ± 3.2†	0.1 ± 0.0
APB-t-constant	-8.7 ± 0.8	-4.8 ± 0.8†	-6.9 ± 0.7†	-9.7 ± 1.6

Data expressed as mean ± SEM. * $P < 0.05$ vs sham operated animals, ** $P < 0.05$ vs BDE and PPVL rats, *** $P < 0.05$ vs sham, TAA and PPVL rats, $^{\Delta}P < 0.05$ vs sham, BDE and PPVL rats, $^{\dagger}P < 0.05$ vs sham and PPVL rats. Abbreviations: TAA, thioacetamide; BDE, bile duct excised; PPVL, partial portal vein ligated; AST, aspartate aminotransferase; γGT, gamma-glutamyltransferase; ABT-k, aminopyrine breath test constant

Creatinine clearances of all groups were comparable. Biochemically, cirrhotic rats showed increased aminotransferases as well as γGT levels. Impaired hepatocyte microsomal function was clearly shown in cirrhotic rats.

3.2. Hepatic NOS activity

In TAA and BDE rats, intrahepatic NOS activity was markedly decreased compared to sham-operated animals ($P < 0.05$). PPVL rats had values similar to sham-operated rats (Fig. 2).

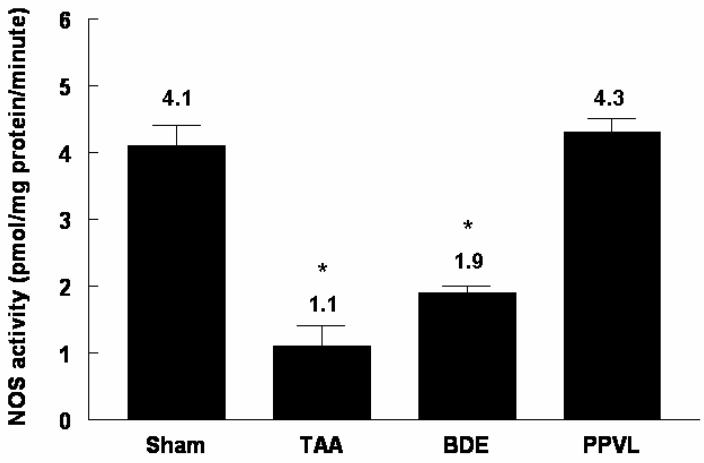


Fig. 2. Specific NOS activity on liver homogenates in the different models of PHT (n=8 per group). Both cirrhotic groups, TAA and BDE, showed significantly decreased NOS activity. (*$P < 0.05$ vs sham-operated rats).

3.3. eNOS western blot analysis and immunohistochemistry

Western blotting performed on liver homogenates showed decreased amounts of eNOS protein in TAA-cirrhosis, which by densitometric analysis reached 75 ± 5 % of the signal obtained in sham-operated controls ($P < 0.05$) (Fig. 3.A). In the two other PHT models, the amount of eNOS protein expression was comparable to that of control rats (Fig. 3).

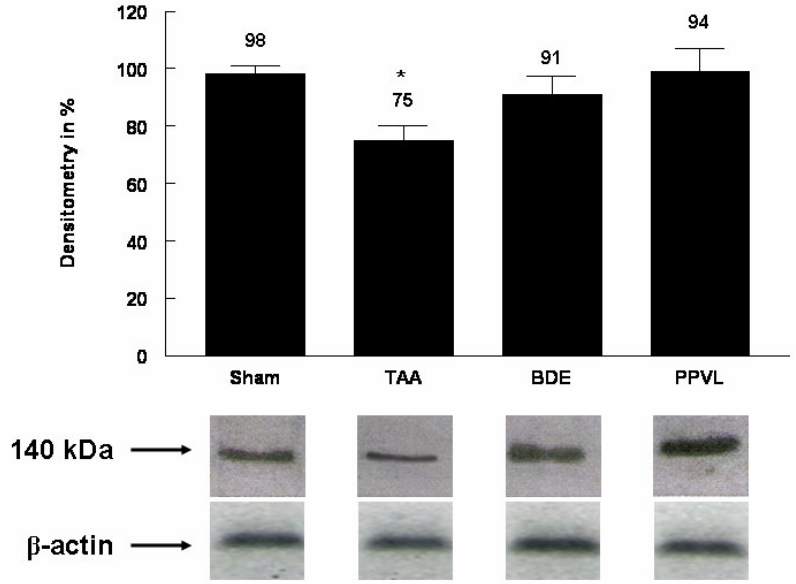
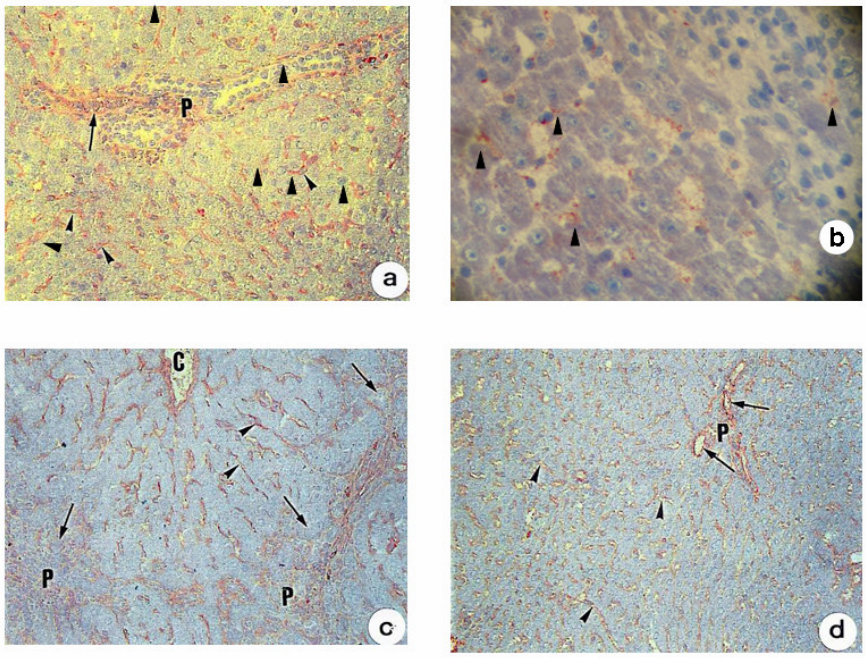


Fig. 3. Densitometric analysis of Western blots from sham-operated, TAA-cirrhotic, BDE and PPVL rats (n=5 per group) (*$P < 0.05$ vs sham-operated rats).

A representative blot of eNOS protein for the different experimental groups is shown.

A



B

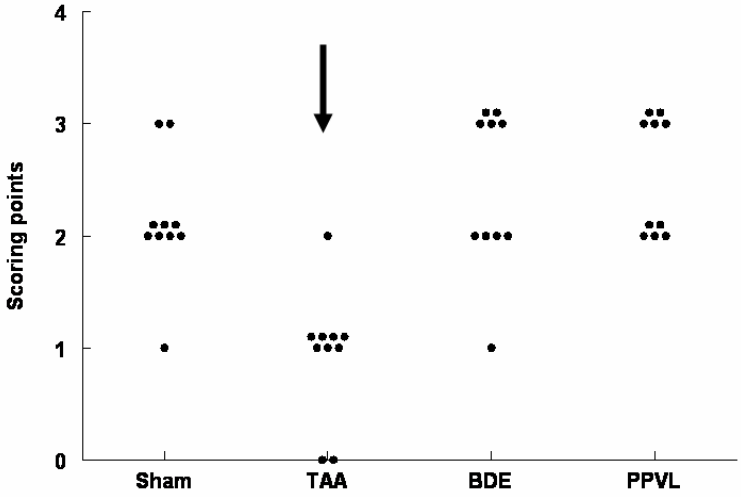


Fig. 4. A. eNOS immunohistochemistry. Liver biopsies whereby the brown colour in the sinusoidal lining cells and endothelium of portal tract vessels signals the eNOS protein. Portal tract (P), central vein (C):

a) Sham operated rats (magnification x 25): eNOS reactivity in the portal vessel endothelium (arrow); homogenous eNOS reactivity in the sinusoidal lining cells (arrowheads);
b) TAA-cirrhosis (magnification x 100): diminished eNOS reactivity in the sinusoidal lining endothelial cells (arrowheads) as compared to the sham-operated animals;
c) BDE (magnification x 25): eNOS expression (arrowheads) comparable to that of sham control; bile ductules (arrows);
d) PPVL (magnification x 25): eNOS reactivity (arrowheads) similar to that of sham and BDE liver biopsies; portal vessels (arrows).

B. Semi-quantitative evaluation of eNOS immunohistochemistry in liver biopsies in the different rat models: no (0), weak (1), moderately strong (2), strong reactivity (3) and maximal reactivity (4). (vertical arrow, $P < 0.001$ versus other groups).

Immunoreactivity for eNOS in normal liver and in the models of PHT, was seen homogeneously distributed in endothelial cells lining portal tract vessels and sinusoids. Only TAA cirrhotic livers showed a decreased sinusoidal expression (Fig. 4.A.b). A semi-quantitative score of the eNOS immunohistochemical expression in the different rat models, is shown in Fig. 4.B.

3.4. Plasma levels of ADMA and SDMA

The plasma concentration of ADMA in sham-operated rats (0.69 ± 0.37 μM) and in TAA cirrhotic rats (0.58 ± 0.10 μM) were similar, while in BDE rats levels were significantly higher (2.92 ± 0.59μM) ($P < 0.001$ vs other groups) (Fig. 5).

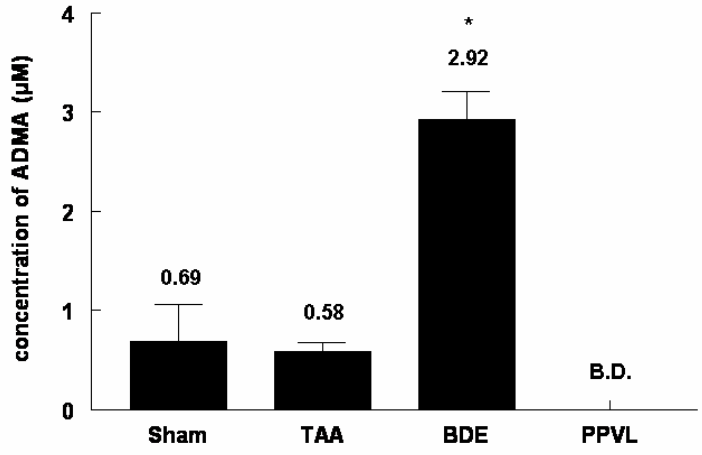


Fig. 5. Plasma levels of ADMA. BDE rats showed significantly higher levels than all other groups (*$P < 0.001$) (n=8 per group). B.D. = below detection limit.

Plasma SDMA levels were 0.42 ± 0.13 μM for sham-operated rats, 0.33 ± 0.17 μM for TAA cirrhotic rats and 0.46 ± 0.22 μM for biliary cirrhotic rats (P = NS between sham, TAA and BDE). ADMA and SDMA levels of PPVL rats were below detection limit.

3.5. The hepatic vascular response to ADMA in the perfused rat liver

3.5.1. Normal rats

In methoxamine-preconstricted normal rat livers injected with vehicle, an incremental vasorelaxation in response to cumulative doses of acetylcholine was observed (Fig. 6).

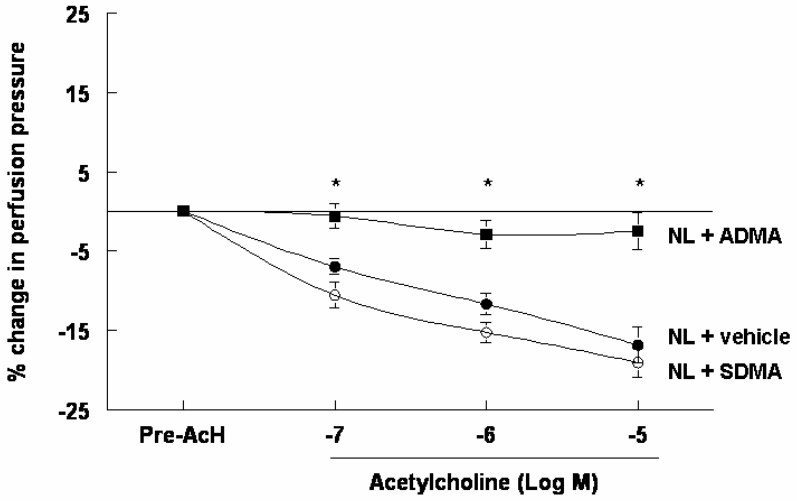


Fig. 6. Dose-response curves to cumulative doses of acetylcholine in in-situ perfused normal rat livers (n=5 for each condition): comparison of normal livers incubated with vehicle (●) versus with ADMA 10^{-3}M (■) or SDMA 10^{-3}M (o). *P < 0.001 (■) versus (●) and (o) (ANOVA). Abbreviations: NL, normal liver; ADMA, asymmetric dimethylarginine; SDMA, symmetric dimethylarginine.

In contrast, livers incubated with ADMA, exhibited markedly less relaxation to acetylcholine at 10^{-7} M (-0.6 ± 1.6% versus -7.0 ± 0.7% [ADMA versus vehicle], P = 0.006), 10^{-6} M (-2.9 ± 1.8% versus -11.7 ± 1.3%, P = 0.016) and 10^{-5} M (-2.5 ± 2.4%

versus -16.9 ± 2.3%, $P = 0.002$) (Fig. 4). SDMA, the vasoinactive stereoisomer of ADMA, showed a similar concentration-effect curve as vehicle (10^{-7} M: -10.6 ± 1.9% versus -7.0 ± 0.7%; 10^{-6} M: -15.3 ± 1.7% versus -11.7 ± 1.3%; 10^{-5} M: -18.6 ± 1.6% versus -16.9 ± 2.3%, all NS) (Fig. 4).

When ADMA was compared to L-NAME, no significant differences were noted: 10^{-7} M: -0.6 ± 1.6% for ADMA versus -2.3 ± 1% for L-NAME; 10^{-6} M: -2.9 ± 1.8% versus -5.7 ± 1%; 10^{-5} M: -2.5 ± 2.4% versus -8.4 ± 2.2%, all NS (Fig. 7).

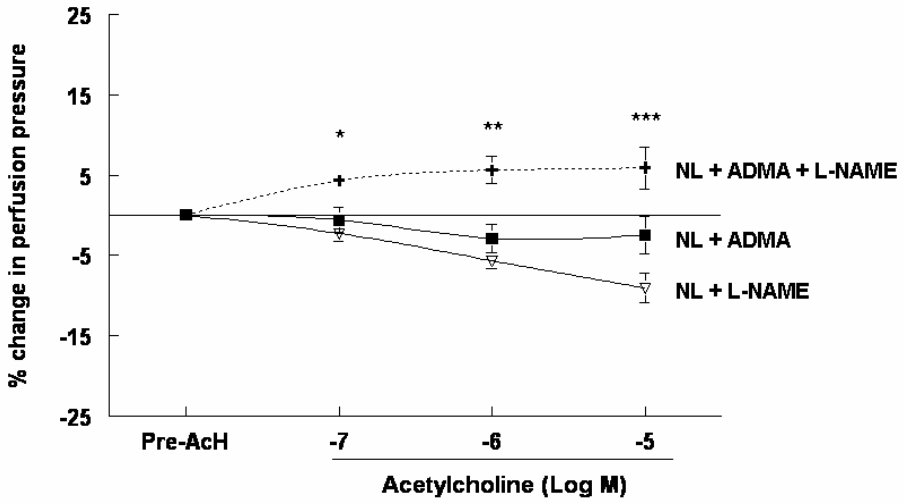


Fig. 7. Dose-response curves to cumulative doses of acetylcholine in in-situ perfused normal rat livers (n=5 for each condition): comparison of normal livers incubated with ADMA 10^{-3}M (■) versus with L-NAME 10^{-3}M (∇) or combined ADMA 10^{-3}M + L-NAME 10^{-3}M (+) . *$P < 0.05$ (+) versus (■) and (∇), **$P < 0.001$ (+) versus (■) and (∇), ***$P < 0.05$ (+) versus (∇) (ANOVA). Abbreviations: NL, normal liver; ADMA, asymmetric dimethylarginine; L-NAME, N^G-nitro-L-arginine-methyl ester

As for ADMA, a similar significant difference was noted for L-NAME versus vehicle (10^{-7} M: $P = 0.005$, 10^{-6} M: $P = 0.006$, 10^{-5} M : $P = 0.028$). When preincubation of ADMA was combined with L-NAME, a similarly increased perfusion pressure for all concentrations of acetylcholine was noted (10^{-7} M: 4.3 ± 0.8, 10^{-6} M: 5.6 ± 1.7, 10^{-5} M : 5.9 ± 2.6, P=0.590) (Fig. 5). This increased perfusion pressure was significant compared to L-NAME or ADMA alone (for each concentration of Ach, $P < 0.001$)

3.5.2. BDE cirrhotic rats

In BDE cirrhotic rats, the effect of acetylcholine was blunted compared to normal livers preincubated with vehicle: 10^{-7}M: -1.7 ± 0.9% versus -7.0 ± 0.7% ($P = 0.002$), 10^{-6} M: -5.7 ± 0.8% versus -11.7 ± 1.3% ($P = 0.005$) and 10^{-5} M: -8.1 ± 0.9% versus -16.9 ± 2.3% ($P = 0.007$) (Fig. 8).

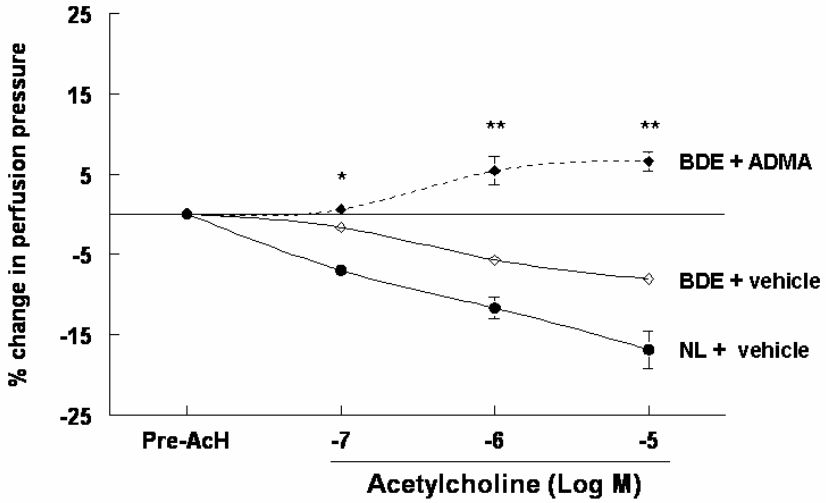


Fig. 8. Dose-response curves to cumulative doses of acetylcholine in in-situ perfused rat livers: comparison of BDE cirrhotic rat livers with (♦) or without preincubation of ADMA (◇) vs normal rat livers with vehicle (●). *$P < 0.001$ (♦) versus (●), **$P < 0.001$ (♦) versus (◇) and (●).

This impaired relaxation was further impaired in BDE rats when preincubated with ADMA 10^{-3}M, which resulted in paradoxical vasoconstriction (at 10^{-7}M 0.6 ± 0.1%, at 10^{-6} 5.4 ± 1.8% and at 10^{-5} 6.6 ± 1.2%, all $P < 0.05$ vs BDE liver incubated with vehicle) (Fig. 8).

3.5.3. TAA cirrhotic rats

As in BDE rats, pre-ascitic TAA cirrhotic rats showed endothelial dysfunction compared to normal livers when preincubated with vehicle: 10^{-7}M: -0.8 ± 0.6% versus -7.0 ± 0.7% (P = 0.008), 10^{-6} M: -1.9 ± 1.6% versus -11.7 ± 1.3% (P = 0.001) and 10^{-5} M: -5.0 ± 1.8% versus -16.9 ± 2.3% (P = 0.004). Addition of ADMA to perfused TAA cirrhotic livers did not significantly alter the response to acetylcholine when compared to TAA cirrhotic liver incubated with vehicle (at 10^{-7}M 0.6 ± 1.1%, at 10^{-6} -1.2 ± 1.6% and at 10^{-5} -2.6 ± 2.2%, all NS compared to TAA cirrhosis without ADMA) (Fig. 9).

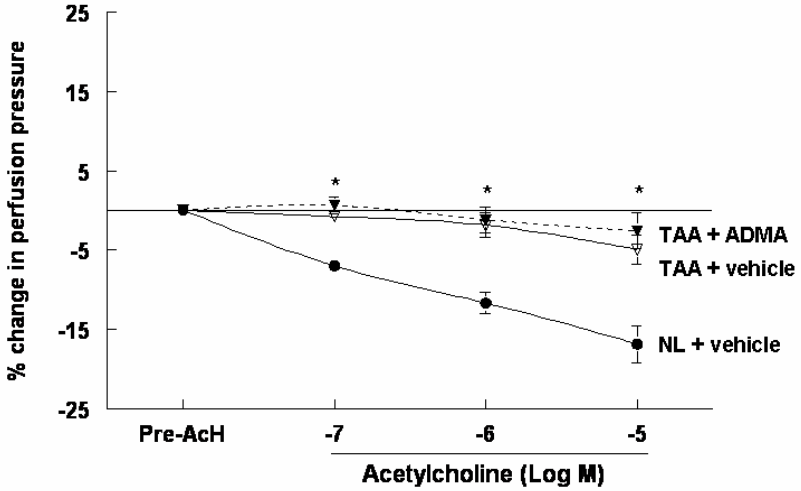


Fig. 9. Dose-response curves to cumulative doses of acetylcholine in in-situ perfused rat livers: comparison of TAA cirrhotic lives with (▼) or without preincubatioin with ADMA (∇) versus normal rat livers with vehicle (●). *P < 0.05 (▼) and (∇) versus (●).

3.6. NOx in perfusates

Comparison of NOx concentration before methoxamine administration and after the dose-response to acetylcholine, showed a comparable decrease in NOx levels in healthy livers incubated with ADMA or L-NAME : -29.6 ± 3.1 nM and -29 ± 10.9 nM respectively ($P < 0.05$ vs SDMA and vehicle). Normal livers incubated with both L-NAME and ADMA showed a further decrease in NOx levels (-52.9 ± 5.4 nM), which approached significance (P=0.062 vs normal rats incubated with ADMA or L-NAME alone) (Fig. 10).

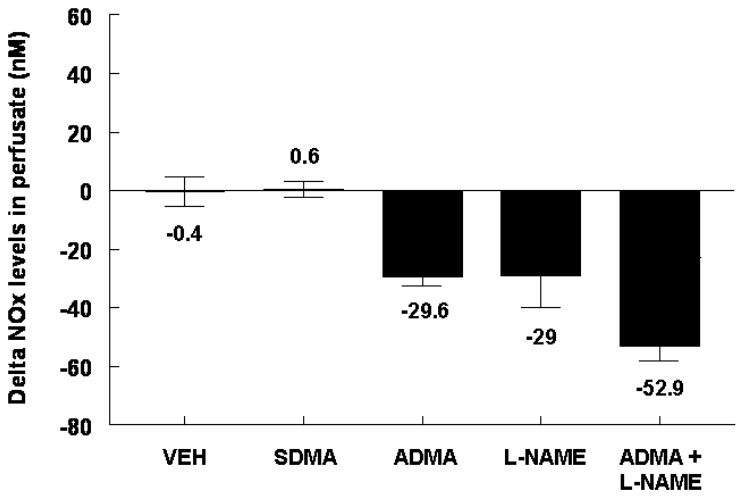


Fig. 10. Difference in NOx concentration in normal perfused rat livers before the administration of methoxamine and immediately after the end of the dose-response to acetylcholine in the different conditions. *$P < 0.05$ versus SDMA and VEHICLE.

3.7. ADMA in bile and perfusates

In a subset of BDE rats (n=4), bile was obtained by puncture of the extrahepatic bile duct. ADMA was undectable in bile.

In perfusate samples taken either just before the administration of methoxamine or at the end of an experiment in normal, TAA and BDE rats infused with vehicle, ADMA was undetectable. When incubated with 10^{-3} M ADMA, at the end of the perfusion experiment 264 ± 53.8µM and 290.7 ± 32.3 µM was retrieved in the perfusate of normal (n=5) and TAA rats (n=5), respectively. In BDE rats (n=5) the recovery was significantly higher : 656.8 ± 59.9 µM (P = 0.007). The associated removal rates are shown in Fig. 11.

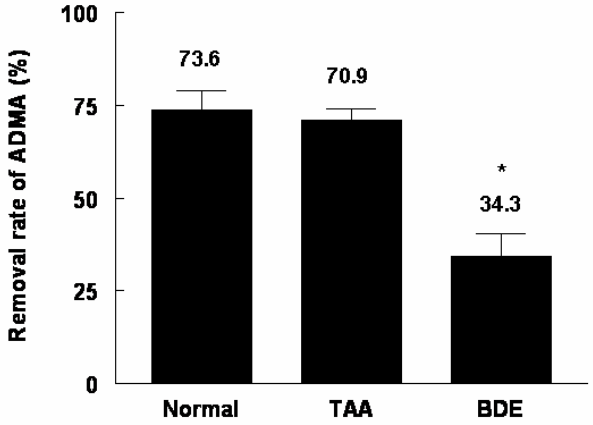


Fig. 11. Removal rates at the end of dose-response curves to acetylcholine in normal, TAA and BDE rats preincubated with or without 10^{-3}M ADMA (*P < 0.001 versus normal and TAA rats).

4. DISCUSSION

Decreased eNOS-derived NO production is presumed to play a pivotal role in the increased IHVR in cirrhotic portal hypertension (4-6,22). However, different morphological types of cirrhosis and portal hypertension exist depending on the etiology (23). We therefore investigated whether the pathophysiology of PHT might differ amongst these different conditions. For this purpose, we used three rat models of PHT, namely TAA, BDE and PPVL, which are representative of different conditions of portal hypertension seen in humans.

Upon characterization of the different models with regard to eNOS, we observed decreased eNOS activity in both cirrhotic animal models, in agreement with what is generally accepted (4). However, eNOS protein, assayed immunohistochemically in endothelial cells lining portal vessels and sinusoids and by western blot of liver homogenates, was decreased only in TAA cirrhosis, suggesting decreased eNOS enzyme level in this model, consistent with previous reports (24). In rats with CCl_4 cirrhosis, another non-biliary cirrhotic rat model, we previously documented a similarly decrease in eNOS expression and showed that restoration of hepatic eNOS by gene transfer led to a decrease in portal hypertension, further supporting the hypothesis that eNOS enzyme levels are diminished (8). Other groups have shown decreased eNOS activity in CCl_4 cirrhotic rats in the presence of unaltered eNOS expression and suggested that NO deficiency is caused by dysfunctional co-factors of eNOS such as caveolin and Akt (9,10). This merely illustrates the complexity of the abnormal intrahepatic eNOS-regulation depending on different conditions and hightlights the need for further study.

In biliary cirrhosis, however, normal eNOS protein, both by immunohistochemistry and by western blot, was found despite decreased NOS activity. These findings suggest that the pathogenesis of deficient intrahepatic NO production might differ depending on the

etiology of cirrhosis. Further support for this hypothesis comes from the observation that eNOS gene transfer in BDE rats did not restore a normal vasodilatory response whereas in CCl_4 cirrhotic rats it did (8,25).

Since the level of eNOS enzyme is unaltered in our biliary cirrhotic rats, the cause of decreased NOS activity remains to be explained. Theoretically, eNOS malfunction might originate either from a direct inhibition of eNOS or indirect through dysfunctional co-factors. Shah et al. (25,26) supported the latter hypothesis by showing that enhanced hepatic caveolin-1 protein levels in BDE rats could reduce NOS activity since NOS activity was partially restored when excess calmodulin, a protein that competitively binds eNOS from caveolin, was added to liver lysates.

Data supporting direct NOS inhibition intrahepatically have not been reported yet, but a role for ADMA has been proposed (13,14). In the current study, we investigated whether ADMA could be related to intrahepatic endothelial dysfunction. Plasma ADMA levels were increased only in biliary cirrhotic rats. However, increased plasma levels do not necessarily imply intrahepatic NOS inhibiting features and subsequent hemodynamic effects. Therefore, we assessed the vasomotor endothelial function by measuring the vasorelaxing response to acetylcholine. Acetylcholine couples to its endothelial muscarinic M_3 receptor and stimulates eNOS to produce the vasodilatory NO (7,27). We could demonstrate an impaired endothelium-dependent vasodilator reaction, also called "endothelial dysfunction", when we perfused normal livers with ADMA. In contrast to ADMA, SDMA, its vasoinactive stereoisomer, did not induce this impaired vasomotor reaction, corroborating its vasoinactive properties. The effect of ADMA mimicked those of L-NAME, a well-known NOS inhibitor (28). ADMA induced a decrease in NOx levels, suggesting that ADMA causes intrahepatic endothelial dysfunction via NOS inhibition. When ADMA was administrated togheter with L-NAME a synergism arose towards a

positive perfusion pressure, or paradoxical vasoconstriction, which was associated with a further decrease in NOx levels. In this perfusion system, this probably results from the concurrent vasoconstrictor response following endothelial stimulation via acetylcholine and the total loss of eNOS stimulation since in the combined ADMA-L-NAME incubated rats the dose-related respons to acetylcholine is immediately lost and rises to a steady-state positive perfusion pressure (7,27). In perfused BDL and TAA cirrhotic rats, endothelial dysfunction was already present upon preincubation with vehicle. This was as expected in the chronically injured liver, an observation documented by others (7,25). However, when ADMA was added in BDE rats, the endothelial dysfunction was further aggravated and resulted in paradoxical vasoconstriction, which would seem evident in an environment where vasoconstrictors are highly upregulated (1,6,29,30) and an already dysfunctional eNOS were to be further impeded or even fully inhibited. In contrast, in TAA rats the decreased vasorelaxing capacity was not further impaired, which further supports the hypothesis that decreased eNOS enzyme levels are causative.

The last question involves elucidating why ADMA plasma concentrations were highest in biliary cirrhosis. Renal and hepatic function as well as the degree of portal hypertension in BDE rats were similar to that seen in TAA rats and can therefore not explain the difference between our models. The presence of cholestasis, a cardinal feature of biliary cirrhosis, might suggest that biliary constituents are causative for elevated ADMA levels. Dimethyl-arginine dimethylaminohydrolase (DDAH), the enzyme responsible for the degradation of ADMA, is highly expressed in the liver, rendering the liver a key organ in the degradation of ADMA (12,31). We showed that the removal rate of ADMA in BDE liver is lower than in normal or non-biliary cirrhotic livers. This argues in favour of decreased DDAH activity in BDE rats. Cooke and colleagues (32) have suggested that DDAH is oxidant labile, and thus subject to inhibition by oxidants derived from endothelial superoxide. Recent evidence

suggests that cholestasis causes liver injury by mechanisms involving mitochondrial oxidative stress (33-36). Therefore, a decrease in DDAH activity in cholestatic livers caused by oxidative damage to the enzyme, might explain the increased plasma ADMA levels in BDE rats. The possibility that ADMA accumulation may be due to mechanical biliary obstruction in BDE rats, was ruled out by indectectable bile levels of ADMA.

The apparent discrepancy between measured plasma levels of ADMA (10^{-6}M) in biliary cirrhotic rats and the concentration of ADMA needed (10^{-3}M) in the perfused healthy rat liver can be explained by the rather high Michaelis constant (K_M) of DDAH (above 100 μM), which is the substrate concentration at which the reaction rate is half of its maximal value (12). Under certain conditions, inhibition of DDAH is known to result in very high local concentrations of ADMA, further raising the question as to whether plasma levels adequately reflect biologically active ADMA or indeed represent a marker of high intracellular levels (12,37,38).

In conclusion, we demonstrated that the pathogenesis of defective intrahepatic NO production depends on the etiology of the underlying cirrhosis. Whereas in TAA cirrhosis the decreased intrahepatic NO bioavailability originates from a lowered eNOS enzyme level and activity, in our rats with biliary cirrhosis the eNOS enzyme level was unaltered. In this latter condition, the decreased NOS activity should therefore arise from eNOS dysfunction. ADMA might be one of the molecules responsible for this NOS inhibition.

5. REFERENCES

1. Bosch J, Garcia-Pagan JC. Complications of cirrhosis. I. Portal hypertension. J Hepatol 2000; 32(Suppl. 1): 141-156.
2. Gupta TK, Chen L, Groszmann RJ. Pathophysiology of portal hypertension. Baillieres Clin Gastroenterol 1997; 11: 203-219.
3. Bhatal PS, Grossman HJ. Reduction of the increased intrahepatic vascular resistance of the isolated perfused cirrhotic rat liver by vasodilators. J Hepatol 1985; 1: 325-337.
4. Wiest R, Groszmann RJ. The paradox of nitric oxide in cirrhosis and portal hypertension: Too much, not enough. Hepatology 2002; 35: 478-491.
5. Gupta TK, Toruner M, Chung MK, Groszmann RJ. Endothelial dysfunction and decreased production of nitric oxide in the intrahepatic microcirculation of cirrhotic rats. Hepatology 1998; 28: 926-931.
6. Rockey DC. The cellular pathogenesis of portal hypertension: stellate cell contractility, endothelin and nitric oxide. Hepatology 1997; 25: 2-5.
7. Graupera M, Garcia-Pagan JC, Pares M, et al. Cyclooxygenase-1 inhibition corrects endothelial dysfunction in cirrhotic rat livers. J Hepatol 2003; 39: 515-521.
8. Van de Casteele M, Omasta A, Janssens S, et al. In vivo gene transfer of endothelial nitric oxide synthase decreases portal pressure in anaesthetised carbon tetrachloride cirrhotic rats. Gut 2002; 51: 440-445.
9. Shah VJ, Toruner M, Haddad F, et al. Impaired endothelial nitric oxide synthase activity associated with enhanced caveolin binding in experimental cirrhosis in the rat. Gastroenterology 1999; 117: 1222-1228.
10. Moralez-Ruiz M, Cejudo-Martin P, Fernandez-Varo G, et al. Transduction of the liver with activated Akt normalizes portal pressure in cirrhotic rats. Gastroenterology 2003; 125: 522-531.
11. Vallance P, Leone A, Calver A, Collier J, Moncada S. Accumulation of an endogenous inhibitor of nitric oxide synthesis in chronic renal failure. Lancet 1992; 339: 572-576.
12. Vallance P, Leiper J. Cardiovascular biology of the asymmetric dimethylarginine : dimethylarginine dimethylaminohydrolase pathway. Arterioscler Thromb Vasc Biol 2004; 24: 1-9.
13. Nijveldt RJ, Teerlink T, Siroen MPC, et al. The liver is an important organ in the metabolism of asymmetrical dimethylarginine (ADMA). Clin Nutr 2003; 22: 17-22.
14. Nijveldt RJ, Teerlink T, Van der Hoven B, et al. Asymmetrical dimethylarginine (ADMA) in critically ill patients: high plasma ADMA concentration is an independent risk factor of ICU mortality. Clin Nutr 2003; 22: 23-30.
15. Langer DA, Shah VH. A gas, an amino acid, and an imposter: the story of nitric oxide, L-arginine, and ADMA in portal hypertension. Hepatology 2005; 42: 1255-1257.
16. Kountouras J, Billing BH, Scheuer PJ. Prolonged bile duct obstruction: a new experimental model for cirrhosis in the rat. Br J Exp Path 1984; 65: 305-311.
17. Blanchet L, Lebrec D. Changes in splanchnic blood flow in portal hypertensive rats. Eur J Clin Invest 1982; 12: 327-330.
18. Van Roey G. Pathogenesis of sodium retention and of ascites formation in experimental cirrhosis in rats. Acta Biomedica Lovaniesa 137. 1996.
19. Van de Casteele M, Omasta A, Janssens S, et al. In vivo gene transfer of endothelial nitric oxide synthase decreases portal pressure in anaesthetised carbon tetrachloride cirrhotic rats. Gut 2002; 51: 440-445.
20. Bradford MM. A rapid and sensitive method for the quantitation of microgram quantities of protein utilizing the principle of protein dye binding. Anal Biochem 1976; 72: 248-254.
21. Teerlinck T, Nijveldt RJ, de Jong S, Van Leeuwen P. Determination of arginine, asymmetrical dimethylarginine and symmetric dimethylarginine in human plasma and other biological samples by high performance liquid chromatography. Anal Biochem 2002; 303: 131-137.
22. Shah VJ. Cellular and molecular basis of portal hypertension. Clin Liv Dis 2001; 5: 629-644.
23. Roskams T, Baptista A, Bianchi L, et al. Histopathology of portal hypertension: a practical guideline. Histopathology 2003; 42: 2-13.
24. Petermann H, Vogl S, Schulze E, Dargel R. Chronic liver injury alters basal and stimulated nitric oxide production and 3H-thymidine incorporation in cultured sinusoidal endothelial cells from rats. J Hepatol 1999; 31: 284-292.
25. Shah V, Cao S, Hendrickson H, Yao J, Katusic ZS. Regulation of hepatic eNOS by caveolin and calmodulin after bile duct ligation in rats. Am J Physiol Gastrointest Liver Physiol 2001; 280: G1209-1216.

26. Hendrickson H, Chatterjee S, Cao S, et al. Influence of caveolin on constitutively activated recombinant eNOS: insights into eNOS dysfunction in BDL rat liver. Am J Physiol Gastrointest Liver Physiol. 2003; 285: G652-660.
27. Aleixandre de Artinano A, Lopez-Miranda Gonzalez V. Endothelial dysfunction and hypertensive vasoconstriction. Pharmacol Res 1999; 40: 113-124.
28. Pfeiffer S, Leopold E, Schmidt K, Brunner F, Mayer B. Inhibition of nitric oxide synthesis by N^G-nitro-L-arginine methyl ester (L-NAME): requirement for bioactivation to the free acid, N^G-nitro-L-arginine. Br J Pharmacol 1996;118:1433-1440.
29. Rockey DC. Vascular mediators in the injured liver. Hepatology 2003; 37: 4-12.
30. Tieche S, De Gottardi A, Kappeler A, et al. Overexpression of endothelin-1 in bile duct ligated rats: correlation with activation of hepatic stellate cells and portal pressure. J Hepatol 2001; 34: 38-45.
31. Cam TL, Leiper JM, Vallance P. The DDAH/ADMA.NOS pathway. Atherosclerosis Supplements 2003; 4: 33-40.
32. Stuhlinger MC, Abbasi F, Chu JW, et al. Relationship between insulin resistance and an endogenous nitric oxide synthase inhibitor. JAMA 2002; 287: 1420–1426.
33. Zhong Z, Froh M, Wheeler MD, et al. Viral gene delivery of superoxide dismutase attenuates experimental cholestasis-induced liver fibrosis in the rat. Gene Ther 2002; 9: 183-191.
34. Perez MJ, Macias RI, Duran C, Monte MJ, Gonzalez-Buitrago JM, Marin JJ. Oxidative stress and apoptosis in fetal rat liver induced by maternal cholestasis. Protective effect of ursodeoxycholic acid. J Hepatol 2005; 43: 324-332.
35. Sokol RJ, Straka MS, Dahl R, et al. Role of oxidant stress in the permeability transition induced in rat hepatic mitochondria by hydrophobic bile acids. Pediatr Res 2001; 49: 519-531.
36. Ljubuncic P, Fuhrman B, Oiknine J, Aviram M, Bomzon A. Effect of deoxycholic acid and ursodeoxycholic acid on lipid peroxidation in cultured macrophages. Gut 1996; 39: 475-478.
37. MacAllister RJ, Parry H, Kimoto M, et al. Regulation of nitric oxide synthesis by dimethylarginine dimethylaminehydrolase. Br J Pharmacol 1996; 119: 1533-1540.
38. Ito A, Tsao PS, Adimoolam S, Kimoto, Ogawa T, Cooke JP. Novel mechanisms for endothelial dysfunction: dysregulation of dimethylarginine dimethylaminehydrolase. Circulation 1999; 99: 3092-3095.

Chapter 6

Both thromboxane A_2, a vasoconstrictive cyclooxygenase-metabolite, and nitric oxide are involved in the increased intrahepatic vascular tone associated with thioacetamide-induced cirrhosis in the rat

W. Laleman, L. Van Landeghem, T. Severi, I. Vander Elst, M. Zeegers,
J. Fevery and F. Nevens

Department of Hepatology,
University Hospital Gasthuisberg, KU Leuven, Belgium

1. INTRODUCTION

From the previous studies, it is clear that the vascular endothelium has emerged as an important modulator of vascular tone (1-5). In physiological conditions, the vascular tone is stably maintained through a balanced synthesis of various vasodilating and vasoconstricting substances that act in a paracrine fashion on an underlying contractile effector (Fig. 1) (1,2). Perturbation of this balance results in endothelial dysfunction, which is defined as an imbalance between the synthesis, release or effect of those vasoactive endothelial factors and which is considered one of the main pathological mechanisms in the increased vascular tone observed in disorders such as essential hypertension, pulmonary hypertension, diabetes and atherosclerosis (6). More specifically in these conditions, endothelial dysfunction has been attributed to decreased nitric oxide (NO) bioavailability secondary to either decreased production or to increased degradation of NO (7-10). Alternatively, increased production of vasoconstrictors has also been implicated, such as endothelin-1 (11,12), vasopressin (13), catecholamines (14), the renin-angiotensin-aldosterone system (15) and PGH_2/thromboxane A_2 (TXA_2) (16-19).

In cirrhosis, a similar imbalance between the expression of vasoconstrictors (endothelins, catecholamines, angiotensin-II, vasopressin, …) and the release of the vasodilator NO (as shown in chapter 4 and 6), may result in increased intrahepatic vascular tone, leading to portal hypertension (1-5,20,21). Furthermore, the vascular territory of the cirrhotic liver also exhibits a hyperresponsiveness to most of the previously mentioned vasoconstrictors (22,23). It has been suggested that both mechanisms could account for a reduced NO biodisponibility (21). However, the ultimate mechanism responsible for these events has not been fully elucidated.

Recent studies regarding endothelial dysfunction in the context of essential hypertension have stressed the importance of prostaglandins, in particular TXA_2. Prostaglandins are

formed following the oxygenation of arachidonic acid by the cyclooxygenase (COX) pathway. Two COX iso-enzymes (COX-1 and COX-2) are known. COX-1 is a constitutive enzyme that is expressed in nearly all tissues under basal conditions and is involved in immediate prostanoid biosynthesis within minutes after stimulation (24,25). COX-2 is an inducible enzyme that may be expressed in many cell types in response to several stimuli, such as cytokines and endotoxin, and is involved in delayed prostanoid biosynthesis (26-30). Normal rat liver has been shown to express COX-1 but not COX-2 protein (31). In cirrhotic human liver on the other hand, COX-2 expression has recently been described in hepatocytes (32). In addition, isolated Kupffer cells from rat livers with steatonecrosis and cirrhosis were found to present an imbalance in COX metabolites with an overproduction of TXA_2 and a decrease of prostaglandin E_2 (33). It seems therefore possible that the binding of different vasoconstrictors to G-protein coupled receptors increases the release of arachidonic acid and results in an overproduction of vasoconstrictive prostanoids, contracting the hepatic vascular bed and contributing to the observed increase in IHVR of cirrhotic livers. Moreover, many endothelium-derived factors, such as NO and prostaglandins, share a number of common functions although they are part of different metabolic pathways (23). In vascular endothelial cells, pharmacological manipulation of one pathway has been shown to result in cross-modulation of the other, but whether this also happens in the cirrhotic liver remains unknown (23, 32-35). We therefore aimed to evaluate the role of thromboxane A_2 (TXA_2), a COX-derived vasoconstrictor prostanoid, in the increased intrahepatic vascular tone associated with cirrhosis, and to evaluate a possible interaction with NO (Fig 1).

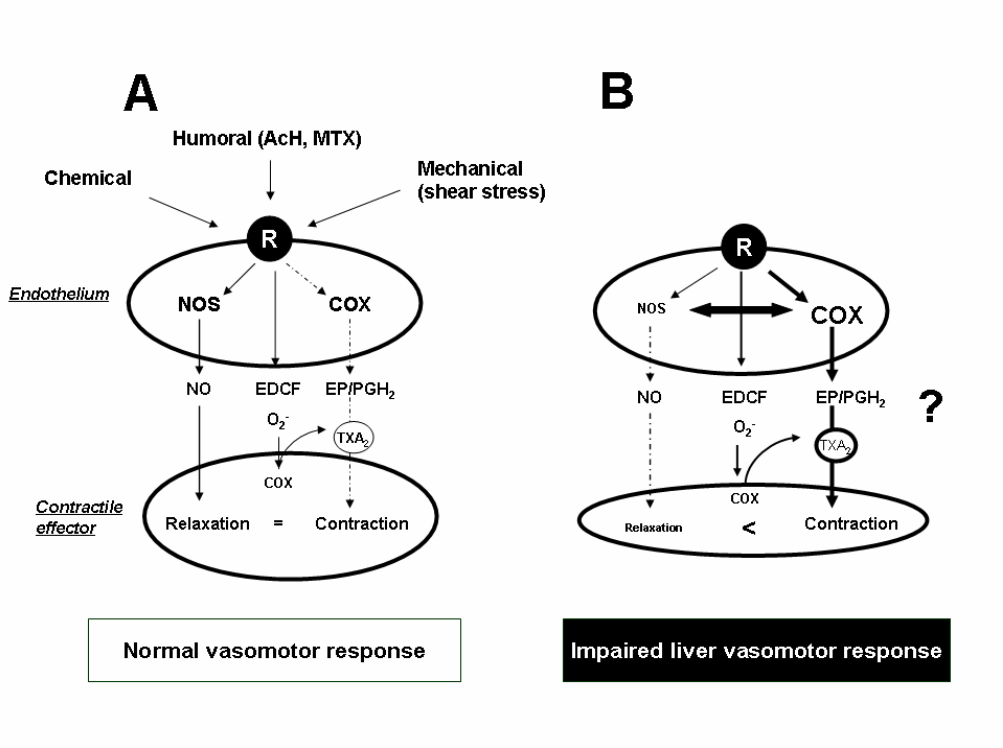


Fig. 1: A. Normal endothelium. B. Proposed hypothesis of mode of action of TXA_2 in the increased intrahepatic vascular tone and its relation to NOS. (Ach, acetylcholine; MTX, methoxamine; NOS, nitric oxide synthase; COX, cyclooxygenase; NO, nitric oxide; EDCF, endothelial constricting factor; O_2^-, superoxide, EP, endoperoxides; PGH_2, prostaglandin H_2; TXA_2, thromboxane A_2)

2. MATERIALS AND METHODS

Materials and methods used for these experiments have been described in chapter 3 or chapter 4. Additional information regarding certain aspects of the experiments are given below.

2.1. TAA-induced cirrhosis

All studies were performed in cirrhotic animals (n= 60 in total) that underwent chronic exposure to TAA, given in drinking water for 18 weeks, as described in chapter 4. Normal rats were used as internal controls in the perfusion experiments (n=35) and for the isolation of hepatic stellate cells (n=3).

2.2. In-situ rat liver perfusion study

Increased intrahepatic vascular tone was assessed through the evaluation of endothelial function (n=5 per condition) and responsiveness to vasoconstrictors (n=5 per condition), as described earlier. Experimental design of the perfusion studies:

2.2.1. Effect of NOS-inhibition

To evaluate the effect of NO-inhibition on endothelial function and portal pressure response to methoxamine, the NOS-inhibitor L-NAME 10^{-3}M was preincubated.

2.2.2. Involvement of cyclooxygenase-metabolites or prostanoids

To test the the hypothesis that cyclooxygenase-metabolites were involved, the non-isoform-selective cyclooxygenase-inhibitor flurbiprofen was used. Flurbiprofen (125 and 250μM) or vehicle (DMSO : isotonic saline) were added to the perfusate of perfused cirrhotic rats after the stabilization period. The preparation was allowed to stabilize for 15 minutes before the start of the experiment.

2.2.3. Involvement of TXA_2, a vasoconstrictive cyclooxygenase-metabolite

To support the intrahepatic hemodynamic effects of TXA_2 , a dose-effect curve was established using the TXA_2–analogue U-44619 (Caymann Chem, Michigan, USA).

Additionally, the effect of the TXA_2-receptor antagonist SQ 29,548 (Caymann Chem) was evaluated on endothelial function and responsiveness to methoxamine in the cirrhotic rat liver.

Two mL samples of the perfusate were taken before and after the experiment assessing endothelial function in order to determine TXB_2-production (Caymann Chem), a stable metabolite of TXA_2. TXB_2-production was expressed as the absolute increment over baseline before methoxamine administration.

2.2.4. Effect of combined NOS- and COX-inhibition

For this purpose, L-NAME was preincubated together with flurbiprofen for both the experiments assessing endothelial function and hyperresponsiveness to methoxamine.

2.3. Western blot for TXA_2-synthase and receptor in normal and TAA cirrhotic liver

Fresh liver was homogenized in sucrose-buffer to a final concentration of 0.25g wet weight of liver/mL. Samples were homogenized, sonicated and heated for 5 min at 70°C. After centrifugation at 10000xg for 15 min, protein concentration of the supernatant was determined by the standard Bradford method. Protein samples (30µg) were loaded onto a 12% Tris-Cl gel (Biorad Laboratories, Nazareth, Belgium). Electrophoresis was carried out using the Mini Protean II module (Biorad) according to the manufacturers instructions. After blotting the proteins onto a PVDF membrane (Bio-Rad) the membrane was rinsed in 5% blocking solution (milkpowder) in PBS for 1 h at room temperature to avoid nonspecific binding. Blots were incubated overnight with primary antibodies against thromboxane synthase and receptor (1:800; rabbit Thromboxane synthase/receptor, Minnesota, USA). The next day, the membranes were incubated with horseradish peroxidase-conjugated secondary antibody (SwaR-HRP 1:1000 Prosan, Merelbeke, Belgium) and immunoreactivity was visualized using chemiluminescence detection (ECL-plus, Amersham Biosciences). Densitometric quantification of Western blot signal intensity

was performed with Un-Scan-IT Gel Software (Silk Scientific, Utah, USA) and calculated as the percentage of the mean value from control livers.

2.4. In vitro hepatic stellate cell contraction assay

To prove that HSCs were sensitive to TXA_2-mediated contraction, a subset of collagen matrices were preincubated with 1 and 2.5µM of the TXA_2-receptor antagonist SQ29,548 before adding 5µM U44619, a stable TXA_2-analogue. The effect of flurbiprofen (250µM) and vehicle (DMSO) on FCS-promoted contraction was evaluated by preincubating these compounds before addition of FCS 10%. All data are from experiments using at least 3 sets of 3 collagen lattices containing culture-activated HSCs from 3 different rat HSC isolations (passage 1 to 3).

3. RESULTS

3.1.Evaluation of endothelial function and hyperresponsiveness to methoxamine

As shown in figure 2 and 3 (see also fig. 7.B & 5.C (Chapter 3)), cirrhotic livers, compared to control livers, showed less relaxation to acetylcholine, illustrating the phenomenon of endothelial dysfunction, and exhibited an aggravated response to methoxamine, demonstrating the phenomenon of hyperresponsiveness to methoxamine.

3.2. Pathophysiological characterization of endothelial dysfunction and hyperresponsiveness to methoxamine

3.2.1. Role of NOS in endothelial dysfunction and hyperresponsiveness

Preincubation with L-NAME, a NOS-inhibitor, significantly blunted the acetylcholine-dependent vasorelaxation in normal rat livers.

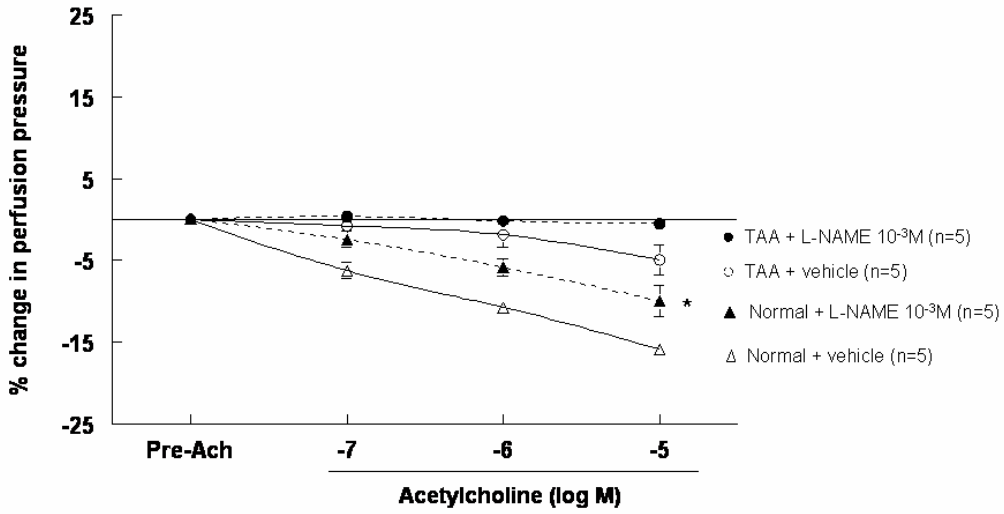


Fig. 2: Effect of NOS-inhibition with L-NAME on the perfusion pressure dose-response curve to acetylcholine in control and cirrhotic rat livers (* $P < 0.001$ vs normal + vehicle).

Preincubation with L-NAME increased the response to methoxamine in normal livers ($P < 0.005$), while in cirrhotic rat livers, pre-treatment with L-NAME did not further aggravate the hyperresponse to methoxamine.

Despite the inhibition of NO-release in both normal and cirrhotic rat livers, cirrhotic livers still exhibited a hyperresponse to methoxamine (Fig. 3).

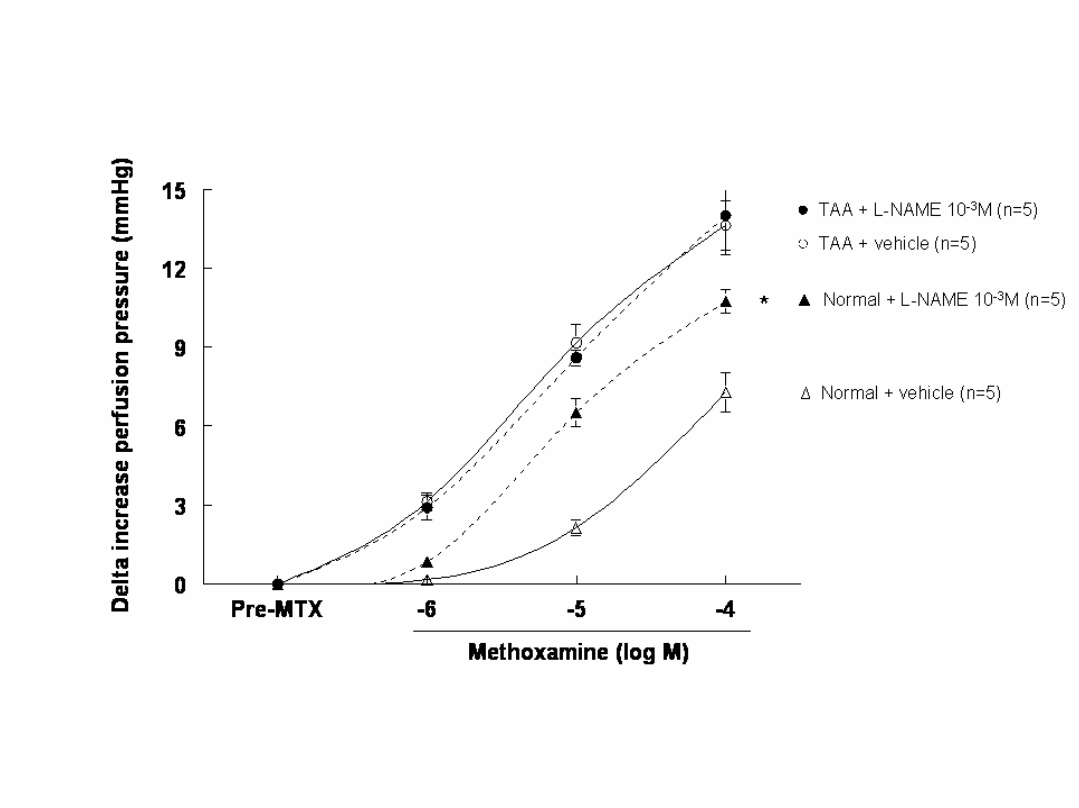


Fig. 3. Effect of NOS-inhibition with L-NAME on the perfusion pressure dose-response curve to methoxamine in control and cirrhotic rat livers (* $P < 0.005$ vs normal + vehicle, TAA + vehicle and L-NAME).

3.2.2. Role of cyclooxygenase-metabolites in the increased intrahepatic vascular tone

In normal livers, preincubation with flurbiprofen 250µM did not significantly modify the response to acetylcholine (% change in perfusion pressure in flurbiprofen pretreated normal livers vs % change in vehicle pretreated normal livers: 10^{-7}M: -6.5 ± 0.9 vs -6.3 ± 1%; 10^{-6}M: -11.1 ± 0.9 vs -10.8 ± 0.7%; 10^{-5}M: -16.3 ± 1.1 vs -15.9 ± 0.4%; all NS) (not shown). In contrast, flurbiprofen preincubation markedly improved the vasodilatory response to acetylcholine in TAA-induced cirrhotic liver (Fig. 4).

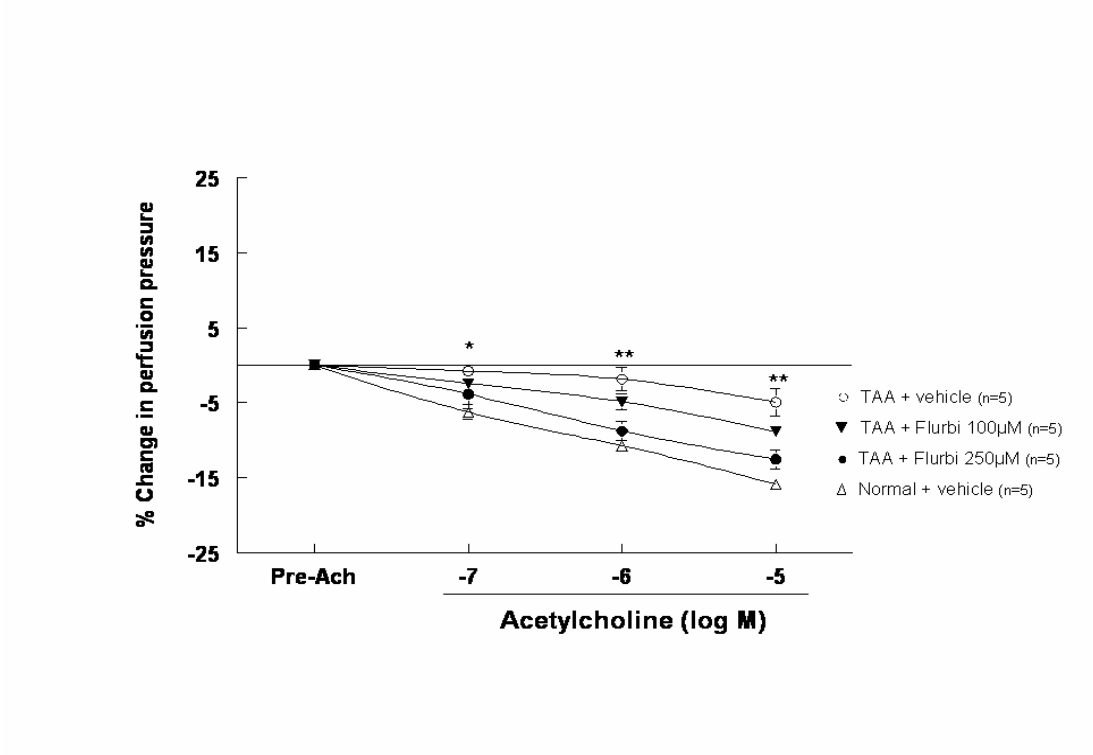


Fig. 4: Effect of flurbiprofen 100 and 250µM preincubation or vehicle on the perfusion pressure dose-response curve to acetylcholine in cirrhotic rat livers versus normal livers with vehicle (*$P < 0.05$ TAA+vehicle vs normal liver, **$P < 0.05$ TAA+vehicle vs normal liver and TAA + 250µM flurbiprofen).

Moreover, this improvement was dose-dependent (TAA + flurbi 100µM vs TAA + flurbi 250µM: 10^{-6}M: -4.9 ± 1.0 vs -8.8 ± 1.2%, *P*=0.040; 10^{-5}M: -8.9 ± 1.0 vs -12.5 ± 1.2%, *P*= 0.045), to the point that there was no longer a difference between flurbiprofen pretreated cirrhotic (250µM) and normal livers.

In terms of the hyperresponsiveness to methoxamine, flurbiprofen preincubation significantly attenuated portal perfusion pressure response to methoxamine in cirrhotic rat livers (Fig. 5).

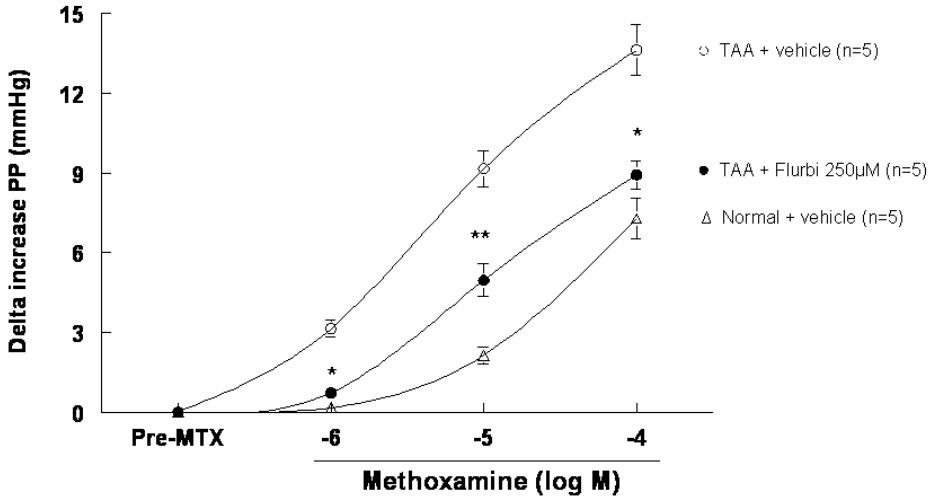


Fig. 5: Effect of flurbiprofen 250µM or vehicle on the perfusion pressure dose-response curve to methoxamine in cirrhotic rat livers versus normal livers with vehicle (*$P < 0.05$ TAA + flurbi vs TAA + vehicle, ** $P < 0.05$ TAA + flurbi vs TAA + vehicle and normal + vehicle).

In normal livers, there was a tendency toward a slight decrease following flurbiprofen preincubation (Δ increase in perfusion pressure at methoxamine 10^{-6}M: 0.4 ± 0.1 vs 0.2 ± 0.1 mmHg for vehicle alone, *P*=0.193; 10^{-5}M: 1.4 ± 0.1 vs 2.1 ± 0.3mmHg, *P*=0.062; 10^{-4}M: 5.4 ± 0.4 vs 7.3 ± 0.8mmHg, *P*=0.061) (data not shown).

3.2.3. Involvement of TXA_2, a vasoconstrictive cyclooxygenase-metabolite,in the increased vascular tone.

When TXB_2 production (an end-product of TXA_2) was measured in the perfusate of the experiment assessing the effect of the COX-inhibitor flurbiprofen (100 and 250µM) on endothelial dysfunction in TAA cirrhotic rats, we observed a dose-dependent decrease in TXB_2 production (Fig. 6), in parallel to the dose-related hemodynamic effect in this same experiment (Fig. 4).

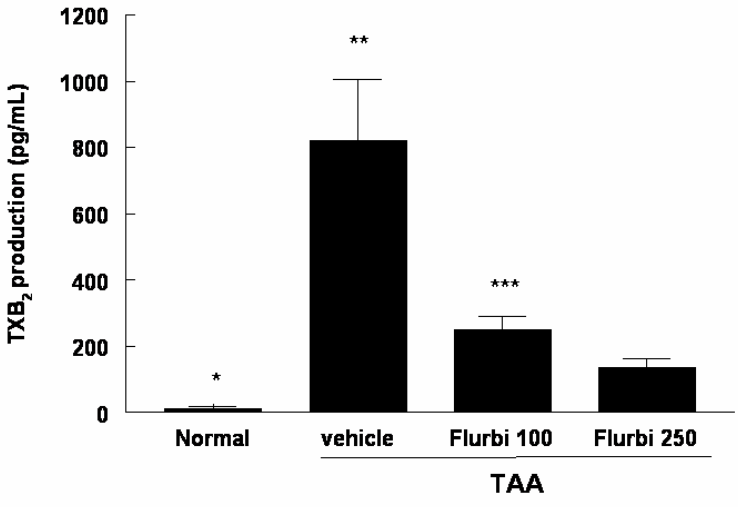


Fig. 6: TXB_2 (the end metabolite of TXA_2) production in normal perfused liver and cirrhotic liver preincubated with either vehicle, flurbiprofen 100µM (flurbi 100µM) or 250µM (flurbi 250µM) (*$P < 0.001$ normal vs all other groups, **$P < 0.001$ TAA + vehicle vs TAA + flurbi 100 and 250µM, **$P < 0.005$ TAA + flurbi +100µM vs TAA + flurbi 250µM).

To prove that TXA_2 was indeed of importance in the increased intrahepatic vascular resistance associated with cirrhosis, we next performed a dose-response curve to U44619, a TXA_2-analogue, in both normal and TAA cirrhotic rats (Fig. 7).

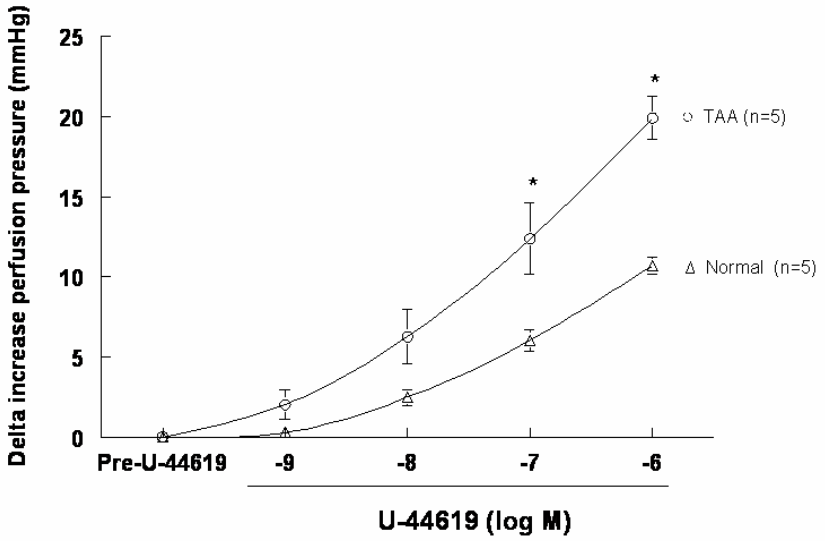
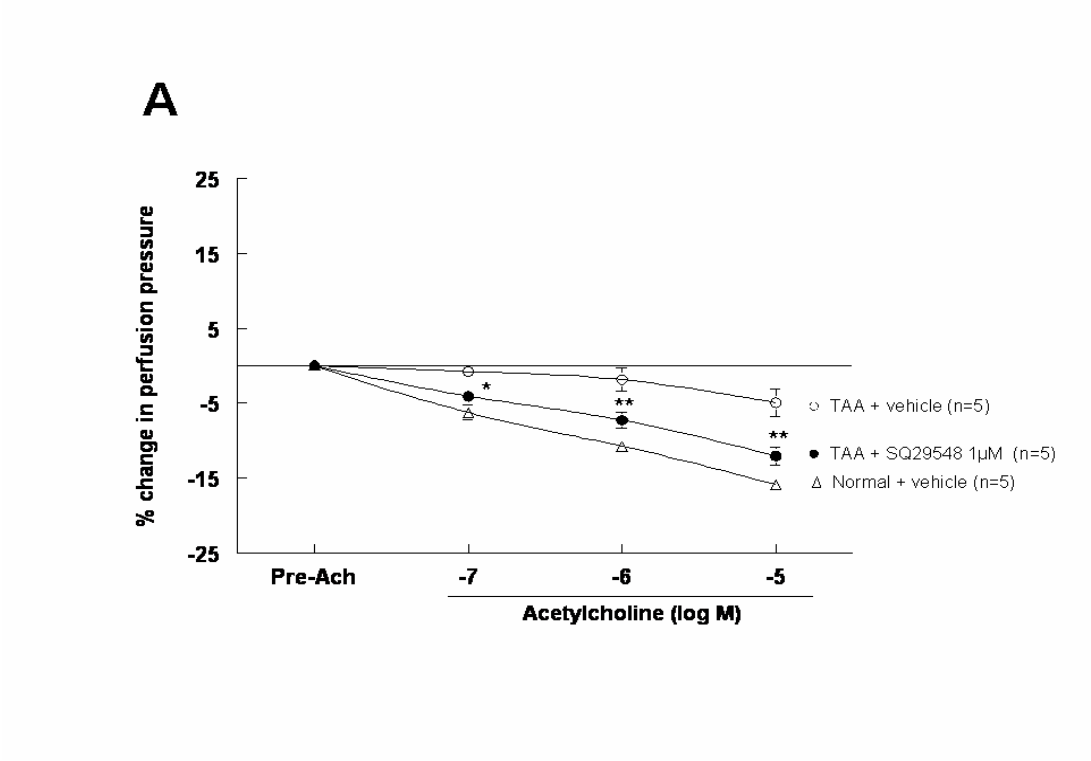


Fig. 7: Portal perfusion pressure dose-response curve to U44619, a TXA_2-analogue, in both normal and TAA cirrhotic rat livers (*$P < 0.05$ vs normal liver at same concentration).

U44619 produced a significant dose-dependent increase in portal perfusion pressure in both control and TAA cirrhotic livers with an aggravated response at higher doses in the cirrhotic perfused rat liver compared to normal rat liver (10^{-9}M: 2.0 ± 0.9 vs 0.3 ± 0.1mmHg, *P*=0.097; 10^{-8}M: 6.3 ± 1.7 vs 2.5 ± 0.5mmHg, *P*=0.062; 10^{-7}M: 12.4 ± 2.2 vs 6.0 ± 0.7mmHg, *P*=0.026; 10^{-6}M: 19.9 ± 1.3 vs 10.7 ± 0.5, $P < 0.001$).

Additionally, preincubation with SQ29548, a TXA_2-receptor antagonist, significantly improved endothelial dysfunction (Fig. 8.A) and attenuated the hyperresponse to methoxamine (Fig. 8.B), thereby confirming the involvement of TXA_2.



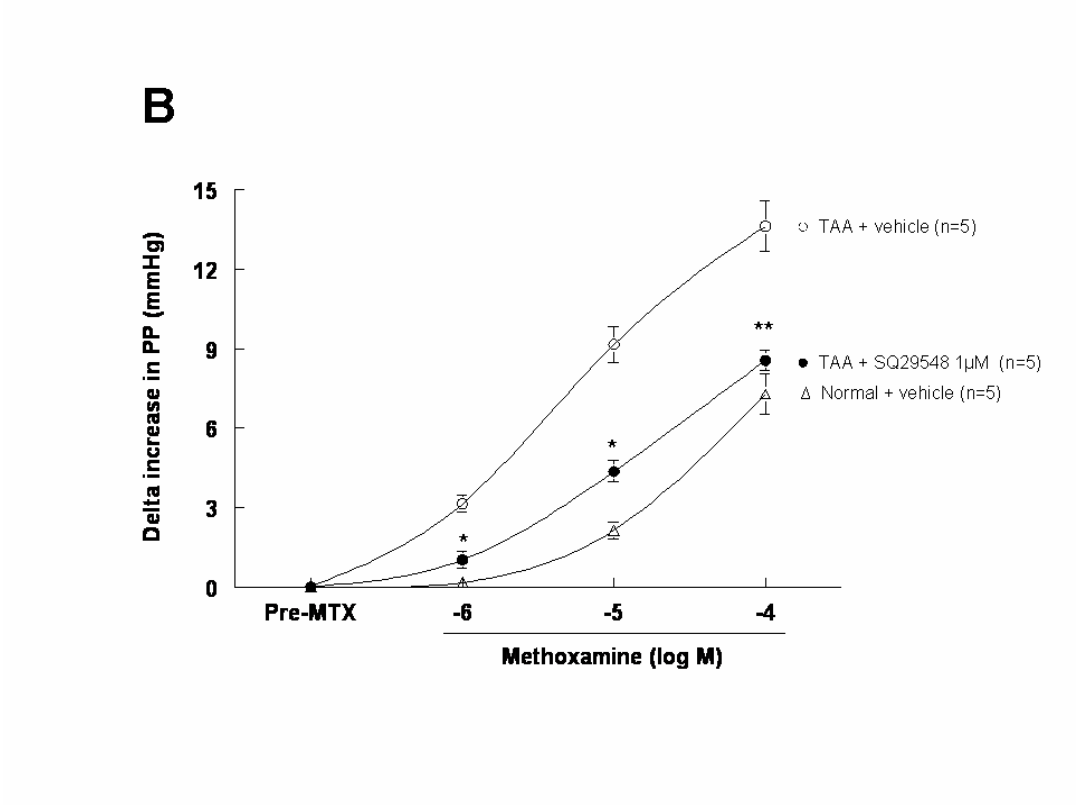


Fig. 8. A. Effect of TXA_2-blockade with SQ29548 on the portal perfusion response curve to acetylcholine in cirrhotic rats compared to normal rats (*P<0.05 vs TAA + vehicle, **P < 0.05 vs TAA + vehicle and normal + vehicle). B. Effect of SQ29548 preincubation on portal perfusion pressure dose-response to methoxamine in cirrhotic rat livers compared to normal perfused rat liver (*P < 0.05 vs TAA + vehicle and normal + vehicle, **P < 0.05 vs TAA + vehicle)

Lastly, TXA_2-synthase and -receptor were detected by western blotting in normal and cirrhotic rat liver (Fig. 9). In the cirrhotic rat liver, TXA_2-synthase was upregulated (densitometric analysis: 222.5 ± 3.2% of the signal obtained in normal rats, $P < 0.001$), whereas the TXA_2-receptor was downregulated (24 ± 3% of the signal obtained in normal rats, $P < 0.001$) (Fig. 9).

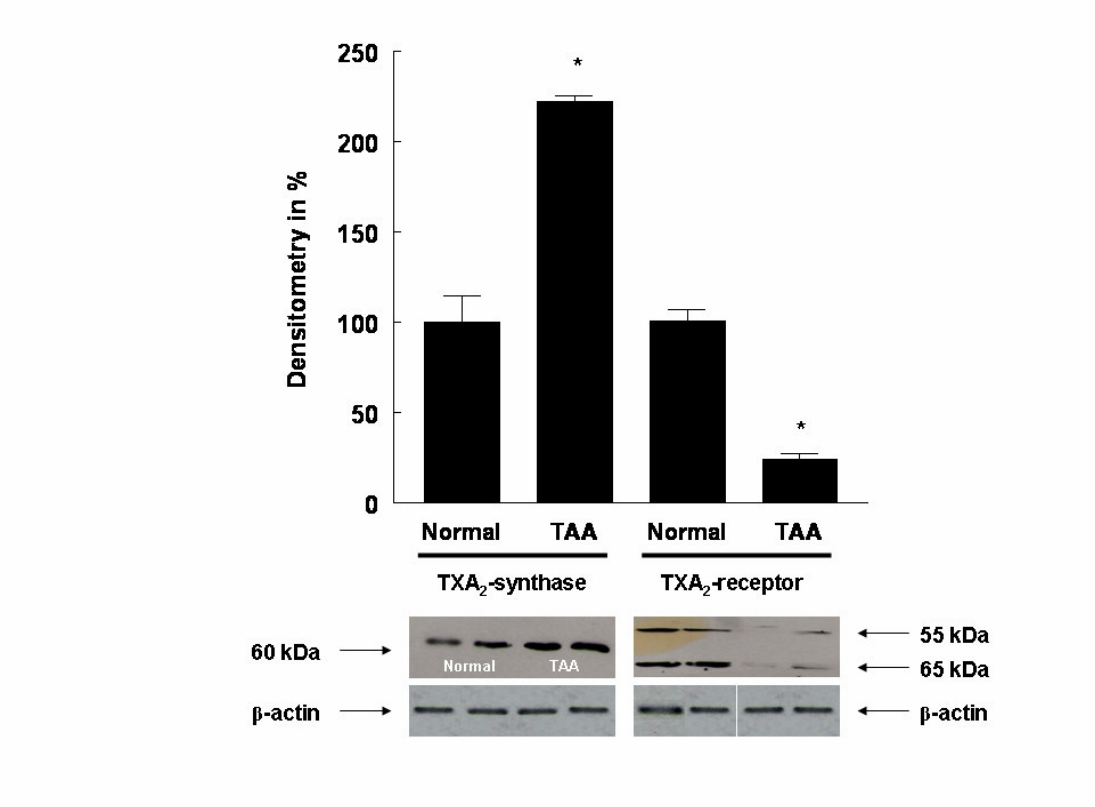


Fig. 9: Densitometric analysis of Western blot for TXA_2-synthase and –receptor in normal and TAA-cirrhotic rats (n=5 per group) (*$P < 0.001$ vs normal rats). A representative blot of TXA_2-synthase and –receptor for the different experimental groups is shown.

3.2.4. Effect of both COX- and NOS-inhibition on endothelial dysfunction and hyperresponsiveness to methoxamine (Fig. 10-11)

In cirrhotic livers, preincubated with a combination of L-NAME 10^{-3}M and flurbiprofen 250µM, it was clear that the correcting effect of flurbiprofen on endothelial dysfunction was markedly attenuated at 10^{-6} and 10^{-5}M acetylcholine, suggesting an interaction between COX-metabolites and NO-synthase (10^{-6}M AcH: -5.6 ± 0.5 vs -8.8 ± 1.2% for flurbiprofen alone, P=0.042; 10^{-5}M AcH: -8.4 ± 0.6 vs -12.6 ± 1.2%, P=0.015).

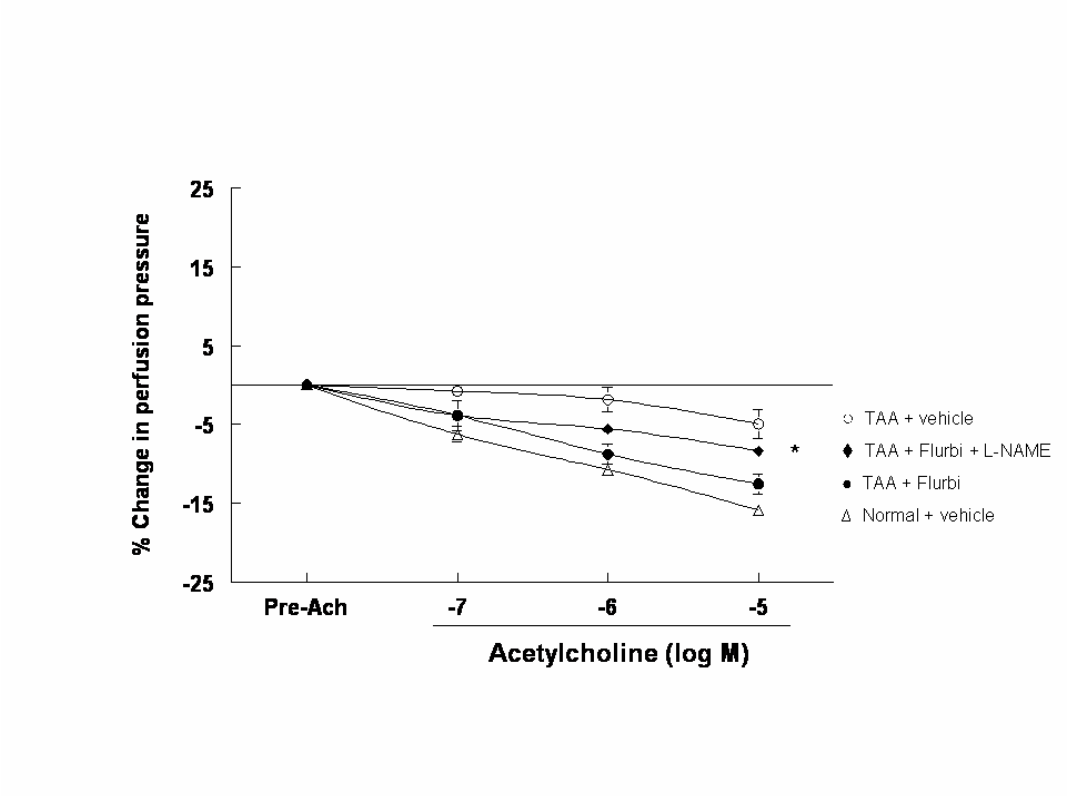


Fig. 10: Improvement of endothelial dysfunction by flurbiprofen in the TAA cirrhotic rat is attenuated by L-NAME, a known NOS-inhibitor, suggesting an interaction between COX-metabolites and NO (TAA + flurbi vs TAA + flurbi + L-NAME, *P<0.05 at 10^{-5} and 10^{-6}M acetylcholine).

With regard to hyperresponsiveness to methoxamine in L-NAME-preincubated cirrhotic livers, the attenuating effect of flurbiprofen was significantly reduced at 10^{-6}M methoxamine and even prevented at 10^{-5} and 10^{-4} M (Fig. 11).

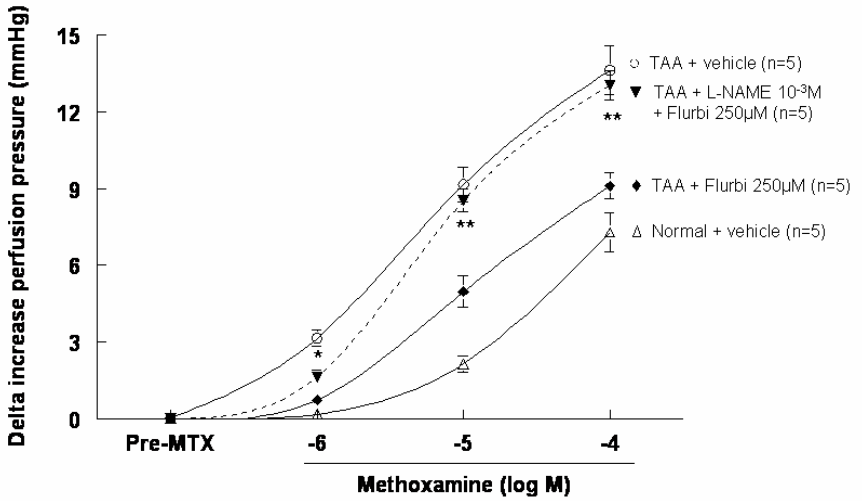


Fig. 11: Improvement of hyperresponsiveness to methoxamine by flurbiprofen in the TAA cirrhotic rat is attenuated by L-NAME, a known NOS-inhibitor, suggesting an interaction between COX-metabolites and NO (* $P < 0.05$ TAA + Flurbi + L-NAME vs TAA + vehicle and normal + vehicle, ** $P < 0.001$ TAA + Flurbi + L-NAME and TAA + vehicle vs both other groups).

3.3. Effect of TXA_2 on HSC contraction in vitro

We next assessed the direct effect of TXA_2 on the driving force of the increased intrahepatic vascular tone, more specifically HSC contraction. We observed that U44619, a stable TXA_2-analogue, led to HSC contraction (51.8 ± 1.5% vs 15.3 ± 3.8% for vehicle,

$P < 0.001$), which was dose-dependently decreased following pre-incubation with SQ29,548, a TXA_2-receptor antagonist (Fig. 12.A). Preincubation with flurbiprofen resulted in a slight decrease in FCS-promoted HSC contraction ($P < 0.001$ versus FCS alone) (Fig. 12.B). Cytotoxicity of flurbiprofen was excluded in vitro by use of a colorimetric cell proliferation assay based on the tetrazolium salt sodium 3,3'-{1-[(phenylamino)carbonyl]-3,4-tetrazolium}-bis (4-methoxy-6-nitro) benzene sulfonic acid hydrate (XTT) (Roche Diagnostics, Vilvoorde, Belgium) (data not shown).

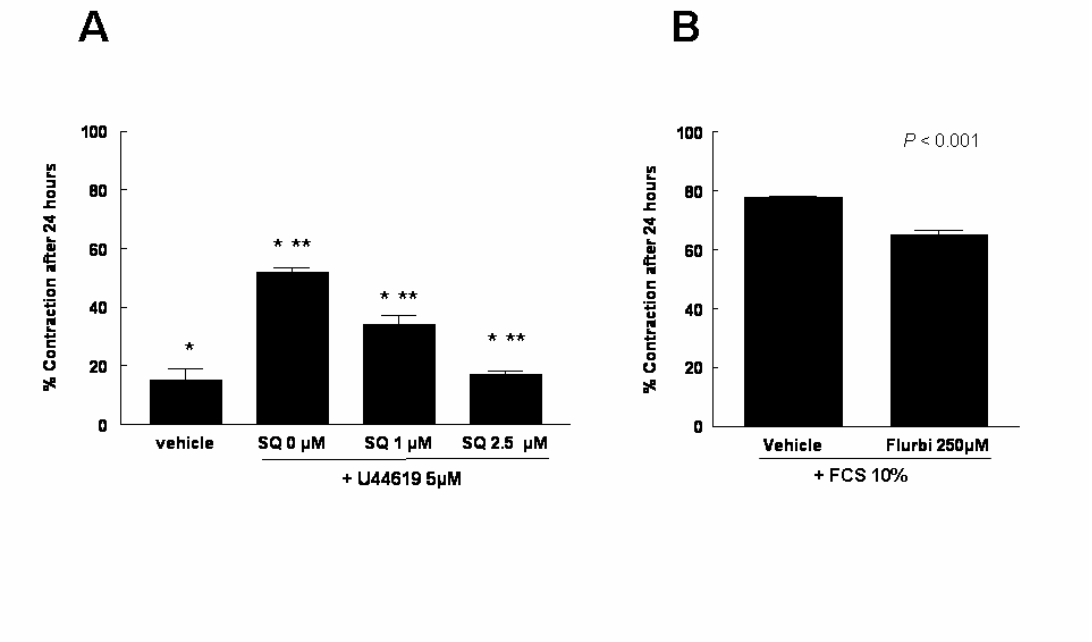


Fig. 12. A. U44619, a TXA_2-analogue, promotes contraction in HSCs, which is dose-dependently decreased following addition of increasing concentration of SQ29,548, a TXA_2-receptor antagonist (*P<0.05 vs U44619 alone, **P<0.05 1µM SQ29,548 vs 2.5µM), B. Flurbiprofen slightly attenuates FCS-promoted HSC contraction (*P<0.001 vs FCS alone).

4. DISCUSSION

Similar to pathological conditions in other vascular territories, such as essential hypertension and primary pulmonary hypertension, the cirrhotic liver is not only characterized by alterations in the contractile properties of a driving effector (see chapter 5) but also exhibits endothelial dysfunction (7-9,21). The underlying mechanism of the latter results from a change in the equilibrium between the effect of relaxing and contracting factors released by the endothelium. More specifically, there is decreased synthesis/availability of vasodilatory mediators (such as NO), increased production of vasoconstrictors (such as endothelin, catecholamines, and angiotensin II) and increased sensitivity to vasoconstrictors and/or resistance of contractile effectors to endothelial vasodilators (1,2,21-23,38).

With regard to decreased synthesis of vasodilatory mediators, a reduction in the biological actions of NO has been implicated as a major causative factor in the endothelial dysfunction of the cirrhotic liver (1-5,20,21,39). In our TAA rat model of cirrhosis, we could document and confirm these abovementioned features, including reduced NOS activity, decreased endothelial NOS expression and impaired endothelial-dependent vasorelaxation following cumulative doses of acetylcholine (cfr. chapter 4). By preincubating L-NAME, a NOS-inhibitor, we corroborated that the response to acetylcholine in the normal perfused liver is partially NO-mediated since L-NAME significantly blunted vasorelaxation. Similarly, L-NAME increased the response to methoxamine, suggesting also its involvement in the phenomenon of responsiveness to methoxamine. In TAA cirrhotic rats on the other hand, L-NAME preincubation did not worsen the hyperresponsiveness to methoxamine further nor the impaired endothelium-dependent vasorelaxation. Taking into consideration the effect exerted by NO in the normal perfused liver (as shown by inhibition with L-NAME) and the fact that there is decreased

NOS activity and expression in the TAA cirrhotic liver, both the phenomenon of impaired endothelium-dependent vasorelaxation and hyperresponsiveness could be accounted for by insufficient NO biodisponibility. An argument against this premise, at least in the phenomenon of hyperresponsiveness, is the fact that despite the inhibition of the potent vasodilator NO, cirrhotic livers in the present study still exhibited a hyperresponse to methoxamine compared to normal livers preincubated with L-NAME. This observation might suggest that the reduced NO-production in cirrhotic livers is not the only factor involved in the phenomenon of hyperresponsiveness to vasoconstrictors. The ultimate mechanism therefore remains to be elucidated.

Increased production of vasoconstrictors and increased sensitivity to these agents, might represent an additional component in intrahepatic endothelial dysfunction. In this context, recent studies have pointed out a role for vasoconstrictive prostanoids, produced by stimulation of cyclooxygenases (COX). In spontaneous hypertensive rats, for example, COX-expression was found to be increased and pretreatment of these rats with selective COX-1 inhibitors led to the restoration of the endothelium-dependent vasodilatory response to acetylcholine, suggesting a major role for vasoconstrictor endoperoxides or prostanoids (16-18). Furthermore, it was shown in other vascular territories that the activation of G-protein-coupled receptors, such as those for (nor)epinephrine, vasopressin and endothelin-1, promotes the release of arachnidonic acid for the biosynthesis of vasoactive-derived prostaglandins and thromboxanes (25,40,41). This observation suggests that the phenomenon of hyperresponsiveness emerges principally through prostanoids. In our pre-ascitic TAA-induced cirrhotic rats, the non-selective COX-inhibitor flurbiprofen dose-dependently improved the impaired endothelium-dependent vascular relaxation and attenuated the hyperresponsiveness to methoxamine, suggesting that vasoconstrictive

prostanoids are indeed involved in the pathogenesis of the intrahepatic endothelial dysfunction.

The nature of the putative COX-dependent vasoconstrictor responsible for the intrahepatic endothelial dysfunction is not completely defined. Analogous to other vascular territories (42-44), a likely candidate to fulfil this role is thromboxane A_2 (TXA_2). The results of our study strongly support a role for this COX-metabolite. First of all, we recorded increased levels of 11-dehydro-TXB_2 (a stable non-renal- nor platelet-derived metabolite of thromboxane A_2 in the serum of TAA cirrhotic rats (chapter 4) as well as increased TXB_2-levels in the experiments illustrating intrahepatic endothelial dysfunction. Secondly, non-selective COX-inhibition attenuated the hyperresponsiveness to methoxamine and improved the impaired intrahepatic endothelial vascular relaxation. Moreover, in this latter condition, the hemodynamic improvement was dose-dependent and was paralleled by a dose-dependent decrease in TXB_2-levels. The importance of this observation is further emphasized by the finding of increased expression of TXA_2-synthase in the TAA cirrhotic rat liver compared to normal liver. Thirdly, we proved that TXA_2 causes intrahepatic vasoconstriction. *In vitro*, we documented that U44619, a stable TXA_2-analogue, led to HSC contraction, which was dose-dependently decreased following pre-incubation with SQ29,548, a TXA_2-receptor antagonist. Inhibition of COX, and therefore TXA_2-synthesis, only mildly modulated HSC contraction, suggesting that HSCs act most likely as an effector for TXA_2 rather than as a cellular source, which by Graupera et al. (45) was attributed mainly to the sinusoidal endothelial cell. Recent work (46) further supports this premise by showing that arachidonic acid incubation promoted a significant increase in TXA_2 release by isolated sinusoidal endothelial cells from cirrhotic rat livers, while this was not observed sinusoidal endothelial cells from normal livers. Furthermore, prostaglandin $F_{2\alpha}$ (a vasoconstrictor prostaglandin) and prostacyclin (PGI_2, a vasodilator

prostaglandin) were not found increased after arachidonic acid incubation, compared to endothelial cells from normal livers. Moreover, this same group documented that COX-1 is the responsible upstream isoenzyme to the production of TXA_2 since selective inhibition of COX-1, and not of COX-2, was associated with an attenuation in TXA_2-production. This finding might oppose the dogmatic theory that TXA_2-synthase, the terminal enzyme that metabolizes prostaglandin H_2 to TXA_2, preferentially utilizes COX2-derived PGH_2 (30). However, it has been shown that when arachidonic acid supplies increase, COX-1 derived PGH_2 can be efficiently metabolized to TXA_2 (30). These data not only clearly support our hypothesis concerning the intrahepatic vasoconstrictive role of TXA_2, they also point out a dominant role for the sinusoidal endothelial cell as the source of TXA_2 and suggest COX-1 as the responsible isoenzyme.

In the perfused liver, preincubation with SQ29548, a TXA_2-receptor antagonist, significantly improved endothelial dysfunction and attenuated the hyperresponse to methoxamine, further demonstrating the involvement of TXA_2. Even more relevant, the TXA_2-receptor agonist U44619 produced a significant dose-dependent increase in portal perfusion pressure in both normal and cirrhotic rats. The response to U44619 was aggravated at higher doses of U44619 (10^{-7}-10^{-6}M) in cirrhotic compared to normal rat liver, indicating a different sensitivity of the TXA_2-receptor depending on the state of liver disease. Remarkably enough, on western blot, the expression of the TXA_2-receptor was decreased. A normal physiological mechanism in the face of continued or excessive stimulation is the suppression of cellular responsiveness, also called desensitization (47,48). This phenomenon is considered critical for the cell to integrate the myriad signals being received, and for adaptation to physiologic and pathological states. Desensitization develops in either the context of dysfunction of downstream signalling pathways and/or a decrease in receptor expression (termed downregulation) (47-49). Recent reports have

shown that this desensitization can be masked by more substantial increases in the activity of signalling elements downstream from the receptors, resulting in sustained and anomalous responses in the face of continued receptor stimulation (50). These latter findings might explain the apparent contrasting functional increased responsiveness to U44619 and the decreased expression of the TXA_2-receptor in cirrhotic rat livers. Another explanation for the decreased expression of the receptor might involve a mere decrease in the number of intracellular reserve receptors without affecting the number of membrane-incorporated receptors.

Taken togheter, these data would suggest that TXA_2, but not NO, is of importance in both intrahepatic endothelial dysfunction and hyperresponsiveness to methoxamine. The illustration that the correcting effect of flurbiprofen on both phenomena was markedly attenuated when L-NAME, a well-known NOS-inhibitor, was preincubated, however, prompts the need to correct the former hypothesis. A possible explanation was suggested by Ashton et al. (51,52) who documented an interaction between COX-metabolites and eNOS in human umbilical vein endothelial cells. Increased COX-activity in these cells led to increased TXA_2 production, which in turn caused down-regulation of Akt, a serine-threonine kinase and known co-factor of eNOS, causing dysfunction of this latter enzyme. In the CCl_4-cirrhotic liver, deficiency of Akt has been shown to be a major factor in eNOS dysfunction and cirrhotic portal hypertension, which was restored by gene-transfer of this apparent important co-factor (53). This observation therefore discloses a new aspect in the complexity of intrahepatic interactions of vasoactive substances (Fig 13).

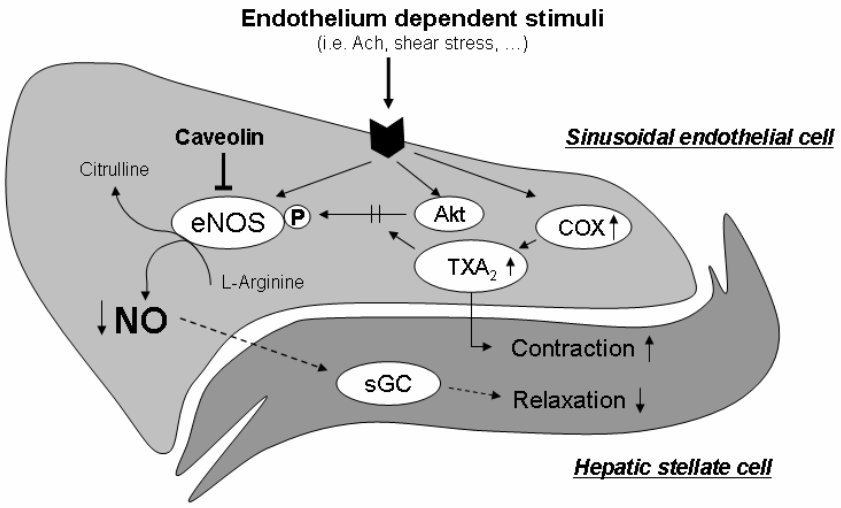


Fig. 13: Suggested pathogenetic mechanism through which TXA_2 exerts control on NO-production. Stimulation of cyclooxygenases (COX) lead to increased TXA_2-production, which besides a direct paracrine effect on the hepatic stellate cell also decreases Akt-stimulated activation of NO-synthase (eNOS) and downstream signalling pathways (sGC, soluble guanylate cyclase).

In conclusion, the present study shows that besides low NO bioavailability excessive intrahepatic production of the vasoconstrictor cyclooxygenase-metabolite TXA_2 plays a major role in the pathogenesis of endothelial dysfunction and in the hyperresponsiveness to vasoconstrictors associated with TAA-induced cirrhosis. Therefore, strategies aiming to decrease TXA_2 might be of therapeutic relevance in the treatment of portal hypertension.

5. REFERENCES

1. Laleman W, Omasta A, Van de Casteele M, et al. A role for asymmetric dimethylarginine in the pathophysiology of portal hypertension in rats with biliary cirrhosis. Hepatology 2005; 42: 1382-1390.
2. Van de Casteele M, Omasta A, Janssens S, et al. In vivo gene transfer of endothelial nitric oxide synthase decreases portal pressure in anaesthetised carbon tetrachloride cirrhotic rats. Gut 2002; 51: 440-445.
3. Laleman W, Van Landeghem L, Wilmer A, Fevery J, Nevens F. Portal hypertension: from pathophysiology to clinical practice. Liver Int 2005; 25: 1079-1090.
4. Rockey DC. The cellular pathogenesis of portal hypertension: stellate cell contractility, endothelin and nitric oxide. Hepatology 1997; 25: 2-5.
5. Laleman W, Vander Elst I, Zeegers M, et al. A stable model of cirrhotic portal hypertension in the rat: thioacetamide revisited. Eur J Clin Invest 2006; 36: 242-249.
6. De Artinano AA, Gonzalez VL. Endothelial dysfunction and hypertensive vasoconstriction. Pharmacol Res 1999; 40: 113-124.
7. Giaid A, Saleh D. Reduced expression of endothelial nitric oxide synthase in the lungs of patients with pulmonary hypertension. N Engl J Med 1995; 27; 333: 214-221.
8. Panza JA, Quyyumi AA, Brush JE Jr, Epstein SE. Abnormal endothelium-dependent vascular relaxation in patients with essential hypertension. N Engl J Med 1990; 323: 22-27.
9. Shimokawa H, Flavahan NA, Vanhoutte PM. Loss of endothelial pertussis toxin-sensitive G protein function in atherosclerotic porcine coronary arteries. Circulation 1991; 83: 652-660.
10. Harrison DG, Widder J, Grumbach I, et al. Endothelial mechanotransduction, nitric oxide and vascular inflammation. J Intern Med 2006; 259: 351-363.
11. Saito Y, Nakao K, Mukoyama M, Imura H. Increased plasma endothelin level in patients with essential hypertension. N Engl J Med 1990; 322: 205.
12. Stewart DJ, Levy RD, Cernacek P, Langleben D. Increased plasma endothelin-1 in pulmonary hypertension: marker or mediator of disease? Ann Intern Med 1991; 114: 464-469.
13. Padfield PL, Brown JJ, Lever AF, Morton JJ, Robertson JI. Changes of vasopressin in hypertension: Cause or effect? Lancet 1976; 1: 1255-1257.
14. Esler M. The sympathetic system and hypertension. Am J Hypertens 2000; 13: 99S-105S.
15. McFarlane SI, Kumar A, Sowers JR. Mechanisms by which angiotensin-converting enzyme inhibitors prevent diabetes and cardiovascular disease. Am J Cardiol 2003; 91: 30H-37H.
16. Ge T, Hughes H, Junquero DC, Wu KK, Vanhoutte PM, Boulanger CM. Endothelium-dependent contractions are associated with both augmented expression of prostaglandin H synthase-1 and hypersensitivity to prostaglandin H_2 in the SHR aorta. Circ Res 1995; 76: 1003-1010.
17. Luscher TF, Aarhus LL, Vanhoutte PM. Indomethacin improves the impaired endothelium-dependent relaxations in small mesenteric arteries of the spontaneously hypertensive rat. Am J Hypertens 1990; 3: 55-58
18. Kato T, Iwama Y, Okumura K, Hashimoto H, Ito T, Satake T. Prostaglandin H2 may be the endothelium-derived contracting factor released by acetylcholine in the aorta of the rat. Hypertension 1990; 15: 475-481.
19. Zhao WG, Richardson JS. Prostacyclin, thromboxane A_2, and hypertension. Clin Invest Med 1990; 13: 343-352.
20. Rockey DC. Vascular mediators in the injured liver. Hepatology 2003; 37: 4-12.
21. Gupta TK, Toruner M, Chung MK, Groszmann RJ. Endothelial dysfunction and decreased production of nitric oxide in the intrahepatic microcirculation of cirrhotic rats. Hepatology 1998; 28: 926-931.
22. Grossman HJ, Grossman VL, Bhathal PS. Enhanced vasoconstrictor response of the isolated perfused cirrhotic rat liver to humoral vasoconstrictor substances found in portal venous blood. J Gastroenterol Hepatol. 1992; 7: 283-287.
23. Elliot AJ, Vo LT, Grossman VL, Bhathal PS, Grossman HJ. Endothelin-induced vasoconstriction in isolated perfused liver preparations from normal and cirrhotic rats. J Gastroenterol Hepatol 1997; 12: 314-318.
24. Crofford LJ. COX-1 and COX-2 tissue expression: implications and predictions. J Rheumatol 1997;24 (Suppl 49):15-19.

25. Xing M and Insel PA. Protein kinase C-dependent activation of cytosolic phospholipase A_2 and mitogen-activated protein kinase by alpha 1-adrenergic receptors in Madin-Darby canine kidney cells. J Clin Invest 1996;97:1302–1310.
26. Herschman HR. Prostaglandin synthase 2. Biochim Biophys Acta 1996;1299:125-140.
27. Geng Y, Blanco FJ, Cornelisson M, Lotz M. Regulation of cyclooxygenase-2 expression in normal human articular chondrocytes. J Immunol 1995;155:796-801.
28. Feng L, Xia Y, Garcia GE, Hwang D, Wilson CB. Involvement of reactive oxygen intermediates in cyclooxygenase-2 expression induced by interleukin-1, tumor necrosis factor alpha, and lipopolysaccharide. J Clin Invest 1995;95:1669-1675.
29. Bishop-Bailey D, Pepper JR, Larkin SW, Mitchell JA. Differential induction of cyclooxygenase-2 in human arterial and venous smooth muscle: role of endogenous prostanoids. Arterioscler Thromb Vasc Biol 1998;18:1655-1661.
30. Ueno N, Murakami M, Tanioka T, et al. Coupling between cyclooxygenase, terminal prostanoid synthase, and phospholipase A_2. J Biol Chem 2001;276: 34918–34927.
31. Suzuki-Yamamoto T, Yokoi H, Tsuruo Y, Watanabe K, Ishimura K. Identification of prostaglandin F-producing cells in the liver. Histochem Cell Biol 1999;112:451-456.
32. Cheng J, Imanishi H, Iijima H, et al. Expression of cyclooxygenase 2 and cytosolic phospholipase A_2 in the liver tissue of patients with chronic hepatitis and liver cirrhosis. Hepatol Res 2002;23:185-195.
33. Reactive oxygen intermediates and eicosanoid production by Kuppfer cells and infiltrated macrophages in acute and chronic liver injury induced by rats by CCl_4. Inflamm Res 2000;49:700-707.
34. Vassalle C, Domenici C, Lubrano V, L'Abbate A. Interaction between nitric oxide and cyclooxygenase pathways in endothelial cells. J Vasc Res 2003; 40: 491-499.
35. Fernandez M, Garcia-Pagan JC, Caadevall M, et al. Acute and chronic cyclooxygenase blockade in portal hypertensive rats: influence on nitric oxide biosynthesis. Gastroenterology 1996; 110: 1529-1535.
36. Ashton AW, Ware JA.Thromboxane A_2 receptor signaling inhibits vascular endothelial growth factor-induced endothelial cell differentiation and migration. Circ Res 2004; 95: 372-379.
37. Gao Y, Yokota R, Tang S, Ashton AW, Ware JA. Reversal of angiogenesis in vitro, induction of apoptosis, and inhibition of AKT phosphorylation in endothelial cells by thromboxane A_2. Circ Res 2000; 87: 739-745.
38. Loureiro-Silva MR, Iwakiri Y, Abraldes JG, Haq O, Groszmann RJ. Increased phosphodiesterase-5 expression is involved in the decreased vasodilator response to nitric oxide in cirrhotic rat livers. J Hepatol 2006; 44: 886-893.
39. Rockey DC, Chung JJ. Reduced nitric oxide production by endothelial cells in cirrhotic rat liver: endothelial dysfunction in portal hypertension. Gastroenterology 1998;114: 344-351.
40. Athari A, Hanecke K, Jungermann K. Prostaglandin F_2 alpha and D_2 release from primary Ito cell cultures after stimulation with noradrenaline and ATP but not adenosine. Hepatology 1994; 20: 142-148.
41. Wiest R, Tsai MH, Groszmann RJ. Octreotide potentiates PKC-dependent vasoconstrictors in portal-hypertensive and control rats. Gastroenterology 2001; 120: 975-983.
42. Dai FX, Diederich A, Skopec J, Diederich D. Diabetes-induced endothelial dysfunction in streptozotocin-treated rats: role of prostaglandin endoperoxides and free radicals. J Am Soc Nephrol 1993; 4: 1327-1336.
43. Dai FX, Skopec J, Diederich A, Diederich D. Prostaglandin H_2 and thromboxane A_2 are contractile factors in intrarenal arteries of spontaneously hypertensive rats. Hypertension 1992; 19: 795-798.
44. Maruyama J, Yokochi A, Maruyama K, Nosaka S. Acetylcholine-induced endothelium-derived contracting factor in hypoxic pulmonary hypertensive rats. J Appl Physiol 1999; 86: 1687-1695.
45. Graupera M, March S, Engel P, Rodes J, Bosch J, Garcia-Pagan JC. Sinusoidal endothelial COX-1-derived prostanoids modulate the hepatic vascular tone of cirrhotic rat livers. Am J Physiol Gastrointest Liver Physiol. 2005; 288: G763-770.
46. Gracia-Sancho J, Lavina, Rodriguez-Vilarrupla A, Bosch J, Garcia-Pagan J. Enhanced prostaglandin H2 production by sinusoidal endothelial cells increase the vascular tone by cirrhotic livers. Hepatology 2006;44 (suppl 1):356:44A.
47. Bristow MR, Ginsburg R, Minobe W, et al. Decreased catecholamine sensitivity and β-adrenergic receptor density in failing human hearts. N Engl J Med 1982; 307: 205-211.
48. Brodde OE, Michel MC. Adrenergic and muscarinic receptors in the human heart. Pharmacol Rev 1999; 51: 651-689.

49. McGraw DW, Liggett SB. Molecular mechanisms of β_2-adrenergic receptor function and regulation. Proc Am Thorac Soc 2005; 2: 292-296.
50. Slotkin TA, Seidler FJ. Anomalous regulation of β-adrenoreceptor signaling in brain regions of the newborn rat. Brain Res 2006; 1077: 54-58.
51. Ashton AW, Ware JA.Thromboxane A_2 receptor signaling inhibits vascular endothelial growth factor-induced endothelial cell differentiation and migration. Circ Res 2004; 95: 372-379.
52. Gao Y, Yokota R, Tang S, Ashton AW, Ware JA. Reversal of angiogenesis in vitro, induction of apoptosis, and inhibition of AKT phosphorylation in endothelial cells by thromboxane A_2. Circ Res 2000; 87: 739-745
53. Morales-Ruiz M, Cejudo-Martin P, Fernandez-Varo G, et al. Transduction of the liver with activated Akt normalizes portal pressure in cirrhotic rats. Gastroenterology 2003; 125: 522-531.

Chapter 7

Nitroflurbiprofen, a nitric oxide-releasing cyclooxygenase-inhibitor, improves cirrhotic portal hypertension in the rat.

W. Laleman, L. Van Landeghem, I. Vander Elst, M. Zeegers,
J. Fevery and F. Nevens

Department of Hepatology,
University Hospital Gasthuisberg, KU Leuven, Belgium

Resubmitted

1. INTRODUCTION

Although the knowledge concerning the pathophysiology of portal hypertension has improved tremendously over the past 25 years, the therapeutic armamentarium has not assumed equal proportions (1). As a result, non-selective beta-blockers, since their introduction more than 20 years ago, have remained the mainstay of pharmacological therapy for portal hypertension (1-4). Undeniably, these drugs have proven to be of value since they have reduced the risk of variceal (re)bleeding and bleeding-related mortality on a short-term basis. In addition, they also decrease the risk of developing long-term complications, such as ascites, spontaneous bacterial peritonitis and hepatorenal syndrome, and improve long-term survival (4-7). Nonetheless, a sustained decrease in portal pressure is only achieved in less than half of the treated patients, urging the need for potential new or additive drugs (1,6,8).

Recent advances in the knowledge of the pathophysiology of cirrhotic portal hypertension indicates that the increased intrahepatic vascular resistance, which in part is determined by increased hepatic vascular tone, is a reasonable therapeutic target (9). The increased vascular tone is mainly driven by activated hepatic stellate cells (HSCs) and results from an imbalance between vasodilator and vasoconstrictor forces (1,10-14). More specifically, there is an increased intrahepatic production of vasoconstrictors, including thromboxane A_2 (TXA_2), a cyclooxygenase (COX)-derived prostanoid, which has recently been suggested to play a major role in the intrahepatic endothelial dysfunction and the aggravated response to vasoconstrictors ("hyperresponsiveness") in the cirrhotic liver (Chapter 7). Additionally, there is decreased availability of vasodilators, of which nitric oxide (NO) is the most renowned (10-14). A possible pharmacological strategy in the treatment of portal hypertension would therefore be to abrogate the generation of TXA_2 in combination with a replenishment of the decreased hepatic NO bioavailability. Additionally, the vasodilatory

effect of this drug should remain limited to the hepatic microcirculation to avoid further worsening of the associated splanchnic and systemic vasodilatory syndrome, which is currently the major impediment to the use of nitrovasodilators such as isosorbide-5-mononitrate (1,11).

In the present study, we examined the hemodynamic effect and safety-profile of administration of nitro-flurbiprofen (HCT-1026), a cyclooxygenase-inhibitor with liver-specific NO-donating properties (Fig. 1), in rats with established cirrhotic portal hypertension and associated hyperdynamic circulation.

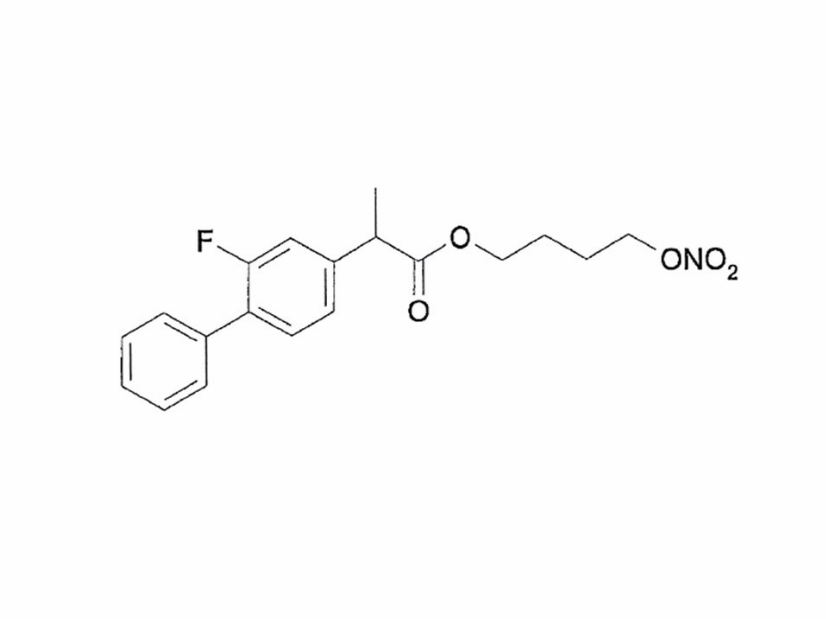


Fig. 1: Nitroflurbiprofen (HCT-1026) : 2-fluoro-α-methyl[1,1'-biphenyl]-4-acetic acid 4-(nitroxy)butylester

2. MATERIALS AND METHODS

Materials and methods used for these experiments are described in chapter 3. Additional information regarding certain aspects of the experiments are given below.

2.1. Rat model of TAA-induced cirrhosis.

2.2. In vivo experiments

After 18 weeks of TAA administration, cirrhotic rats were equally (n=8/group) and randomly allocated to one of the following groups: intraperitoneal injection 24 hours and 1 hour prior to the measurements with nitroflurbiprofen (45 mg/kg) (HCT-1026, Nicox, Sophia Antipolis Cedex, France), flurbiprofen (30mg/kg, equimolar concentration to nitroflurbiprofen) (Sigma, St. Louis, USA) or vehicle (250µL dimethylsulfoxide [DMSO]: 250µL isotonic saline). Rats were then instrumented for in vivo hemodynamic measurements (portal pressure, mean arterial pressure and mesenteric blood flow), as described in chapter 3.

2.3. In-situ rat liver perfusion study

The effect of intraperitoneal injection - 24 hours and 1 hour prior to measurement - of nitroflurbiprofen (HCT-1026, 45mg/kg), flurbiprofen (30mg/kg) or vehicle on the total intrahepatic vascular resistance was evaluated in 15 additional cirrhotic rats (n=5/group) by performing flow-pressure curves (increase with 5mL/min every 5 minutes) (n=5 for each condition).

To test the direct effect of these drugs on the increased intrahepatic vascular tone, nitroflurbiprofen (HCT-1026) (250µM), flurbiprofen (250µM) (also see chapter 7) or vehicle (DMSO : isotonic saline) was added to the perfusate of an additional group of treatment-naive perfused cirrhotic rats (n=30 in total) after the stabilization period. Thereafter, the preparation was allowed to stabilize for 15 minutes.

The increased intrahepatic vascular tone was assessed through the evaluation of endothelial function (n=5 per condition) and responsiveness to vasoconstrictors (n=5 per condition). In the experiments assessing endothelial function (concentration-effect curves to cumulative doses of acetylcholine), 2 mL samples of the perfusate were taken before and after the experiment for the measurement of TXB_2 production (Caymann Chem), a stable metabolite of TXA_2. TXB_2 production was expressed as the absolute increment over baseline before methoxamine administration.

2.4. In vitro hepatic stellate cell contraction assay

The effect of nitroflurbiprofen (HCT-1026) (25-50-100-250µM), flurbiprofen (250µM) and vehicle (DMSO) on FCS-promoted contraction was measured by preincubating these compounds before addition of FCS 10%, as described earlier.

2.5. Serum and liver nitrite/nitrate

To determine the degree of systemic NO-release, nitrate/nitrite (NOx) content, a parameter of NO production, was assayed by a fluorometric method using 2,3-diaminonaphtalene in the serum of the differently treated groups of cirrhotic rats, used in the in vivo hemodynamic study, as described (14,15). Additionally, NOx levels were determined in homogenates of these cirrhotic rat livers (final concentration of 0.25g wet weight of liver/mL sucrose buffer) (n=6/group) in order to determine hepatic NO-release.

2.6. Assesment of NSAID-related side-effects in vivo

To evaluate potential adverse effects to the use of HCT-1026 and flurbiprofen, typical reported side-effects of NSAIDs, such as nephrotoxicity, hepatotoxicity and gastrointestinal ulceration were investigated (16,17). Rats receiving either nitroflurbiprofen (HCT-1026), flurbiprofen or vehicle were housed individually in metabolic cages for 24 hours before the in vivo hemodynamic study (i.e. after the first intraperitoneal injection) in order to collect urine and to determine creatinin clearance as a measure of renal glomerular filtration rate.

Blood, taken by puncture of the aortic bifurcation at the end of the hemodynamic measurements, was collected in dry Vacutainer tubes. Liver function tests were assayed by standardized automated procedures. The stomach and small intestines of each animal (n=24) were excised and treated with 2% formalin for fixation of tissue walls. They were opened along the mesenteric attachment and examined for the presence of ulcers or erosions. The area (mm^2) of macroscopically visible lesions was measured, summed per small intestine, and used for lesion score, as described (18).

3. RESULTS

3.1. In vivo study

At laparotomy, all animals clearly showed pre-ascitic macronodular cirrhosis with splenomegaly. General characteristics are shown in table 1 and did not reveal any differences between the groups.

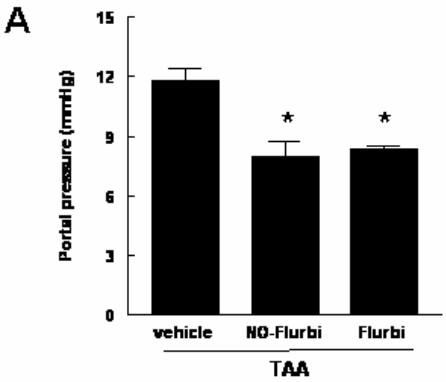
Table 1: General characteristics of the different groups

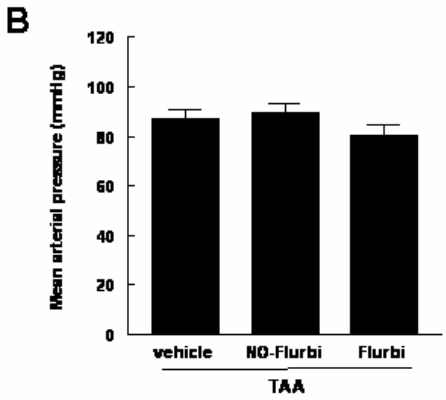
Parameter	**Administration**			***P***
	Vehicle (n=8)	**Nitroflurbiprofen (n=8)**	**Flurbiprofen (n=8)**	
Body weight (g)	301.4 ± 6.9	282.3 ± 3.4	292 ± 13.8	0.350
Liver (g/100g b.w.)	7.0 ± 0.3	6.6 ± 0.3	6.3 ± 0.4	0.425
Spleen (g/100g b.w.)	0.58 ± 0.04	0.62 ± 0.07	0.56 ± 0.07	0.757

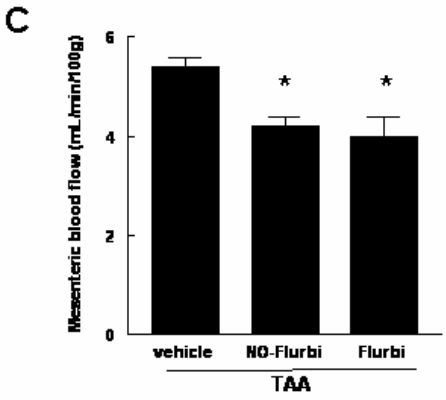
Upon hemodynamic characterization, we observed a similar decrease in portal hypertension after treatment with HCT-1026 and flurbiprofen as compared to the vehicle-treated group (8 ± 0.8 mmHg and 8.4 ± 0.1 mmHg vs 11.8 ± 0.6 mmHg, respectively, $P<0.001$) (Fig. 2.A). The rather low mean arterial pressure, indicative of the hyperdynamic state, as documented previously (17,18), remained unchanged between the different groups (86.4 ± 3.6 mmHg [vehicle], 89.3 ± 4.1 mmHg [HCT-1026] and 80.6 ± 4.1 mmHg [flurbiprofen], P=0.291) (Fig. 2.B). Splanchnic hyperemia was attenuated in both the HCT-1026- and flurbiprofen-treated group of cirrhotic rats (4.2 ± 0.2 and 4.0 ± 0.4 mL/min/100g vs 5.4 ± 0.2 mL/min/100g for TAA+vehicle, $P=0.004$) (Fig. 2.C).

Fig. 2: Effect of nitroflurbiprofen (HCT-1026), flurbiprofen and vehicle on portal pressure (A), mean arterial pressure (B) and mesenteric blood flow (C) in the different treatment groups of cirrhotic rats (n=8/group). *$P < 0.005$ vs vehicle-treated cirrhotic rats.

Abbreviations: TAA, thioacetamide; NO-flurbi, nitroflurbiprofen; flurbi, flurbiprofen.


A
Portal pressure (mmHg)
15
12
9
6
3
0
*
*
vehicle
NO-Flurbi
Flurbi
TAA


B
Mean arterial pressure (mmHg)
120
100
80
60
40
20
0
vehicle
NO-Flurbi
Flurbi
TAA


C
Mesenteric blood flow (mL/min/100g)
6
4
2
0
*
*
vehicle
NO-Flurbi
Flurbi
TAA

3.2. In-situ perfusion experiments

3.2.1. Effect on the total intrahepatic resistance in pretreated cirrhotic rats (Fig. 3).

TAA cirrhotic rats, injected with vehicle 24 and 1 hour prior to the perfusion experiment, showed significantly increased perfusion pressures with increasing flow in comparison with non-cirrhotic control animals, suggesting an increased total intrahepatic vascular resistance (slope values: 0.43 ± 0.01 mmHg.min/mL vs 0.07 ± 0.02 mmHg.min/mL, $P<0.001$). Pre-treated TAA cirrhotic rats with nitroflurbiprofen (HCT-1026) or flurbiprofen had markedly reduced total intrahepatic vascular resistance (0.16 ± 0.02 mmHg.min/mL and 0.14 ± 0.01 mmHg.min/mL respectively, $P<0.001$ vs TAA + vehicle).

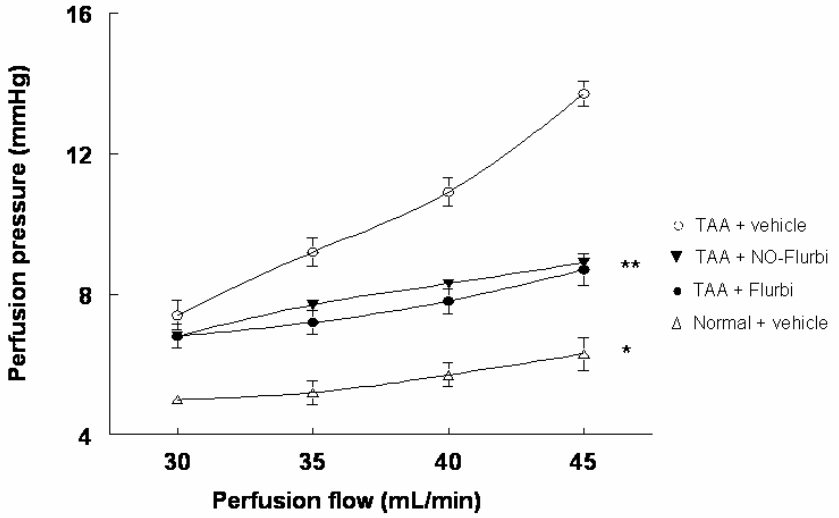


Fig. 3: Nitroflurbiprofen (HCT-1026) and flurbiprofen reduce total intrahepatic vascular resistance in the perfused TAA cirrhotic rat liver (*$P<0.001$ normal vs TAA+ vehicle, **$P<0.001$ TAA+ flurbi and TAA + NO-flurbi vs normal and TAA + vehicle). Abbreviations: TAA, thioacetamide; NO-flurbi, nitroflurbiprofen; flurbi, flurbiprofen.

3.2.2. Effect on the increased intrahepatic vascular tone

A. Effect on endothelial dysfunction

Similar to flurbiprofen 250µM, pre-incubation with 250µM nitroflurbiprofen attenuated the impaired vasodilatory response to acetylcholine of cirrhotic livers to the point that there were no longer differences between nitroflurbiprofen- or flurbiprofen-pretreated cirrhotic and control livers (Fig. 4).

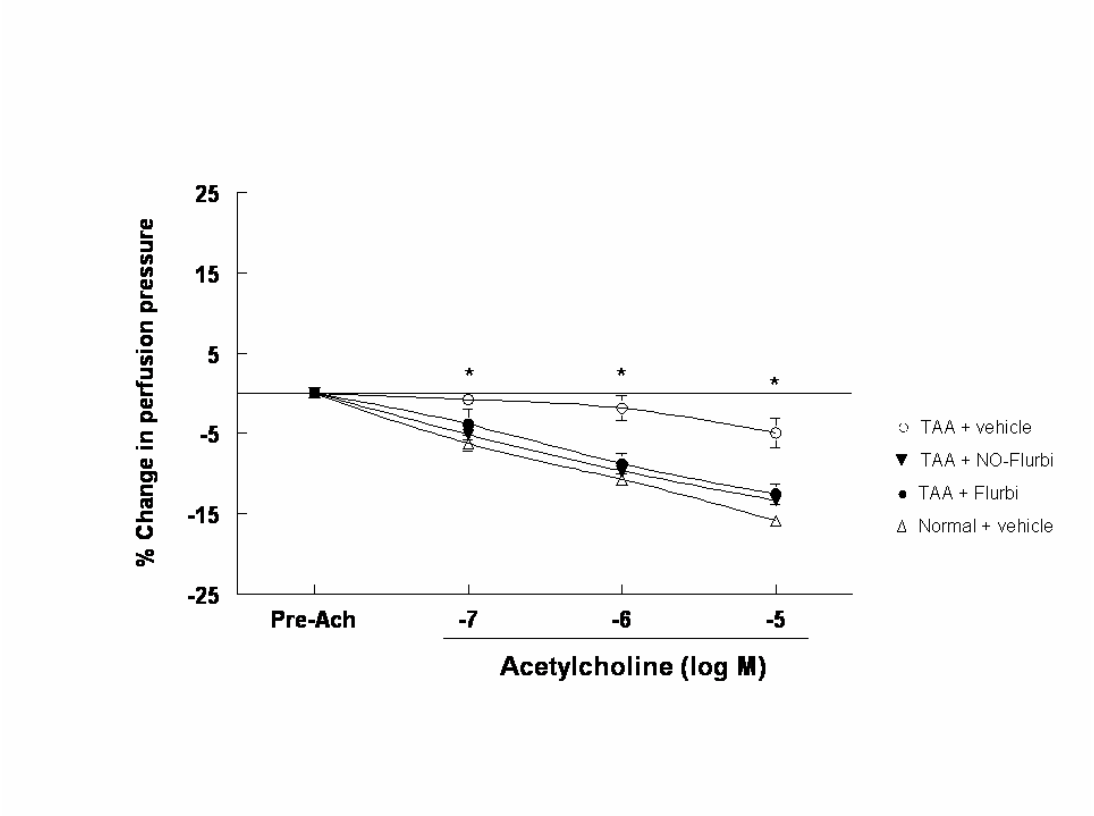


Fig. 4: Nitroflurbiprofen (HCT-1026) and flurbiprofen improve the impaired vasodilatory response to acetylcholine (endothelial dysfunction) in the TAA cirrhotic rat liver (*P<0.001 TAA + vehicle vs all).

This marked improvement in endothelial function after administration of either nitroflurbiprofen or flurbiprofen, was associated with an equally decreased production of TXB_2 in these animals (control: 10.3 ± 6.7 pg/mL, TAA: 820.5 ± 185.4 pg/mL, TAA + 250µM nitroflurbiprofen: 129.5 ± 48.3 pg/mL, TAA + 250µM flurbiprofen: 135.6 ± 26.5 pg/mL, *P*<0.001TAA + nitroflurbiprofen or flurbiprofen vs control and TAA alone) (Fig. 5).

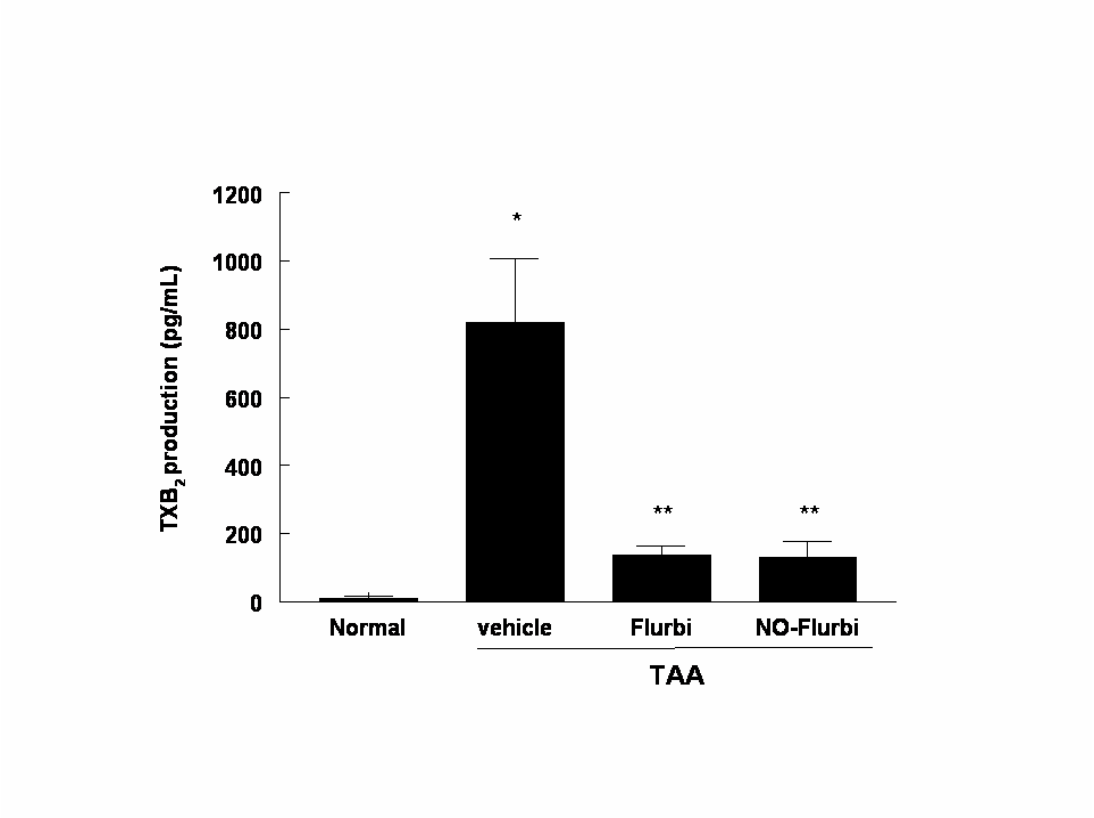


Fig. 5: TXB_2 production after acetylcholine in TAA cirrhotic rat liver preincubated with nitroflurbiprofen (n=5), flurbiprofen (n=5) or vehicle (n=5) and normal liver with vehicle (n=5) (**P*<0.001 TAA + vehicle vs all other groups, ***P*<0.001 TAA + nitroflurbi and flurbi vs normal and TAA + vehicle).

B. Effect on intrahepatic hyperresponsiveness to methoxamine (Fig.6).

Preincubation with 250µM nitroflurbiprofen attenuated the exaggerated response to methoxamine in the perfused TAA cirrhotic rat liver to the point that this hyperresponse almost completely disappeared (10^{-6}M: 0.07 ± 0.1 mmHg vs 0.2 ± 0.1 mmHg, *P*=0.342 vs healthy control; 10^{-5}M: 3.3 ± 0.4 vs 2.1 ± 0.3 mmHg, *P*=0.074; 10^{-4}M: 7.06 ± 0.3 mmHg vs 7.3 ± 0.8, *P*=0.776). Pretreatment with flurbiprofen (250µM) resulted in a similar effect, however, less firm (10^{-6}M: 0.7 ± 0.2 mmHg, *P*=0.029 vs TAA+nitroflurbiprofen; 10^{-5}M: 5.0 ± 0.6 mmHg, *P*=0.05; 10^{-4}M: 9.1 ± 0.5 mmHg, *P*=0.013).

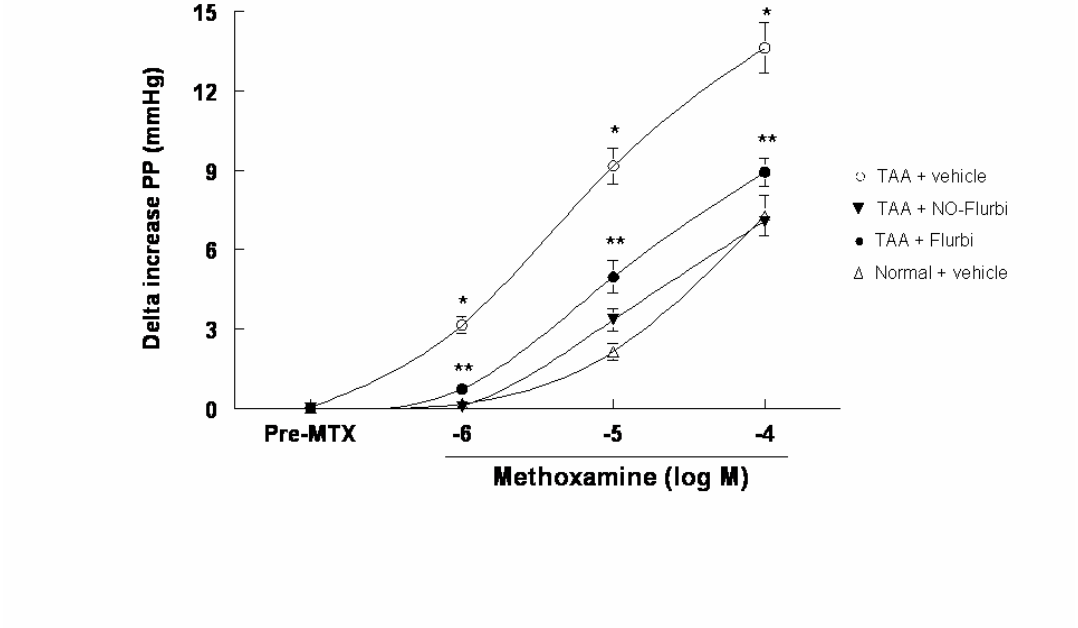


Fig. 6: Nitroflurbiprofen, more than flurbiprofen, attenuates the intrahepatic hyperresponsiveness to methoxamine (*P<0.001 TAA+vehicle vs all other groups, **P ≤ 0.05 TAA + flurbiprofen vs TAA + nitroflurbiprofen).

3.3. In vitro HSC contraction

Preincubation with nitroflurbiprofen resulted in a dose-dependent decrease in FCS-promoted HSC contraction (P<0.001 versus FCS alone) (Fig. 7) . However, cyclooxygenase-inhibition alone, accomplished by flurbiprofen, resulted in a less obvious decrease in FCS-mediated contraction (P<0.001 flurbiprofen 250µM vs nitroflurbiprofen 250µM).

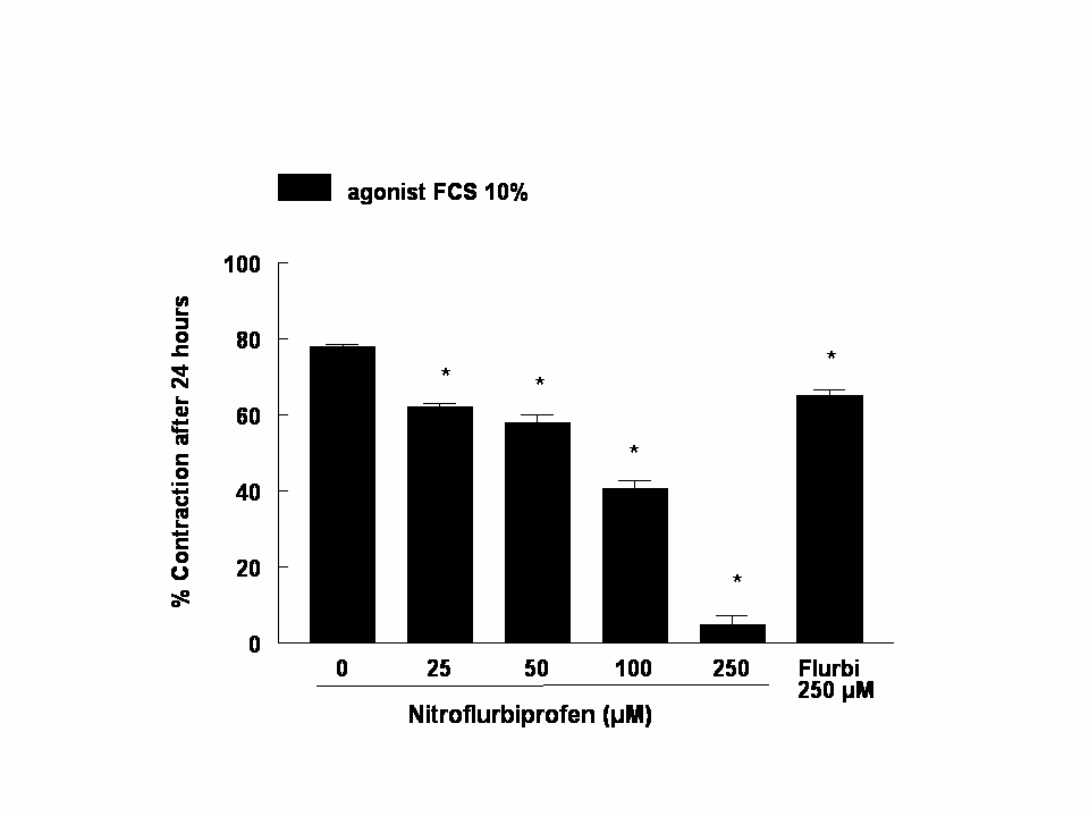


Fig. 7. Nitroflurbiprofen dose-dependently inhibits FCS-promoted HSC contraction (*P<0.001 vs FCS alone).

Cytotoxicity of both drugs and vehicle in the range of concentrations used, was excluded in vitro by use of a colorimetric cell proliferation assay (XTT) (Roche Diagnostics, Vilvoorde, Belgium).

3.4. Nitrite/nitrate levels in serum and liver

Analysis of serum NOx levels of rats used in the in vivo experiments showed no differences, which together with the comparable mean arterial pressure between the different groups, suggests lack of overt systemic NO-release of nitroflurbiprofen (HCT-1026) (Fig. 8.A).

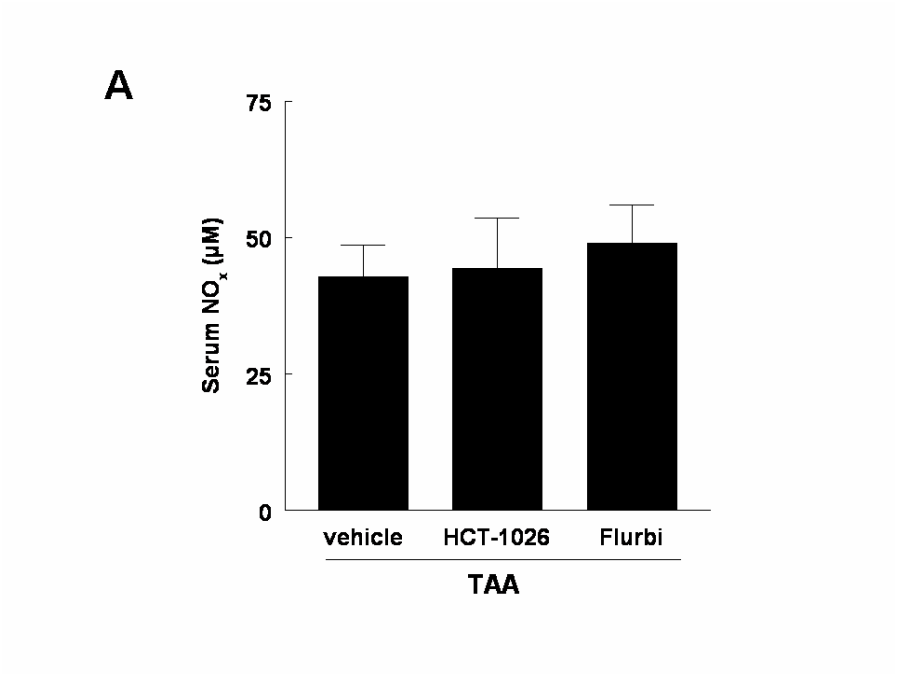


Fig. 8. Serum (A) (n=8/group) and hepatic (B) levels (n=6/group) of nitrite/nitrate in the 3 different groups (*P=0.005 vs others). Abbreviations: NOx, nitrite/nitrate; TAA, thioacetamide; HCT-1026, nitroflurbiprofen; flurbi, flurbiprofen.

In contrast, we documented significantly higher hepatic NOx levels in rats pretreated with nitroflurbiprofen compared to cirrhotic rats treated with either vehicle or flurbiprofen (179.7 ± 29.9 pmol/mg vs 57.5 ± 16.7 and 109.2 ± 16.7 pmol/mg respectively, *P*=0.005) (Fig. 8.B). The levels of liver NOx in the flurbiprofen-treated were notably different from the control cirrhotic rats – approaching statistical significance (*P*=0.059) - further supporting the previously mentioned interaction beween NOS and COX (cfr chapter 7).

3.5. Assesment of NSAID-related side-effects in vivo

Typically associated side-effects of NSAIDs, such as nephrotoxicity, hepatotoxicity and gastrointestinal ulceration complicated with bleeding, were evaluated in rats undergoing the different treatments (Table 2). Except for an almost significant decrease in aspartate aminotransferase, there were no differences in hepatic function. With regard to renal function, flurbiprofen, but not HCT-1026, caused renal impairment. Similarly, animals treated with flurbiprofen, but not HCT-1026, had a significantly higher ulcer index, which in 3 out of 8 treated cirrhotic animals was responsible for gastrointestinal bleeding (Fig. 9).

Table 2: Effect of nitroflurbiprofen, flurbiprofen and vehicle on gastrointestinal ulcerogenicity, liver and renal function in TAA cirrhotic rats

Parameter	**Administration**			***P***
	Vehicle (n=8)	**Nitroflurbiprofen (n=8)**	**Flurbiprofen (n=8)**	
Hepatic function				
AST (U/L)	202 ± 15.6	140.1 ± 9.8	196.9 ± 24.1	0.054
Albumin (g/L)	32.4 ± 1.9	30.9 ± 1.4	28.8 ± 1.5	0.209
Total bilirubin (mg%)	0.21 ± 0.04	0.33 ± 0.04	0.32 ± 0.06	0.219
Renal function				
Serum urea nitrogen (mg%)	42.6 ± 1.3	42.3 ± 3	65.4 ± 3.7*	< 0.001
Serum creatinine (mg%)	0.52 ± 0.01	0.51 ± 0.02	0.69 ± 0.04*	< 0.001
Creatinine clearance (mL/h/100g)	10.4 ± 0.6	12.3 ± 0.7	8.0 ± 0.4*	< 0.001
Gastrointestinal ulcerogenicity				
Ulcer index (mm^2)	2.5 ± 1.0	2.9 ± 0.8	15.6 ± 1.6*	< 0.001
GI bleeding	0/8	0/8	3/8	

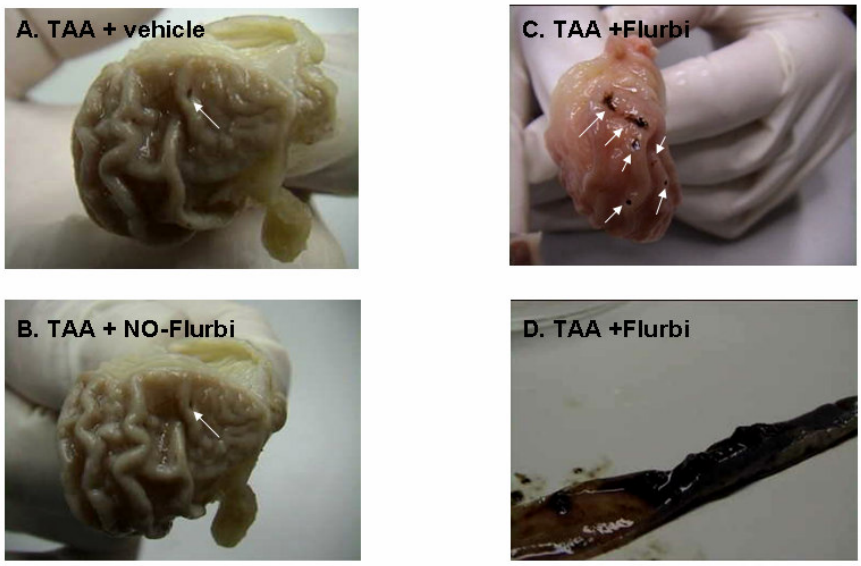


Fig. 9. Evaluation of gastrointestinal ulcerogenicity in the different treatment groups: A. TAA + vehicle (n=8), B. TAA + nitroflurbiprofen (n=8) and C. TAA + flurbiprofen (n=8). A representative excised stomach is shown, ulcers are demarcated by a white arrow. D. Dark-colored, tarry stools in the gut of a rat treated with flurbiprofen, indicative of gastrointestinal bleeding.

4. DISCUSSION

The quest for drugs targeting and decreasing the increased intrahepatic vascular tone has become a major research objective in cirrhotic portal hypertension and is fuelled by advances in the knowledge concerning its pathophysiology. A milestone herein was the finding of an impaired intrahepatic NO production, which stimulated the clinical use of nitrovasodilators for the treatment of portal hypertension (1,10-12). However, many attempts to reduce the increased intrahepatic vascular tone in this way failed due to the lack of liver-selectivity of the currently available nitrovasodilators, leading to a further increase of the already existing splanchnic and systemic vasodilation and to an aggravation of the systemic hypotension with worsening of sodium retention and renal dysfunction (1,7,11).

In the previous chapter, we have shown that TXA_2, a vaso-active prostanoid and cyclooxygenase-metabolite, plays a key role in the increased intrahepatic vascular tone associated with cirrhotic portal hypertension, potentially through an interaction with NO (chapter 7). However, until today, no attempts have been undertaken to explore this molecule for the treatment of portal hypertension since non-selective cyclooxygenase-inhibitors are considered contraindicated in patients with decompensated cirrhosis because of the high-risk of developing renal failure, gastrointestinal ulceration (and bleeding) and refractory ascites (19-21).

The present study tested the potential portal pressure lowering effect of nitro-flurbiprofen (HCT-1026), an NO–donating non-steroidal anti-inflammatory drugs (NO-NSAIDs) (Fig. 1), in an established rat model of TAA-induced cirrhotic portal hypertension.

NO-NSAIDs are a new class of compounds which combine the typical cyclooxygenase (COX)-inhibiting features of NSAIDs with the NO-releasing properties of an added nitroxybutyl-ester group in order to enhance therapeutic efficacy or to reduce side-effects (16-19). We demonstrated that nitroflurbiprofen, as well as its parent NSAID flurbiprofen,

equally decreased portal hypertension in cirrhotic rats, without further compromising the hyperdynamic circulation or splanchnic hyperemia. To elucidate the mechanism of action of nitroflurbiprofen and flurbiprofen, we investigated their vasoactive properties in the in-situ perfused cirrhotic rat liver. Since we used a flow-controlled system, according to Ohm's law, this system provided recording of changes in vascular resistance. Performance of flow-pressure curves, assessing the total intrahepatic vascular resistance (i.e. both passive and active component of resistance), showed that short-term treatment of cirrhotic animals with nitroflurbiprofen and flurbiprofen evenly reduced the increased total intrahepatic resistance. This decrease in total intrahepatic vascular resistance might explain the observed decrease in splanchnic hyperemia as a result of improved rheological conditions, although a direct effect of COX-inhibition on splanchnic hyperemia has also been documented (22). To exclude the possibility that the effect on intrahepatic resistance was attributable to a decrease in fibrosis, since COX-inhibitors have been investigated for this capacity (23), the time-window was kept less than 25 hours from the moment of administration of the compounds to the time of hemodynamic measurements.

To further investigate the observed hemodynamic effect of these drugs, we also evaluated their impact on endothelial dysfunction and hyperresponsiveness to vasoconstrictors, which are considered to be the two main intrinsic features to this vasculogenic component. In our pre-ascitic cirrhotic rats, the COX-inhibitor flurbiprofen and nitroflurbiprofen similarly improved endothelial dysfunction, which was associated with a comparable decrease in TXA_2 production.

When we next evaluated the effect of flurbiprofen and nitroflurbiprofen on the hyperresponsiveness to methoxamine in cirrhotic rats, nitroflurbiprofen attenuated this phenomenon significantly more than flurbiprofen. This can be explained by apparent liver-selective NO-donating properties of nitroflurbiprofen. Indeed, we documented an increased

hepatic NOx concentration without a further increase of systemic NOx levels. Moreover, hepatic NOx-levels in the flurbiprofen-treated were also nearly significantly (*P*=0.059) elevated compared to vehicle-treated cirrhotic rats, as such further supporting the earlier mentioned premise of COX-NOS interaction (chapter 7).

Besides the in vivo and perfused organ study, we finally also proved beneficial effects of nitroflurbiprofen on the cellular level since nitroflurbiprofen modulated HSC contraction. Inhibition of COX, and therefore TXA_2-synthesis, only mildly modulated HSC contraction, whereas nitroflurbiprofen decreased HSC contraction to a much larger extent, suggesting that the in vitro effect of nitroflurbiprofen is largely mediated through its NO-donating properties and that HSCs act most likely as an effector for TXA_2 rather than as a cellular source, which in an alternative way supports the findings of Graupera (24).

The main and possible clinically most relevant advantage of nitroflurbiprofen over flurbiprofen is its safety-profile. Our observations in cirrhotic animals support the lack of hepato- and nephrotoxicity and the lower incidence of gastrointestinal ulcerogenicity associated with these new drugs, which is of particular interest in patients with chronic liver disease who are particularly prone to hepatic, renal and GI complications of NSAIDs (19-21).

In conclusion, the results of the present study demonstrate that nitroflurbiprofen (HCT-1026), a NO-donating NSAID, leads to decreased portal pressure without systemic side-effects in TAA-induced cirrhotic rats. The beneficial effects of this compound are based on the combined approach of abrogated TXA_2 production and the replenishment of the decreased intrahepatic NO-availability as proven in vivo, in the in-situ perfused liver and in vitro.

5. REFERENCES

1. Laleman W, Van Landeghem L, Wilmer A, Fevery J, Nevens F. Portal hypertension: from pathophysiology to clinical practice. Liver Int 2005; 25:1079-1090.
2. Lebrec D, PoynardT, Hillon P, Benhamou JP. Propanolol for the prevention of recurrent gastrointestinal bleeding in patients with cirrhosis: a controlled study. N Engl J Med 1981; 305: 1371-1374.
3. Pascal JP, Cales P. Propanolol in the prevention of first upper gastrointestinal tract hemorrhage in patients with cirrhosis of the liver and esophageal varices. N Engl J Med 1987; 317: 856-861.
4. Abraldes JG, Tarantino I, Turnes J, Garcia-Pagan JC, Rodes J, Bosch J. Hemodynamic response to pharmacological treatment of portal hypertension and long-term prognosis of cirrhosis. Hepatology 2003; 37: 902-908.
5. Groszmann RJ, Bosch J, Grace ND, et al. Hemodynamic events in a prospective randomized trial of propranolol versus placebo in the prevention of a first variceal hemorrhage. Gastroenterology 1990; 90: 1401–1407.
6. Feu F, Garcia-Pagan JC, Bosch J, Luca A, Teres J, Escorsell A, Rodes J. Relation between portal pressure response to pharmacotherapy and risk of recurrent variceal haemorrhage in patients with cirrhosis. Lancet 1995; 346: 1056–1059.
7. Bosch J, Garcia-Pagan JC. Prevention of variceal rebleeding. Lancet 2003; 361: 952-954.
8. Villeneuve JP, Pomier-Layrargues G, Infante-Rivard C, et al. Propranolol for the prevention of recurrent variceal hemorrhage: a controlled trial. Hepatology 1986; 6: 1239-1243.
9. Bhathal PS, Grossman HJ. Reduction of the increased intrahepatic vascular resistance of the isolated perfused cirrhotic rat liver by vasodilators. J Hepatol 1985; 1: 325–337.
10. Rockey DC. The cellular pathogenesis of portal hypertension: stellate cell contractility, endothelin and nitric oxide. Hepatology 1997; 25: 2-5.
11. Gupta TK, Toruner M, Chung MK, Groszmann RJ. Endothelial dysfunction and decreased production of nitric oxide in the intrahepatic microcirculation of cirrhotic rats. Hepatology 1998; 28: 926-931.
12. Wiest R, Groszmann RJ. The paradox of nitric oxide in cirrhosis and portal hypertension: too much, not enough. Hepatology 2002; 35: 478-491.
13. Van de Casteele M, Omasta A, Janssens S, et al. In vivo gene transfer of endothelial nitric oxide synthase decreases portal pressure in anaesthetised carbon tetrachloride cirrhotic rats. Gut 2002; 51: 440-445.
14. Laleman W, Omasta A, Van de Casteele M, et al. A role for asymmetric dimethylarginine in the pathophysiology of portal hypertension in rats with biliary cirrhosis. Hepatology 2005; 42: 1382-1390.
15. Laleman W, Vander Elst I, Zeegers M, et al. A stable model of cirrhotic portal hypertension in the rat: thioacetamide revisited. Eur J Clin Invest 2006; 36: 242-249.
16. Fiorucci S, Antonelli E, Burgaud JL, Morelli A. Nitric oxide-releasing NSAIDs: a review of their current status. Drug Saf 2001; 24: 801-811.
17. Teoh NC, Farrell GC. Hepatotoxicity associated with non-steroidal anti-inflammatory drugs. Clin Liv Dis 2003; 7: 401-413.
18. Mizoguchi H, Hase S, Tanaka A, Takeuchi K. Lack of small intestinal ulcerogenecity of nitric oxide-releasing indomethacin, NCX-530, in rats. Aliment Pharmacol Ther 2001;15:257-267.
19. Keeble JE, Moore PK. Pharmacology and potential therapeutic applications of nitric oxide-releasing non-steroidal anti-inflammatory and related nitric oxide-donating drugs. Br J Pharmacol 2002; 137: 295-310.
20. Lopez-Parra M, Claria J, Planaguma A, et al. Cyclooxygenase-1 derived prostaglandins are involved in the maintenance of renal function in rats with cirrhosis and ascites. Br J Pharmacol 2002; 135: 891-900.
21. Claria J, Kent JD, Lopez-Parra M, et al. Effects of celecoxib and naproxen on renal function in nonazotemic patients with cirrhosis and ascites. Hepatology 2005; 41: 579-587.
22. Fernandez M, Garcia-Pagan JC, Casadevall M, et al. Acute and chronic cyclooxygenase blockade in portal hypertensive rats. Gastroenterology 1996; 110: 1529-1535.
23. Planaguma A, Claria J, Miquel R, et al. The selective cyclooxygenase-2 inhibitor SC-236 reduces liver fibrosis by mechanisms involving non-parenchymal cell apoptosis and PPARgamma activation. FASEB J 2005; 19: 1120-1122.
24. Graupera M, March S, Engel P, et al. Sinusoidal endothelial COX-1-derived prostanoids modulate the hepatic vascular tone of cirrhotic rat livers. Am J Physiol Gastrointest Liver Physiol 2005; 288: G763-G770.

Chapter 9

Summary and conclusions

SUMMARY

Portal hypertension is responsible for the more severe and often lethal complications of cirrhosis such as bleeding oesophageal varices, ascites, renal dysfunction and hepatic encephalopathy and is therefore of great clinical relevance. Recent advances in the knowledge of the pathophysiology of cirrhotic portal hypertension have directed future therapy towards the increased intrahepatic vascular resistance, which, in part, is determined by increased hepatic vascular tone. This increased tone is effectuated mainly by activated hepatic stellate cells and is the result of an imbalance between vasodilator and vasoconstrictor forces. Our present study aimed to clarify and elucidate new pathophysiological aspects of both the celluar and humoral aspects of the increased intrahepatic vascular tone.

In the first part of the results (Chapter 3), we fully characterized a stable, reproducible and homogeneous animal model of cirrhotic PHT, in which we documented the presence of an increased intrahepatic vascular tone associated with increased total intrahepatic vascular resistance which in turn, is a typical feature of cirrhotic PHT.

Focusing subsequently on the cellular effector, the activated hepatic stellate cell, we investigated in vitro the contractile apparatus and the signalling pathways involved in its contraction (Chapter 4). Using a stressed collagen matrix contraction model, we observed a role for both Ca^{2+}-dependent and -independent pathways to a HSC-specific contraction-pattern, as such providing clear distinction of HSCs from smooth muscle cells and myofibroblasts and making assumptions like “smooth-muscle-cell-like” and “myofibroblast-like” in current literature superfluous. The relevance of these in vitro findings, was correlated with the in-situ perfused cirrhotic rat liver in which we observed a hyperresponsiveness of both pathways (Ca^{2+}- dependent and Ca^{2+}-independent) with a predominance of Ca^{2+}-independent signalling pathways.

In chapter 6 and 7, we evaluated humoral aspects involved in the increased intrahepatic vascular tone. More specifically, increased production of vasoconstrictors (*e.g.*, endothelin-1, angiotensin II, adrenergic system) is unopposed due to reduced bioavailability of NO, a potent intrahepatic vasodilator. This imbalance contributes to the intrahepatic endothelial dysfunction. The molecular basis of intrahepatic NO-deficiency has consistently been attributed to a decrease in activity of intrahepatic endothelial NO synthase. However, the mechanisms of this endothelial dysfunction remain ill-defined. In chapter 6, we focus on the impaired intrahepatic vasorelaxing capacity by evaluating the role of an endogenous circulating NOS-inhibitor, asymmetric dimethylarginine (ADMA). We showed that ADMA is involved in the endothelial dysfunction of biliary cirrhotic rats but not of thioacetamide cirrhotic rats, suggesting that the pathophysiology of PHT differs depending on the etiology of cirrhosis. On the other hand, in thioacetamide cirrhotic rats, we documented the involvement of the vasoconstrictive cyclooxygenase-metabolite thromboxane A_2 (TXA_2) in the increased intrahepatic vascular tone (Chapter 6), since its levels were significantly increased in the cirrhotic liver and since inhibition of its production improved endothelial dysfunction, possibly through an interaction with NOS. Since TXA_2 has been reported to act predominantly through Rho-kinase- and protein kinase C-mediated pathways, the increase in TXA_2 levels in TAA cirrhotic rat livers (Chapter 6) might also explain the observed predominance of Ca^{2+}-independent contraction pathways (Chapter 4).

Lastly, we evaluated the effect of nitroflurbiprofen, a non-specific cyclooxygenase-inhibitor which combines NO-donating properties with TXA_2-inhibition, on portal hypertension in thioacetamide cirrhotic rats (Chapter 7). In comparison to flurbiprofen, nitroflurbiprofen decreased PHT by partially reversing the intrahepatic endothelial dysfunction and suppressing the hyperresponsiveness. Notably, this was achieved without

inducing side-effects that are commonly associated with cyclooxygenase-inhibitors, which include, for example, renal impairment, liver toxicity and gastrointestinal ulcerogenicity. Thus, nitroflurbiprofen is an interesting pharmacostrategy in the treatment of PHT.

LIMITATIONS

As with all experimental work, the current thesis is subjected to limitations.

To study humoral and cellular elements that play a role in the increased vascular tone associated with PHT, one is obliged to dissect and tear apart the unity of this aspect to the cellular level (in vitro), organ level (perfused organ level) or to studies in the whole living organism (in vivo). Although each level brings us closer to the "truth", it might also drive us further from it.

"The truth is rarely pure and never simple"

(Oscar Wilde, Irish dramatist, 1854-1900) .

In vitro techniques in the present work involve isolation of hepatic stellate cells from normal rat liver and "activating" them in culture flasks, a "foreign" environment. This in itself might already be a confounding factor since this could lead to changes in expression profile not typically seen in vivo.

"Snatched from a life of obscurity and installed in contemporary glass and plastic palaces, cells are in danger of becoming Pygmalion's protégés. Housed in more traditional residences constructed of water and collagen, instead of plastic or glass, could cells lead primitive, less cultured lives?"

(Elsdale and Bard, 1972)

Investigation of the concept of contractility is even more difficult since this has mainly been investigated in 2-dimensional conditions (like for contraction studies using confocal calcium-imaging or when growing HSCs on top of polymerized collagen lattices).
Inspired by Elsdale and Bard, we applied a three-dimensional stress-relaxed collagen lattice contraction model, which not only allows mimicry of the reciprocal geometric and mechanical relationships with the surrounding matrix but also a mechanical feedback which is missing in classically used contraction assays.
The next level, organ perfusion, was approached by using an in-situ flow-controlled liver perfusion model. This system was shown to be crucial in most of our studies, because it leaves endogenous vasoactive substances and the intrinsic regulatory response of the hepatic portal vasculature itself to control hepatic portal vascular resistance.

"Things should be made as simple as possible, but not any simpler."

Albert Einstein (American scientist, 1879-1955)

The contribution of the hepatic artery and nerves are however eliminated in this closed system. Additionally, the flow-controlled nature of this system is not entirely comparable to the in-vivo situation where flow is adaptable according to physiological needs (e.g. meal-induced hyperemia). Alternatively, pressure-limitation puts us in a similar situation. Therefore, a controlled system inevitably is a system where evaluation of one variable is intended.

"Research is what I'm doing when I don't know what I'm doing".

Werner von Braun (German rocket scientist, 1912-1977)

Finally, studies in the whole living organism: A prerequisite in this context is the need for an animal model, mimicking human cirrhosis and portal hypertension as closely as

possible. Although never ideal, we believe that our rat model of thioacetamide-induced cirrhosis, strongly resembles cirrhosis in humans. Moreover, the model is highly reproducible, homogeneous and is associated with a low mortality rate. Other models were also evaluated. The surgically induced chronic bile duct-excised rat model of cirrhosis can be used after 3 to 5 weeks and is therefore less costly than a hepatotoxin-induced liver damage model. However, this model is characterized by a high mortality (>40%), hemodynamic instability due to the toxic effect of the cholestasis on renal function, a higher susceptibility for sepsis due to the absence of bile in the digestive tract, an exaggerated dilatation of the extrahepatic bile duct causing extrinsic compression on portal vascular structures and a lack of elevated portal venous inflow (when studied under pentobarbital anaesthesia). It is worth noting that all of our studies were done under pentobarbital-anesthesia, which may cause altered systemic hemodynamics, suppression of the sympathic nervous system and reduction of renal plasma flow. Ideally, experiments should be performed on “awake” animals. However, ethical concerns demand some flexibility, and since anesthesia must indeed be used, the consequent increased variability in results must be offset by more careful and consistent administration of anesthesia, the use of appropriate controls, and an increased number of animals in each study.

CONCLUSION AND FUTURE PROSPECTS

In summary, we have elucidated some of the underlying mechanisms, both cellular and humoral, that lead to increased intrahepatic resistance associated with cirrhotic portal hypertension. Not only do these findings recapitulate the everlasting premise of “too much (vasoconstrictors), not enough (vasodilators)” in the cirrhotic liver, but they also emphasize the concept that therapies based on novel pathophysiological insights are worth pursuing.

Hoofdstuk 9

Samenvatting

Portale hypertensie vormt de frequentste complicatie van levercirrose en is verantwoordelijk voor levensbedreigende verwikkelingen zoals bloedende gastro-intestinale varices, ascites, hepatische encephalopathie en het hepatorenaal syndroom. Klassiek wordt de pathogenese van portale hypertensie bekeken naar analogie met de wet van Ohm ($\Delta P=QxR$). Volgens deze laatste, verandert de portale vene druk evenredig aan bloeddebiet en vaatweerstand. In de normale lever verandert de intrahepatisch vasculaire weerstand met variaties in het debiet, zodat de portale druk binnen normale grenzen wordt gehouden. Bij cirrose wordt echter vroegtijdig een verhoogde intrahepatisch vasculaire weerstand vastgesteld, later gevolgd door splanchnische hyperemie en een hyperdynamische circulatie, welke het portaal hypertensief syndroom onderhouden en verder verergeren. Hoewel anatomische "passieve" veranderingen door verlittekening van de lever de hoofdoorzaak zijn van een verhoogde intrahepatisch vasculaire weerstand, werd recent ook een "actieve", "dynamische" en dus moduleerbare component (intrahepatische vasculaire tonus) aangetoond zowel bij proefdieren als bij cirrotische patiënten. De bijdrage van deze actieve intrahepatisch vasculaire weerstand wordt op 30-40% van de totale weerstand geschat, en vormt het aangrijpingspunt voor mogelijke farmacologische interventie. Belangrijke effectoren van deze "actieve" intrahepatisch vasculaire weerstand zijn de hepatische stellaatcellen, ook lipocyten of cellen van Ito genoemd. Hepatische stellaatcellen, die rondom/op de sinusoidale endotheelcellen liggen in de ruimte van Disse, ondergaan immers bij expositie van de lever aan noxen een functioneel transitie-proces ("activatie") tot myofibroblast-achtige cellen. Naast verhoogd fibrogenetisch, proliferatief, chemotactisch en immunomodulatorisch potentieel, verwerven deze "geactiveerde" hepatische stellaatcellen ook het vermogen tot contractie, onder andere door de expressie van α-smooth-muscle actine. Naast de aanwezigheid van een hypercontractiele effector-cel, is er ook een multifactorieel (regulerend) onevenwicht tussen vasoconstrictorische en

vasodilatorische krachten. Meer specifiek, zijn de 3 belangrijkste determinanten in dit onevenwicht : een verhoogde productie van vasoconstrictoren (endothelines, angiotensine II, vasopressine, prostanoiden,…), een verhoogde vasoconstrictor-receptor-densiteit en een verlaagd intrahepatisch vasorelaxerend vermogen door verminderde stikstofmonoxide (NO)-productie. NO, een hyperreactief en labiel molecule, wordt gevormd uit de conversie van L-arginine naar L-citrulline door nitric oxide synthase (NOS)-isoenzymes, welke klassiek worden ingedeeld in constitutief (endotheliaal of neuronaal) of induceerbaar. In cirrose blijkt de intrahepatische NO-release gereduceerd ten gevolge van een endothelial NOS (eNOS)-dysfunctie. Paradoxaal genoeg, wordt er in het splanchnische vaatbed een exces aan NO geproduceerd, leidend tot vasodilatatie (en aldus splanchnische hyperemie) alsook hyporeactiviteit tot endogene vasopressoren. Splanchnische hyperemie, als vermoedelijk secundair fenomeen na primaire verhoogde intrahepatische weerstand, onderhoudt en verergert het portaal hypertensief syndroom.

Het huidig werk had tot doel een beter inzicht te verwerven in de pathofysiologie van cirrotische portale hypertensie, vertrekkende vanuit de “actieve”, “dynamische” intrahepatische vasculaire weerstand, en meer bepaald de effectoren en mediatoren die deze actieve weerstand controleren, gezien dit als een cruciaal primum movens wordt beschouwd in de pathogenese van PHT. Deze kennis zou dan kunnen leiden tot nieuwe perspectieven in de behandeling van het portaal hypertensief syndroom in al zijn dimensies.

In het eerste hoofdstuk van de resultaat-sectie (Hoofdstuk 3), karakteriseerden we een voor ons labo nieuw, reproduceerbaar en homogeen ratmodel van cirrotische PHT door middel van het langdurig toedienen van het hepatotoxine thioacetamide in drinkwater. In dit model toonden we het bestaan aan van een toegenomen intrahepatische vasculaire tonus via de techniek van in-situ lever perfusie.

In een volgend hoofdstuk (Hoofdstuk 4), spitsten we ons dan in eerste instantie toe op de cellulaire effector van deze toegenomen intrahepatische vasculaire tonus, met name de geactiveerde hepatische stellaatcel, en meer bepaald het contractiel apparaat van deze cel en de signaaltransductie-pathways die dit controleren. Door het inbedden van cultuur-geactiveerde hepatische stellaatcellen in collageen matrices, observeerden we in dit in vitro gelcontractie-model een rol voor zowel Ca^{2+}-afhankelijke en –onafhankelijke pathways. Deze bevindingen relativeren de "dogmatische" aangenomen analogie met gladde spiercel contractiliteit, welke strikt en louter Ca^{2+}-afhankelijk is. De relevantie van deze in vitro bevindingen werd verder onderbouwd in de in-situ geperfundeerde cirrotische rattenlever, waarbij Ca^{2+}-onafhankelijke contractie-pathways predominant bleken .

In hoofdstuk 5 en 6, evalueerden we de rol van mogelijk nieuwe humorale factoren in de regulatie van de toegenomen intrahepatische vasculaire tonus. In hoofdstuk 6, focusten we ons specifiek op het verminderd intrahepatisch vasorelaxerend vermogen ten gevolge van een verminderde intrahepatische eNOS activiteit (endotheeldysfunctie), meer specifiek op de rol van een recent beschreven circulerende endogene NOS-inhibitor asymmetrisch dimethylarginine (ADMA). We toonden aan dat ADMA cruciaal was in intrahepatische endotheeldysfunctie geassocieerd met biliaire cirrose maar niet in ratten met toxische cirrose. Dit suggereert dat de pathofysiologie van cirrotische portale hypertensie verschilt naargelang de etiologie van cirrose. In toxische (thioacetamide-geinduceerde) cirrose konden we anderzijds wel de betrokkenheid van thromboxane A_2, een vasoconstrictor cyclooxygenase-metaboliet, aantonen, zowel functioneel (inhibitie van cyclooxygenase resulteerde in correctie van endotheeldysfunctie en hyperresponsiviteit tot vasoconstrictoren), humoraal (toegenomen perfusaat en serumspiegels van thromboxane) als moleculair (toegenomen thromboxane-synthase-expressie) (hoofdstuk 6). Dit brengt ons meteen bij verdere uitdieping van het toegenomen intrahepatisch vasoconstrictorisch

vermogen. Meer nog, een gedeeltelijke verklaring voor het weerstandsverhogende effect van thromboxane A_2 zou te wijten zijn aan een onderdrukking van eNOS. Gezien thromboxane A_2 ook hoofdzakelijk werkt via Ca^{2+}-onafhankelijke signaaltransductie-cascades, zouden de toegenomen thromboxane A_2 spiegels in de cirrotische lever, ook de eerder vernoemde predominantie van Ca^{2+}-onafhankelijke contractie-pathways kunnen verklaren.

Gebruik makend van deze informatie, evalueerden we in het laatste hoofdstuk het therapeutisch nut van nitroflurbiprofen, een niet-selectieve cyclooxygenase-inhibitor die NO-donerende eigenschappen combineert met thromboxane A_2 inhibitie, op portale hypertensie in ratten met thioacetamide-geinduceerde cirrose. In tegenstelling tot flurbiprofen alleen, verbeterde nitroflurbiprofen portale hypertensie in deze dieren zonder de typische nevenwerkingen van een cyclooxygenase-inhibitor, zoals o.a. nierinsufficiëntie, hepatotoxiciteit en gastrointestinale ulcerogeniciteit.

Tot besluit kunnen we stellen dat het huidig werk nieuwe mechanismen, zowel cellulair als humoraal, heeft aangetoond in de pathogenese van de toegenomen intrahepatisch vasculaire weerstand geassocieerd met cirrotische portale hypertensie. Niet alleen herbenadrukken deze bevindingen de complexiteit en interactie tussen de verschillende systemen, ze tonen ook aan dat nieuwe therapieën gebaseerd op nieuwe (en immer vernieuwende) pathofysiologische inzichten, zoals nitroNSAIDs, de moeite waard zijn om verder uit te diepen.

CURRICULUM VITAE

Geboortedatum	6 februari 1975, Poperinge	
Burgerlijke staat	Gehuwd met Katrien Deprez, 2 dochters Elise (°25/11/2002) en Laura (°6/1/2004)	
Diploma's	1994–2000	Geneeskunde, K.U. Leuven, grote onderscheiding
	2002	Brevet acute geneeskunde, Belgian Society of Emergency and disaster medicine (BeSEDiM)
	2005	Licentie radioprotectie en dosimetrie, K.U. Leuven
Hogere studies - opleidingen	2000-2002	Inwendige geneeskunde, AZ Groeninge, Kortrijk
	2000-2006	Inwendige geneeskunde, Universitair Ziekenhuis Gasthuisberg, Leuven
	2002-2006	Doctoraat m.b.t. portale hypertensie (promotor : Prof. Dr. F. Nevens, Hepatologie, U.Z. Leuven)
	2006-…	Specialisatie Gastroenterologie & Hepatologie, Universitair Ziekenhuis Gasthuisberg, Leuven
Erkenningen en wetenschappelijke prijzen	2001	Prijs Prof. Dr. J. De Groote, Faculteit Geneeskunde, K.U. Leuven
	2004-2006	Aspirant-mandaat Fonds voor Wetenschappelijk onderzoek-Vlaanderen
	2004-2005	Aanmoedigingsbeurs Vlaamse Vereniging voor Gastroenterologie (VVGE)
	2005	Award winning abstract – Herfstsymposium NVGE-VVGE, Veldhoven, Nederland
	2005	Presidential poster of distinction- American Association for the Study of the Liver, San Francisco, USA, november 2005.

PUBLICATION LIST

Articles in peer reviewed journals:

- **Laleman W**, Van Landeghem L, Wilmer A, Fevery J and Nevens F. Portal hypertension: from pathophysiology to clinical practice. Liver Int 2005;25:1079-1090.
- **Laleman W**, Omasta A, Van de Casteele M, Zeegers M, Vander Elst I, Vanlandeghem L, Severi T, Van Pelt J, Roskams T, Fevery J and Nevens F. A role for asymmetric dimethylarginine (ADMA) in the pathophysiology of portal hypertension in biliary cirrhotic rats. Hepatology 2005;42:1382-90 + editorial.
- Evenepoel P, **Laleman W**, Wilmer A, Claes K, Maes B, Kuypers D, Bammens B, Nevens F, Vanrenterghem Y. Detoxifying capacity and kinetics of Prometheus – a new extracorporeal system for the treatment of liver failure. Blood Purif 2005;23:349-358.
- **Laleman W**, Wilmer A, Evenepoel P, Verslype C, Fevery J and Nevens F. Non-biological liver support in liver failure: a review of literature. Aliment Pharmacol Therap 2006;23:351-363.
- **Laleman W**, Vander Elst I, Zeegers M, Servaes R, Libbrecht L, Roskams T, Fevery J and Nevens F. A stable model of cirrhotic portal hypertension in the rat: thioacetamide revisited. Eur J Clin Invest 2006;36:242-249.
- Evenepoel P, **Laleman W**, Wilmer A, Claes K, Maes B, Kuypers D, Bammens B, Nevens F, Vanrenterghem Y. PROMETHEUS versus MARS: comparison of efficiency in two different liver detoxification devices. Artif Organs 2006;30:276-284.
- **Laleman W**, Wilmer A, Evenepoel P, Vander Elst I, Zeegers M, Zaman Z, Verslype C, Fevery J and Nevens F. Effect of MARS and Prometheus on systemic hemodynamics and vasoactive agents in patients with acute-on-chronic alcoholic liver failure. Crit Care 2006 Jul 19;10(4):R108 [Epub ahead of print].
- **Laleman W**, Severi T, Bisschops R, Vander Elst I, Van Landeghem L, Roskams T, Cassiman D, Van Pelt J, Fevery J and Nevens F. Hepatic stellate cell contraction pathways and their relevance to the increased intrahepatic vascular resistance

associated with cirrhosis. Am J Physiol Gastrointest Liver Physiol. 2006 Sep 28; [Epub ahead of print]

- **Laleman W**, Van Landeghem L, Severi T, Vander Elst I, Zeegers M, Fevery J and Nevens F. Both thromboxane A_2, a vaso-constrictive cyclooxygenase-metabolite, and nitric oxide are involved in the increased intrahepatic vascular tone associated with thioacetamide-induced cirrhosis in the rat. In preparation.
- **Laleman W**, Van Landegehem L, Vander Elst I, Zeegers M, Fevery J and Nevens F. Nitroflurbiprofen, a nitric oxide releasing derivative of flurbiprofen, improves portal hypertension in the rat without major side-effects. Resubmitted.
- **Laleman W** and Nevens F. Cirrhotic portal hypertension: current and future medical therapy for primary and secondary prevention of variceal bleeding. Minerva Med 2006;97:325-345.
- Trebicka J, Hennenberg M, **Laleman W**, Shelest N, Biecker E, Schepke M, Nevens F, Sauerbruch T, Heller J. Atorvastatin lowers portal pressure in cirrhotic rats via inhibition of RhoA/Rho-kinase and activation of eNOS. Resubmitted

Abstracts, posters and oral presentations:

- Nevens F and **Laleman W**. Prospective cohort study of predictive factors in chronic alcoholic liver disease. 5th International Symposium on Albumin Dialysis in Liver Disease. Rostock, Germany, September 2003, oral presentation.
- **Laleman W**, Nevens F, Wilmer A, Evenepoel P, Zaman Z, Zeegers M, Vander Elst I, Verslype C, Van Pelt J, Fevery J. Improvement in systemic hemodynamics during MARS is associated with a decrease in vasoactive substances in patients with acute on chronic liver failure (AoCLF). Acta Gastroenterol Belg 2004;1:A11. 16th Belgian week of Gastroenterology, oral presentation.
- **Laleman W**, Nevens F, Wilmer A, Evenepoel P, Van Pelt J, Fevery J. Improvement in systemic hemodynamics during MARS is associated with a decrease in vasoactive substances in patients with acute on chronic liver failure (AoCLF). J Hepatol 2004; 40 (Suppl 1):189. European Association for the Study of the Liver, Berlijn, Germany, april 2004, poster presentation.

- Nevens F and **Laleman W**. Novel treatment strategies in Portal Hypertension. UEGW (United European Gastroenterology Week), Prague, Tsjechia, september 2004, State-of-the art lecture.
- **Laleman W** and Nevens F. Alkoholic steatohepatitis : new therapeutic strategies, role of biopsy and MARS ? Vlaamse Vereniging voor Gastroenterologie. Herfstsymposium, Kortrijk, december 2004, Oral presentation.
- **Laleman W**, Omasta A, Van de Casteele M, Zeegers M, Vander Elst I, Roskams T, Fevery J and Nevens F. Asymmetric dimethylarginine causes intrahepatic endothelial dysfunction in biliary but not in toxic cirrhotic rats. Acta Gastroenterol Belg 2005, 68: A02. 17th Belgian Week of Gastroenterology, Spa, oral presentation.
- **Laleman W**, Severi T, Van Landeghem L, Vander Elst I, Roskams T, Fevery J and Nevens F. Hepatic stellate cell contraction: (myo)fibroblast-like or smooth muscle cell-like ? J Hepatol 2005; 42 (Suppl 2): 317. European Association for the Study of the Liver, Paris, France, april 2005, poster presentation.
- **Laleman W**, Omasta A, Van de Casteele M, Vander Elst I, Zeegers M, Roskams T, Fevery J and Nevens F. Asymmetric dimethylarginine (ADMA) is involved in portal hypertension of biliary but not of toxic cirrhotic rats. J Hepatol 2005; 42 (Suppl 2): 170. European Association for the Study of the Liver, Paris, France, april 2005, poster presentation.
- Evenepoel P, Wilmer A, Nevens F, Claes K, Kuypers D, Maes B, Bammens B, **Laleman W**, Vanrenterghem Y. Detoxifying capacity and kinetics of the Prometheus system: contribution of the different filters inbuilt. XLIIth congres of the European Renal Association and European Dialysis and transplant association. Istanbul, Turkey, june 2005, poster presentation.
- Evenepoel P, Wilmer A, Nevens F, Claes K, Kuypers D, Maes B, Bammens B, **Laleman W**, Vanrenterghem Y. Prometheus versus MARS: comparison of efficiency in two different liver detoxification devices. XLIIth congres of the European Renal Association and European Dialysis and transplant association. Istanbul, Turkey, june 2005, oral presentation.
- **Laleman W**, Wilmer A, Evenepoel P, Verslype C, Fevery J, Nevens F. Effect of MARS and Prometheus on systemic hemodynamics and vasoactive agents in patients with acute-on-chronic alcoholic liver failure: the clash of the titans.

Najaarsvergadering Nederlandse en Vlaamse Vereniging voor Gastro-enterologie, Veldhoven, The Netherlands, oktober 2005. Oral presentation.

- **Laleman W,** Vander Elst I, Zeegers M, Fevery J and Nevens F. Asymmetric dimethyl-L-arginine (ADMA): a possible cause of endothelial dysfunction in the bile-duct-excised cirrhotic rat. Najaarsvergadering Nederlandse en Vlaamse Vereniging voor Gastroenterologie, Veldhoven, The Netherlands, oktober 2005. Oral presentation – Presidential Selection NVGE. ***Award winning abstract***.
- **Laleman W**. New drugs and targets for portal hypertension. Liver day in honour of Prof J. Fevery. Leuven, september 2005. Oral presentation.
- **Laleman W,** Vander Elst I, Zeegers M, Fevery J and Nevens F. Asymmetric dimethyl-L-arginine (ADMA): a possible cause of endothelial dysfunction in the bile-duct-excised cirrhotic rat. Hepatology 2005; 42 (Suppl 1): 226A. American Association for the Study of the Liver, San Francisco, USA, november 2005. Oral presentation.
- Evenepoel P, **Laleman W**, Wilmer A, Claes K, Kuypers D, Maes B, Bammens B, Nevens F, Vanrenterghem Y. Comparison of efficiency in two different liver detoxification devices: MARS vs Prometheus. Hepatology 2005; 42 (Suppl 1): 93A. American Association for the Study of the Liver, San Francisco, USA, november 2005. Poster presentation.
- **Laleman W**, Wilmer A, Evenepoel P, Verslype C, Fevery J, Nevens F. Effect of MARS and Prometheus on systemic hemodynamics and vasoactive agents in patients with acute-on-chronic alcoholic liver failure: the clash of the titans. Hepatology 2005; 42 (Suppl 1): 93A. American Association for the Study of the Liver, San Francisco, USA, november 2005. *AASLD Presidential poster of distinction.*
- **Laleman W,** Van Landeghem L, Severi T, Vander Elst I, Cassiman D, Van Pelt J, Fevery J, Nevens F. Hepatic stellate cell contraction pathways and their relevance to the increased intrahepatic vascular resistance associated with thioacetamide cirhrosis. Acta Gastroenterol Belg 2006; 69: A010. 18th Belgian Week of Gastroenterology, oral presentation
- **Laleman W,** Wilmer A, Evenepoel P, Verslype C, Fevery J, Nevens F. Effect of the liver detoxification devices MARS and Prometheus on the systemic circulatory dysfunction associated with acute-on-chronic alcoholic liver failure. Acta Gastroenterol Belg 2006; 69: A02.18th Belgian Week of Gastroenterology, oral presentation.

- **Laleman W**, Van Landeghem L, Severi T, Vander Elst I, Zeegers M, Fevery J and Nevens F. Thromboxane A_2 affects the increased intrahepatic vascular tone of rats with cirrhotic portal hypertension, in part through interaction with nitric oxiede production. Hepatology 2006;44 (suppl 1):356:48A. American Association for the Study of the Liver, Boston, USA, november 2006. Poster presentation.
- **Laleman W**, Van Landeghem L, Vander Elst I, Zeegers M, Fevery J and Nevens F. Nitroflurbiprofen (HCT-1026), a nitric oxide-releasing cyclooxygenase-inhibitor, improves cirrhotic portal hypertension in the rat without major side-effects. Hepatology 2006;44 (suppl 1):356:37A. American Association for the Study of the Liver, Boston, USA, november 2006. Oral presentation.
- Trebicka J, **Laleman W**, Hennenberg M, Biecker E, Nevens F, Sauerbruch T, Heller J. Atorvastatin induces expression of eNOS and activation of NO-signaling in cirrhotic livers and hepatic stellate cells. Hepatology 2006;44 (suppl 1):356:46A. American Association for the Study of the Liver, Boston, USA, november 2006. Poster presentation.
- Nevens F and **Laleman W**. Prevention of variceal bleeding. International association of the Study of the Liver, Cairo, Egypt, september 2006, invited lecture.
- **Laleman W** and Nevens F. Leververvangende therapieën als brug naar transplantatie. Herfstsymposium VVGE, Antwerpen, November 2006.

Other:

- **Laleman W**, Vanderschueren S, Mortelmans L, Knockaert DC. Progressive bouts of acute abdomen: PET the peritoneum. Acta Clin Belg 2001;56:46-50.
- **Laleman W**, Inderadjaja N, Ravelingien I, Gheysens B. Mycobacterium marinum: het loerend gevaar in aquaria. Ts vr Geneeskunde 2004; 60:1233-1240.
- **Laleman W**, Aerts R, Nevens F. Een bijzonder geval van hematemesis. Geneeskundige Dagen van Antwerpen, 17 september 2005, Oral presentation.
- **Laleman W**, Nevens F. Leverdialyse. In: Nevens. F. 101 vragen over leverziektes en –transplantatie. Uitgeverij Lannoo 2006.